



저작자표시-비영리-변경금지 2.0 대한민국

이용자는 아래의 조건을 따르는 경우에 한하여 자유롭게

- 이 저작물을 복제, 배포, 전송, 전시, 공연 및 방송할 수 있습니다.

다음과 같은 조건을 따라야 합니다:



저작자표시. 귀하는 원저작자를 표시하여야 합니다.



비영리. 귀하는 이 저작물을 영리 목적으로 이용할 수 없습니다.



변경금지. 귀하는 이 저작물을 개작, 변형 또는 가공할 수 없습니다.

- 귀하는, 이 저작물의 재이용이나 배포의 경우, 이 저작물에 적용된 이용허락조건을 명확하게 나타내어야 합니다.
- 저작권자로부터 별도의 허가를 받으면 이러한 조건들은 적용되지 않습니다.

저작권법에 따른 이용자의 권리는 위의 내용에 의하여 영향을 받지 않습니다.

이것은 [이용허락규약\(Legal Code\)](#)을 이해하기 쉽게 요약한 것입니다.

[Disclaimer](#)

Doctoral Thesis

Studies of Dendritic Cell-Mediated Cancer
Immunotherapy by Utilizing Functional Nanoparticles

Bongseo Choi

Department of Biological Sciences

Graduate School of UNIST

2018

Studies of Dendritic Cell-Mediated Cancer Immunotherapy by Utilizing Functional Nanoparticles

Bongseo Choi

Department of Biological Sciences

Graduate School of UNIST

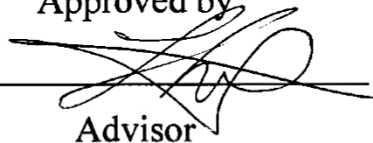
Studies of Dendritic Cell-Mediated Cancer Immunotherapy by Utilizing Functional Nanoparticles

A thesis submitted to the Graduate School of UNIST
in partial fulfillment of the requirements for the degree of
Doctor of Philosophy of Science

Bongseo Choi

6. 11. 2018

Approved by

A handwritten signature in black ink, appearing to read 'Sebyung Kang', is written over a horizontal line. The signature is stylized and cursive.

Advisor

Sebyung Kang

Studies of Dendritic Cell-Mediated Cancer Immunotherapy by Utilizing Functional Nanoparticles

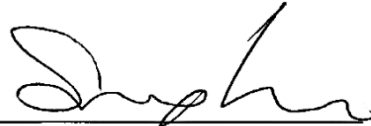
Bongseo Choi

This certifies that the thesis/dissertation of Bongseo Choi is approved.

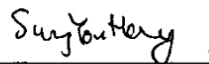
6.11.2018 of submission



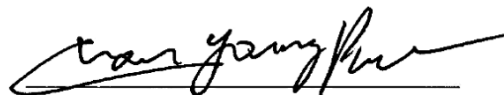
Advisor: Sebyung Kang



Seongho Ryu



Sung You Hong



Chan Young Park



Changwook Lee

Abstract

For the last decades, many of approaches including chemical drugs, therapeutic antibodies, or other reagents have been tried for the regression and the rejection of tumor development. However, the immune escape or tolerance of most tumors are the main hurdles for boosting powerful and robust adaptive immune responses against the cancer antigens. Therefore, the effective generation of antigen specific adaptive immune response is promising, but it is a challenging task for cancer immunotherapy.

In the vaccination process, recognition of non-self-structures and followed antigen presentation by antigen presenting cells, mostly dendritic cells (DCs), are essential through entire stages of adaptive immune responses. However, immunotherapeutic vaccines against the cancer are frequently ignored by the host immune system because of weak immunogenicity of vaccines. Consequently, the developments of effective delivery platforms of vaccines and/or adjuvants are required to the DC mediated adaptive responses.

To achieve the effective delivery of antigenic peptide to DCs, we established encapsulin protein cage nanoparticles as a vaccine carrier and genetically introduced antigenic OT-1 peptide derived from ovalbumin to the encapsulin monomer. In addition, their efficacy is evaluated in activation of DC-mediated antigen-specific T cell cytotoxicity and consequent melanoma tumor rejection *in vitro* and *in vivo*.

A powerful adjuvant for non-self-recognition is required for the activation of DCs to boost and maximize the vaccine efficacy. The imidazoquinoline, clinically approved TLR7 adjuvants, were multivalently conjugated to iron oxide nanoparticles for the induction of TLR mediated DC activation. Multi-step modifications of the adjuvant nanoparticles allow us stable and effective initiation of DC mediated adaptive immune responses against target cancer antigens.

Our studies are to improve the efficacy of cancer vaccine induce robust and powerful activation of DCs and to show the up-regulation of CD8⁺ cytotoxic T cell responses for tumor rejection. The approaches described here may provide opportunities to develop the novel cancer immunotherapy that manipulate the DC activation with subsequent cancer antigen-specific cytotoxicity.

Contents

Abstract	1
Contents	2
List of figures	5
Abbreviations	7
Chapter 1. Introduction	
1.1. Cancer immunotherapy	9
1.1.1. Cancer immunology	9
1.1.2. Adaptive immune responses and Dendritic cells	9
1.1.3. Cancer immunotherapy	13
1.2. Functional nanoparticles	19
1.2.1. Protein cage nanoparticles	19
1.2.2. Encapsulin protein cage nanoparticles	23
1.2.3. Inorganic nanoparticles	25
1.2.4. Iron oxide nanoparticles	25
1.3. Nanoparticle-based cancer immunotherapy	28
1.4. References	32

Chapter 2. Effective Delivery of Antigen-Encapsulin Nanoparticle Fusions to Dendritic Cells Leads to Antigen-Specific Cytotoxic T Cell Activation and Tumor Rejection

2.1. Abstract	36
2.2. Introduction	38
2.3. Materials and Methods	41
2.4. Results	45
2.5. Discussion	59
2.6. References	60

Chapter 3. Covalent Conjugation of Small-Molecule Adjuvants to Nanoparticles Induces Robust Cytotoxic T Cell Responses via DC Activation

3.1. Abstract	66
3.2. Introduction	67
3.3. Materials and Methods	68
3.4. Results	75
3.5. Discussion	83
3.6. References	84

Chapter 4. Conclusion 88

Acknowledgements 89

List of figures

Chapter 1. Introduction

Figure 1.1. Innate and Adaptive immune response	10
Figure 1.2. Pattern recognition receptors in the control of adaptive immunity	12
Figure 1.3. The cycle of cancer immunology	14
Figure 1.4. The mechanism of action of cancer vaccines	15
Figure 1.5. The generation of CAR T cells	17
Figure 1.6. The immune blockade for the elimination of tumor immune suppression	18
Figure 1.7. Space filling models of protein cage nanoparticles	20
Figure 1.8. 3D Ribbon diagrams of various ferritin protein cage nanoparticles	22
Figure 1.9. Structure of the Encapsulin from <i>T. maritima</i>	24
Figure 1.10. Schematic illustration of inorganic nanoparticles	26
Figure 1.11. Representative illustration of application of IONP	27
Figure 1.12. Antigen-specific T cell proliferations and subsequent immune responses induced by ferritin protein cage nanoparticles (FPCNs) carrying OT peptides	29
Figure 1.13. Representative study of cancer immunotherapy in combination with photothermal immune boosting of inorganic nanoparticles with immune checkpoint blockade	31

Chapter 2. Effective Delivery of Antigen-Encapsulin Nanoparticle Fusions to Dendritic Cells Leads to Antigen-Specific Cytotoxic T Cell Activation and Tumor Rejection

Figure 2.1. Schematic representation of OT-1-specific cytotoxic T cell differentiation and tumor rejection induced by OT-1-Encap-mediated prophylactic vaccinations	40
Figure 2.2. Characterization of Encap containing OT-1 peptides at the C-termini	46
Figure 2.3. OT-1 peptides delivered to DCs by OT-1-Encap variants induce OT-1 specific CD8 ⁺ T cell proliferation <i>in vivo</i> and <i>in vitro</i>	48
Figure 2.4. OT-1 peptides delivered to DCs by OT-1-Encap-C induce the differentiation of functional effector CD8 ⁺ T cells in spleens	51
Figure 2.5. Prophylactic vaccination with OT-1-Encap-C suppressed B16-OVA tumor growth	53
Figure 2.6. Therapeutic vaccination with OT-1-Encap-C suppressed B16-OVA tumor growth	57

**Chapter 3. Covalent Conjugation of Small-Molecule Adjuvants to Nanoparticles
 Induces Robust Cytotoxic T Cell Responses via DC Activation**

Figure 3.1. General attributes of Adjuvant-NPs in inducing DC activation and a robust CTL response 69

Figure 3.2. Synthetic scheme of Adjuvant-NPs 76

Figure 3.3. Characterization of Adjuvant-NPs 78

Figure 3.4. Adjuvant effects on *in vivo* DC activation 79

Figure 3.5. Fluorescence imaging studies to examine the internalization of Fluorescein-Adjuvant-NPs
 in DCs 81

Figure 3.6. *In vivo* CTL assay on splenocytes 82

Figure 3.S1. Synthesis of Fluorescein-Adjuvant-NPs 71

Figure 3.S2. A calibration curve of NHS fluorescein 73

Abbreviations

MHC: major histocompatibility class
APC : antigen presenting cell
DC : dendritic cells
CD : cluster of differentiation
IFN- γ : interferon gamma
CAR : chimeric antigen receptor
scFv : single-chain variable fragment
PDL1 : programmed cell death ligand 1
PD1 : programmed cell death 1
CTLA4 : cytotoxic T lymphocyte-associated protein
Treg : regulatory T cells
PEG : polyethylene glycol
GNP : gold nanoparticle
IONPs : iron oxide nanoparticle
VLPs : virus like particles
sHsp : small heat shock protein
NDDS : nanoparticle based drug delivery system
HBV : hepatitis B virus
HBsAg : hepatitis B virus surface antigen
MRI : magnetic resonance imaging
PLGA : poly(lactic-co-glycolic acid)
QD : quantum dot
SPION : superparamagnetic iron oxide nanoparticle
Alum : aluminum salts
PRR : pattern recognition receptor
PAMP : pathogen associated molecular pattern
TLR : Toll-like receptor
CpG ODN : CpG oligodeoxynucleotides
OVA : ovalbumine
TIL : tumor infiltrating lymphocyte
PE : phycoerythrin
TEM : transmission electron micrographic
CTL : cytotoxic T lymphocyte

CFSE : carboxyfluorescein diacetate succinimidyl ester

NP : nanoparticle

DLS : dynamic light scattering

SFP : specific pathogen-free

SDS-PAGE : sodium dodecyl sulfate polyacrylamide gel electrophoresis

1. Introduction

1.1 Cancer immunotherapy

1.1.1 Cancer immunology

The loss of normal cellular characteristics by numerous genetic and epigenetic alterations generates the cancer cells with obtained immortality. In this procedure, neoantigen, which could bound to major histocompatibility class I (MHC I) of antigen presenting cells (APCs) like dendritic cells (DCs), macrophages or B cells for further adaptive immune responses.¹ Even though these neoantigens are suitable for the immunogenicity for antigen specific cancer cytotoxicity for tumor rejection, unusual physiology of cancer cells evades recognition and consequent immune tolerance, including systemic evasion of T cell responses.² Furthermore, in case of cancer elimination by the host immune system, these completion signals may induce immune editing, resulting in the selective growth of less immunogenic and more cancerous cells with the assist of tumor microenvironment.³ These cells gained the survival advantages to develop the solid tumor for accelerate the growth and progress of selected dominant cancer cells. Finally, local immune systems assist the tumor formation, known as an escape stage by the reduction of anticancer response.³⁻⁴

1.1.2 Adaptive immune responses and Dendritic cells

Immune systems are categorized into innate immune response and adaptive immune response and collaboration of immune responses are important to eliminate the cancer cells. Innate immunity related cells including DC, macrophage, nature killer(NK) cells, leukocytes, granulocytes and other related cells recognize and kills the non-self or impaired cells without antigen specificity. Additionally, APCs bridging innate immune response and adaptive immune response by education of antigen specificity to naïve T cells and naïve B cells. Educated T cells differentiated into diverse types of T cell subsets, CD4⁺ helper T cells deliver the antigen specificities to B cells for antibody production and CD8⁺ T cells are directly kills the target cells with exceptional affinity. The most potent antigen presenting cells DCs harmonize this process to control

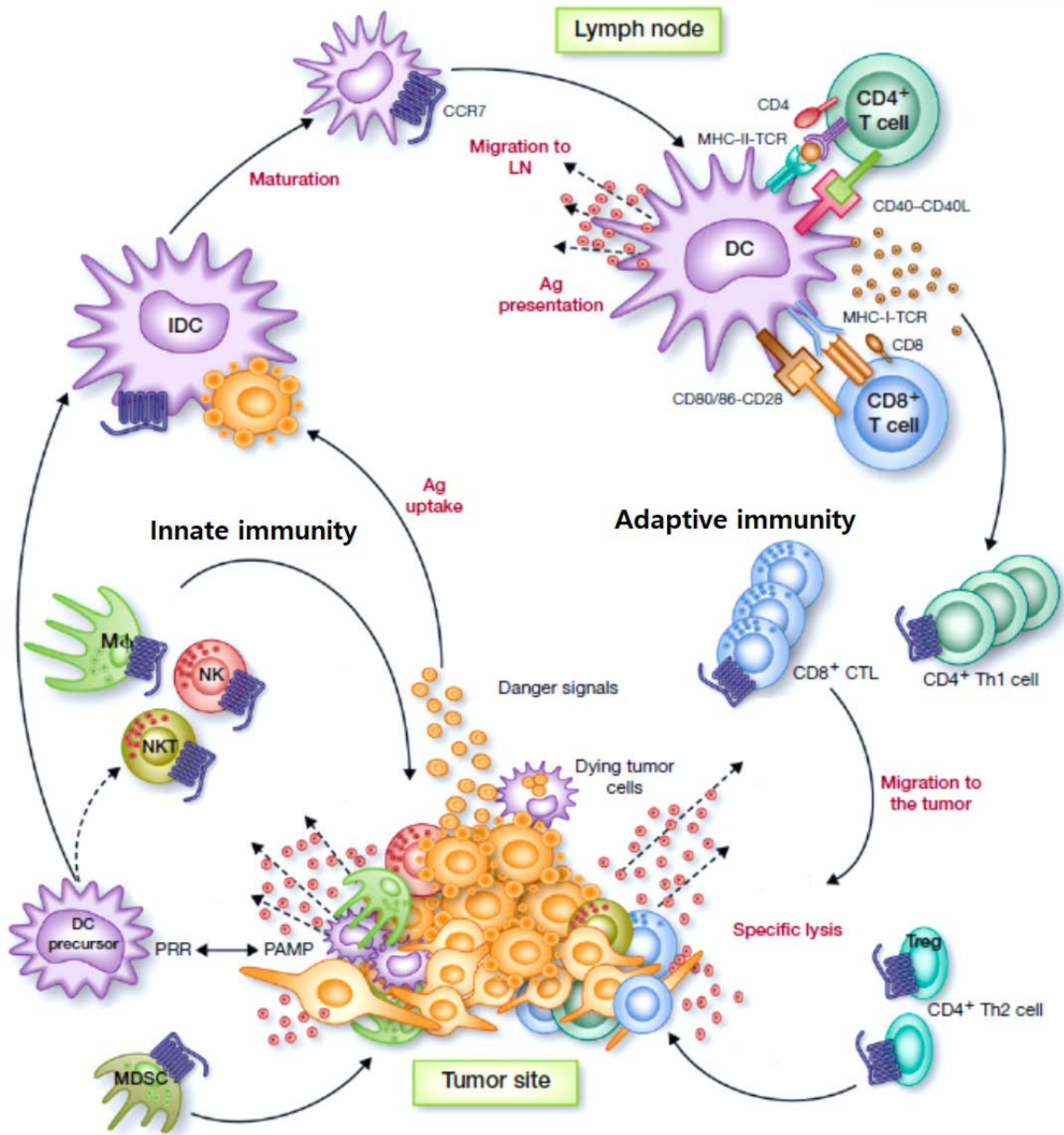


Figure 1.1 Innate and Adaptive immune response

adaptive immune response. Immature DCs are specialized to phagocytosis of non-self or impaired cells, then, they process them and present the immunogenic epitopes to their surface with MHC combined structure. DCs are matured under the interaction of costimulatory molecules and appropriate condition of cytokines. Then, matured DCs migrated into secondary lymphoid organs to educate antigen specific naïve T cells to functionally activated T cell subsets. Educated T cells are differentiated to diverse types of T cells against the antigens with clonal expansion. Consequently, cancer antigen specific cytotoxic CD8⁺ T cells are produced and directly suppress the tumor survival and the formation of tumor microenvironment by the direct killing of tumor cells with of pro-inflammatory cytokine production such as interferon gamma (IFN- γ) (Figure 1.1).⁴⁻⁶

In the initiation of adaptive immune responses, adequate and a powerful role of adjuvants are essential for recognition of outer organisms or impaired self-cells, such as cancer. These signals promoting the effective antigen processing are presented in the vaccine development. Aluminum salts (Alum) were first introduced as vaccine adjuvants and remains the most widely used adjuvant because of their clinical safety and effectiveness. However, alum is not sufficiently immunogenic and preferentially promotes Th2 type responses, which does not efficiently induce cytotoxic T cell responses for viruses and self-antigen derived disease such as neurodegenerative disease or cancer.⁷

Usually, most of the adjuvants decided from constant structural patterns from the organisms to distinguish the self and non-self. Lipopolysaccharides, single-stranded RNA, and bacterial DNA motifs are well studied adjuvants and they have specific pathogen associated molecular patterns (PAMPs) differ from the host. Pattern recognition receptors (PRRs) have specific affinity to PAMPs expressed in the APCs, epithelial cells or fibroblasts for inducing signal transductions of related immune responses. This activation signal facilitates the local innate immune responses and followed antigen specific T cells for adaptive immune responses by the maturation of APCs, DCs, representatively (Figure 1.2).⁸⁻⁹

Due to the constant needs of novel adjuvant and the discovery of PRRs matched with PAMPs, researches on PRRs are an ongoing subject for cancer immunotherapy. Toll-like receptor (TLR) ligands are known to be the most potent and defined PRRs for induction of the innate to adaptive immune response. Moreover, agonists of TLRs have been evaluated as potential adjuvants in vaccine development.

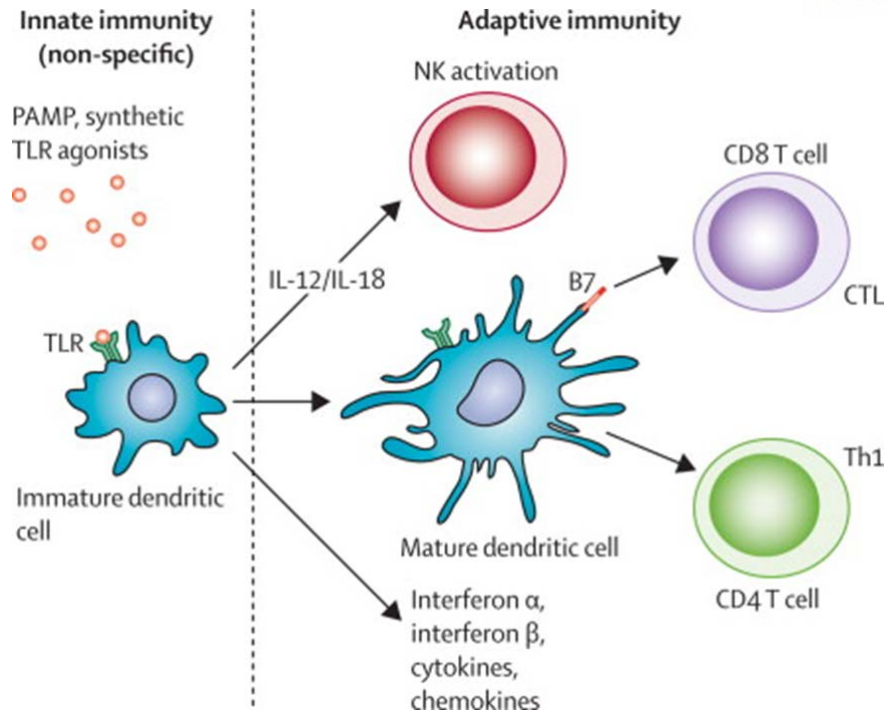


Figure 1.2 Pattern recognition receptors in the control of adaptive immunity

1.1.3 Cancer immunotherapy

Cancer immunotherapy is known to be a new generation of cancer treatment by immunizing the cancer antigens to the host immune system. The beginning of cancer immunotherapy is started with *ex vivo* adoptive cell transfer of cancer antigen specific DCs or T cells to patients. Considerable successes in clinical trials are reported and discovery of cancer associated antigens is one of the key issues for cancer immunotherapy. The heterogeneity of cancer antigens, neoantigens, guides the variance of immune responses against the cancer cells by oncogenesis. Released proteins are primarily recognized by local fibroblasts, neuroendocrine cells, adipose cells and secretion of the cytokines for upregulation and infiltration of DCs for processing. Epitopes of processed neoantigens are presented on the MHC molecules for T cell education following the generation of functional cytotoxic T cells and infiltration to local tumor sites for tumor rejection (Figure 1.3).²

However, cancer immunity cycles sometimes explicit the impaired immune responses because of poor detection of cancer antigens caused by immune editing of cancer cells, so called, “immune tolerance”. They can prevent antigen presentation and the establishment of tumor antigen-specific immune responses through a variety of mechanisms. By switching the differentiation of APCs, preventing the antigen processing and presentation, interfering the DC maturation. Paradoxically, DCs induce the survival and clonogenicity of cancer cells by secretion of pro-angiogenic cytokines.

Therefore, developing the effective and powerful vaccination methods against the cancer antigens for the education of functional cytotoxic CD8⁺ T cells are required for amplification of immune surveillance resulting in tumor rejection and induction of related memory cells for permanent immune responses to cancer antigen.

To achieve this, the most crucial step is priming the antigens to DCs for antigens presentation. Conventionally, *ex vivo* priming of cancer antigens to immature DCs from patients to obtain antigen specific maturation of DCs, and then re-infusing the primed cells back into the host for the cancer antigen specific adaptive immune responses. For improving the efficiency and durability of DC mediated cancer immunotherapy, cancer vaccine development must be configured to elicit cancer antigen-specific CD8⁺ T cell-mediated immune responses for tumor regression and/or rejection. Ultimately, induced CD8⁺ T cells should be shown the high avidity toward antigen–MHC I complex on tumor cells, which could enter the tumor microenvironment to overcome immune ignorance (Figure 1.4).¹⁰⁻¹¹

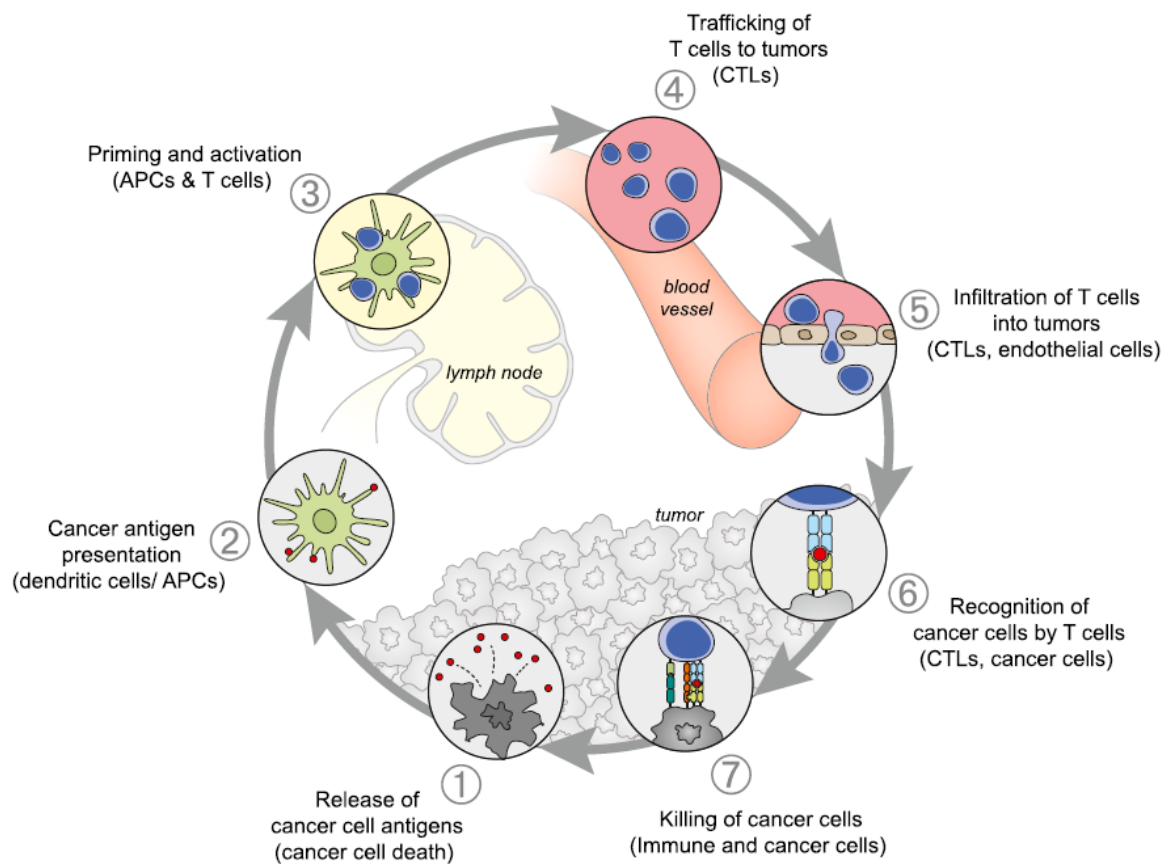


Figure 1.3 The cycle of cancer immunology.

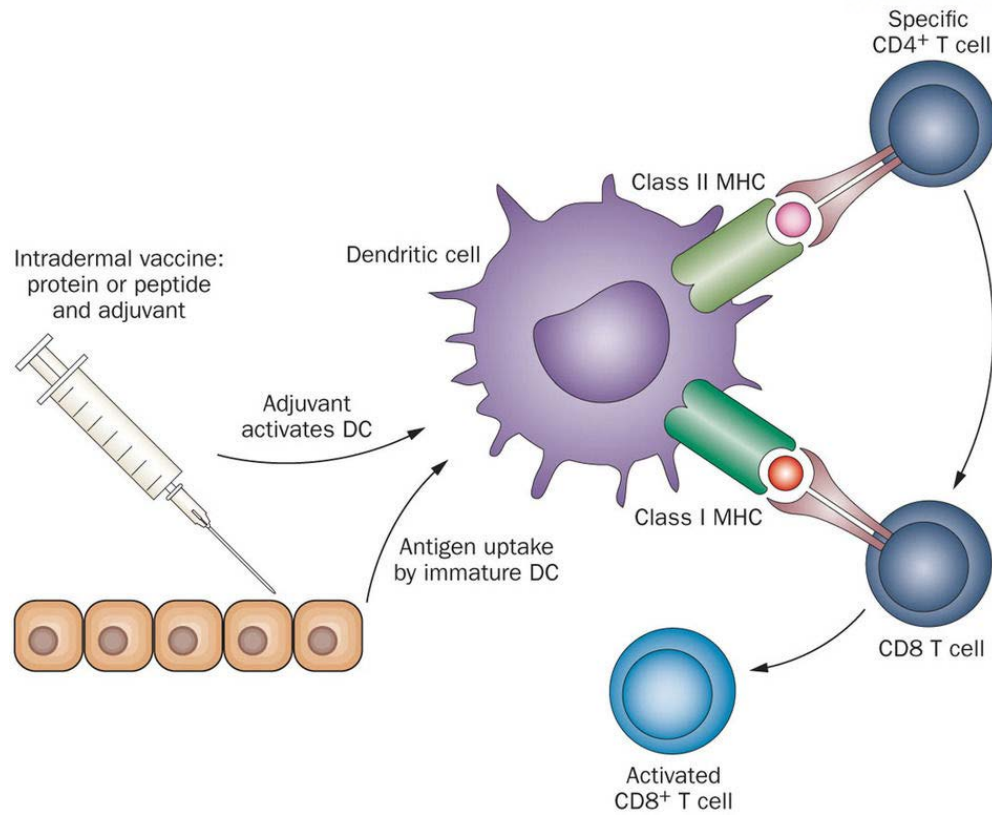
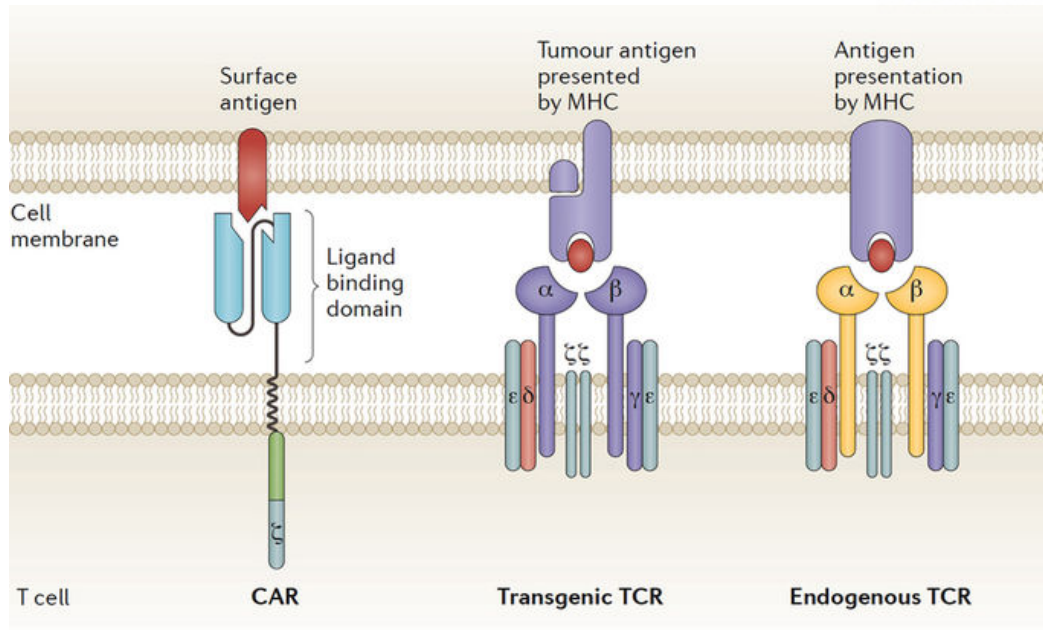


Figure 1.4 The mechanism of action of cancer vaccines.

Other approaches for efficient and powerful induction of cancer specific immune response are direct mutation of T cell receptor (TCR) for biased adaptive immune response or to control the immune checkpoint for up-regulating cancer specific adaptive immune response.

The chimeric antigen receptor (CAR) T cells are developed to obtain forced antigen specificities without antigen presentation of DCs and shown remarkable efficiencies in blood cancers. The single-chain variable fragment (scFv) of immunoglobulin specific to cancer antigens are genetically manipulated into naïve T cells. TCRs are modified with various genetic carriers like transfection. Additionally, CAR T cells can manipulate the other receptors associated with adaptive immune response, such chemoattractant like IL-7 or CCL19 are able to insert at once for enhanced cancer immunotherapy. However, there are still other approaches ongoing due to the limitations in time, cost and labor (Figure 1.5).¹²⁻¹³

Unlike other cancer immunotherapies which are focusing on the development of antigen specific adaptive immune responses, the immune checkpoint blockade focuses on the interfere the mechanisms of anti-immune responses by blocking of immune checkpoint, programmed cell death ligand 1/programmed cell death protein 1 (PDL1/PD1) or cytotoxic T lymphocyte-associated protein 4 (CTLA4). The immune evasion systems of tumor microenvironment induce the immune tolerance by expression of PDL1, the coinhibitory molecules for the PD1 inhibitory receptors expressed on the regulatory T cells (Tregs). Otherwise, CTLA4 receptor expressed on the T cells are for B7 costimulatory molecules of DCs. CTLA4 expression of T cells specifically bound to B7 costimulatory molecules of matured DCs causes the inactivation of T cells. By utilizing the specific antibodies as immune checkpoint blockade, competed inactivation of PDL1/PD1 or CTLA4/ B7 interaction, immune evasion mechanisms no longer interfere the adaptive immune responses and induce subsequent cancer clearance. Along with numerous preclinical and clinical tests are ongoing to develop commercial cancer immunotherapeutic, combination of immune checkpoint blockade and immune boosting agents or vaccines are co-treated for exaggeration of the anti-cancer effect (Figure 1.6).^{4, 14-20}



Nature Reviews | Drug Discovery

Figure 1.5 The generation of CAR T cells. Most transgenic engineered TCRs need to be formed cognate interaction with the antigen loaded DCs. However, CARs only need to be recognized the antigens of cancer cell for adaptive immune responses.

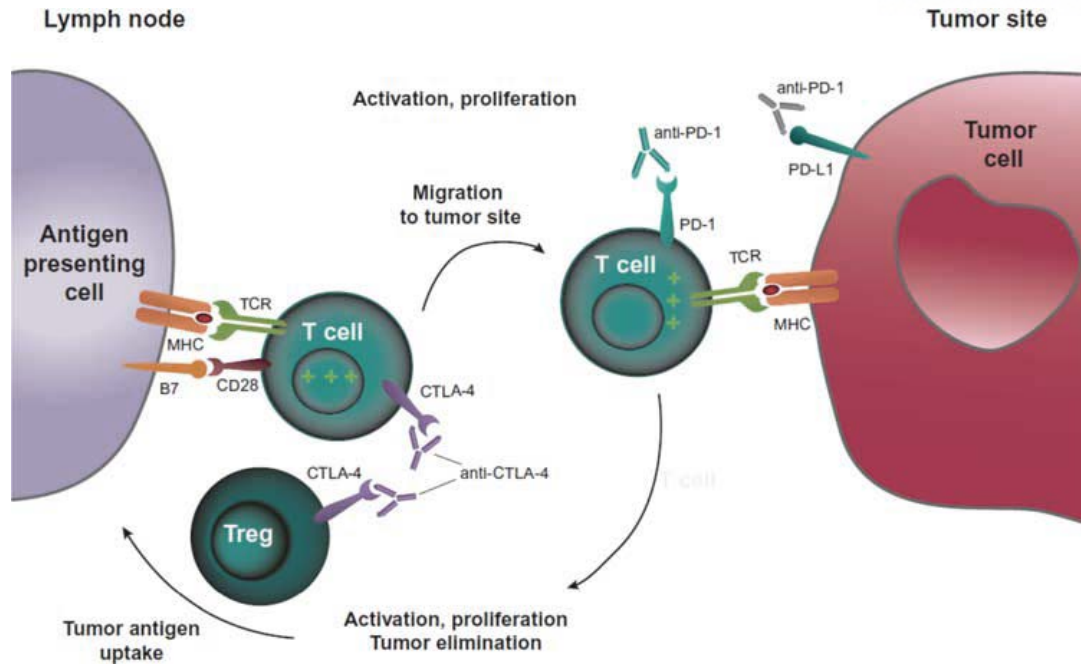


Figure 1.6 CTLA4 and PD1/PDL1, The immune blockade for the elimination of tumor immune suppression.

1.2 Functional Nanoparticles

1.2.1 Protein cage nanoparticle

In the last decades, the development for medical application of nanotechnology has been focused on the field of drug and vaccine delivery. Numerous types of nano-meter-sized carriers are developed and applied in the improvements of cargo delivery. For example, inorganic nanoparticles based on polyethylene glycol (PEG), gold nanoparticles (GNPs), iron oxide nanoparticles (IONPs), dextran and lipid are the most common and established tools due to simple formation and loading. However, poor biocompatibility, biodegradability are the challenging parts to overcome with toxicity for bioapplication.¹⁰

Protein cage nanoparticles are originated from naturally synthesized proteins, and they are utilized as a new delivery system with exceptional biocompatibilities, uniform size, stability and other potentials for both biomedical and material application. Virus like particles (VLPs), collagen, albumin-based and monomer-based nanoparticles are representative and well-established candidates. Recently, protein cage nanoparticles, such as VLPs, ferritin, small heat shock protein (sHsp), Lumazine synthase and encapsulin have been focused because of their appropriate characteristics as carriers like well-defined spherical architecture and accessible biochemical and genetical modification (Figure 1.7). Therefore, nanoparticles derived from natural proteins are affordable for precise incorporation of extra drugs or vaccines through genetic or chemical modifications based on atomic resolution crystal structures. The genetic and chemical modification of the exterior surface or the interior cavity of a protein cage structure allows the site-specific attachment and presentation of several types of molecules including affinity tags, antibodies, fluorophores, carbohydrates, nucleic acids, and targeting peptides. These multivalent functions can be decorated on the interior or the exterior of monomers by labeling with two different reagents sequentially or by an assembly of pre-functionalized subunits in controlled ratios.²¹⁻²³

Nanoparticle based drug delivery systems (NDDSs) are well established and are developing approaches to elevate drug efficiency and longevity in harsh *in vivo* condition. The appropriate size under 100 nm, biocompatibility and surface charge can be controlled by genetic or chemical modifications. Moreover, protein cage nanoparticles can carry a variety of therapeutic and diagnostic agents in a controlled manner. Also, these NDDSs control the drug toxicity by the encapsulation, providing

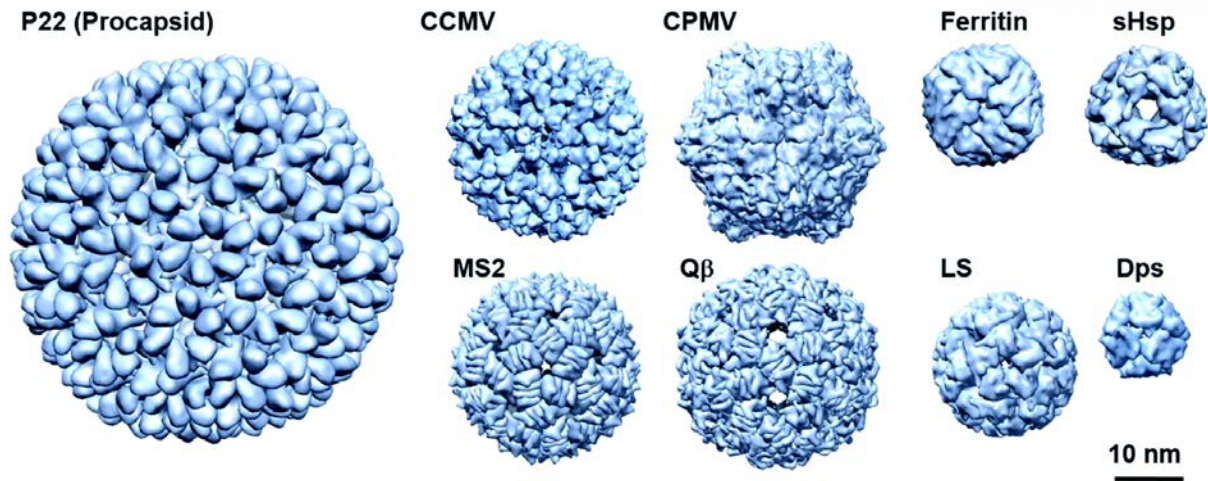


Figure 1.7 Space filling models of protein cage nanoparticles.

wide range of pharmacokinetics pool. Affinity tag such as antibodies, aptamer or affibody conjugated targeting moiety modified NDDS is available for site-specific delivery drug molecules and prolonged reside time to increase the cellular uptake.

Representatively, Ferritins are iron storage proteins found in almost all living organisms from bacteria to animals and studied as an iron supplement for patients with related diseases.²⁴ However, because of their exceptional encapsulating ability and unique characteristics of protein cage nanoparticles, ferritin utilized as a model nanoscale delivery platform. Ferritin isolated from the *Pyrococcus furiosus* is suitable for the bio-application because of the well-defined spherical structure with inner and outer diameters of 8 and 12 nm, respectively, and 24 copies of identical 20 kDa monomers self-assembled easily and accurately, which can be utilized for genetic modifications and chemical bioconjugations.

Recently, ferritin protein cage nanoparticles are utilized as multifunctional protein cage-based delivery nanoplatform, which can hold the cargo molecule inside securely with targeting moiety, and then, artificially release drugs to the targeted cells.²⁵⁻²⁷ Introducing the RGD peptide to ferritin subunits for targeting the cell adhesion molecules of extracellular matrix was used to encapsulate doxorubicin (Dox) and, by using their metal-affinity, Pt-based drugs, cisplatin are loaded and then delivered them to the target sites (Figure 1.8).²⁸

Additionally, various targeting moieties including antibodies added to the surface of ferritin for the targeted delivery.²⁹ Antibodies are practically utilized as ideal moieties for targeted delivery of therapeutics and/or diagnostics because of their high affinity and specificity. Engineered Fc-binding peptides (FcBP) originated from receptor of antibody Fc region were genetically introduced onto the surface of ferritin to capture antibodies without additional alteration of the targeting capability.³⁰ Specific antibodies are decorated on to the FcBP-presenting ferritin and formed stable non-covalent complexes against the HER2 or anti-folate receptor. The specific targeting of ferritin drug conjugates to HER2 expressing breast cancer cells or folate receptor over-expressing cells were respectively demonstrated.³⁰

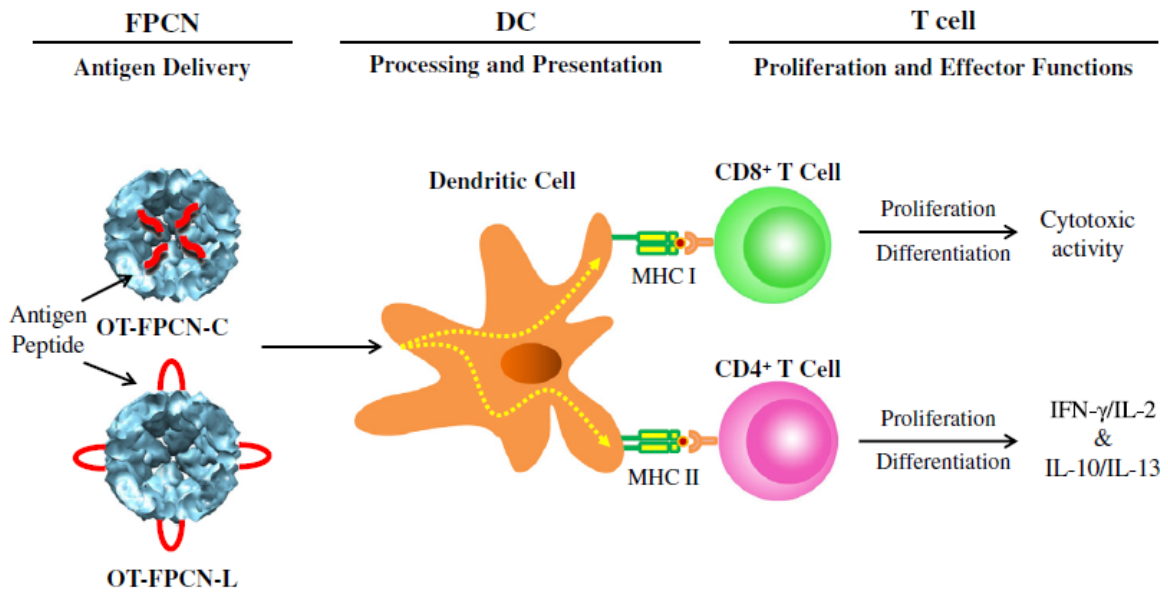


Figure 1.8 Antigen-specific T cell proliferations and subsequent immune responses induced by ferritin protein cage nanoparticles (FPCNs) carrying OT peptides.

1.2.2 Encapsulin protein cage nanoparticles

The first discovered encapsulin protein cage nanoparticle is originated from the cultured supernatant of *Brevibacterium linens*, which suppresses the bacterial activity of other bacterial strains. Also, *Mycobacterium tuberculosis* and *Thermotoga maritima* reported to express a kind of encapsulin without bacteriostatic or proteolytic activity and genomic DNA. Monomers are automatically assembled into icosahedral structure of Encapsulin. There are two structures of encapsulins that are reported for now. a T = 1 icosahedral symmetric Encapsulins of *T. maritima*, *M. tuberculosis* and *Rhodococcus erythropolis/jostii* are composed of 60 monomers, and the 180 monomers self-assembled T = 3 icosahedral encapsulins from *Pyrococcus furiosus* and *Myxococcus xanthus*. Based on the crystal structure of encapsulin protein cage nanoparticles, encapsulin is capable of encapsulate the foreign proteins into the internal cavity which remained their structures with biocompatibility (Figure 1.9). In addition, chemical or genetic addition of appropriate functional moieties on the external surface, encapsulin has the potential to package target proteins in its internal cavity and/or display them on its external surface for further extended delivery system.³¹⁻³⁴

SP94-peptides were presented on the exterior surface of engineered encapsulin through either chemical conjugation or genetic insertion and SP94-encapsulin exhibited specific binding capability to hepatocellular carcinoma cells, HepG2, and an ability to carry imaging probes or prodrug molecules³⁵. In a similar approach, FcBP was introduced onto the surface loop region of encapsulin and FcBP-displaying encapsulin was demonstrated to selectively recognize and specifically bind to squamous cell carcinoma 7 (SCC-7) cells, which overexpress a cell surface glycoprotein CD44 involved in cell-cell interactions, cell adhesion and migration, over HeLa, HepG2, MDA-MB-231 and KB cells³⁶.

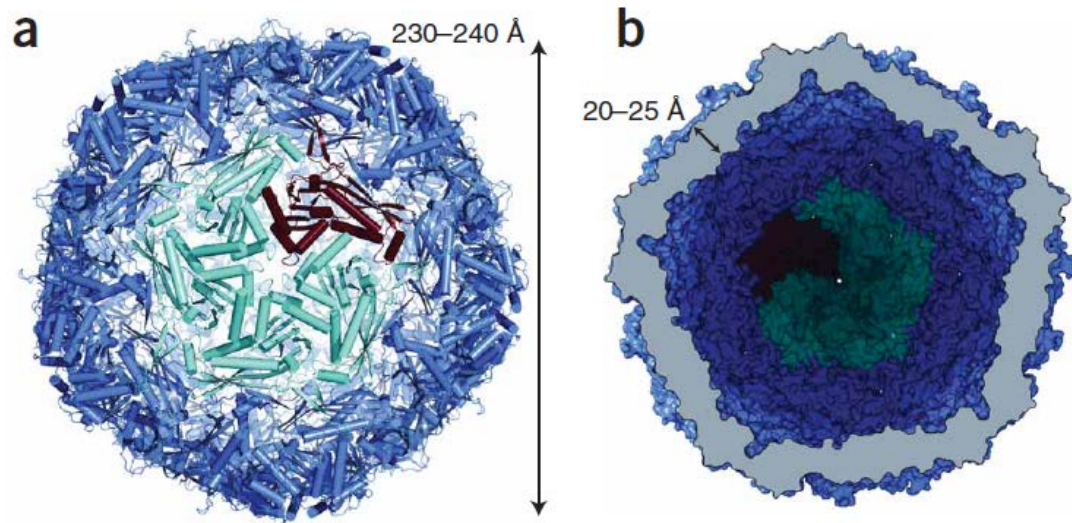


Figure 1.9 Structure of the Encapsulin from *T. maritima*.

1.2.3 Inorganic nanoparticles

Even though numerous efforts and funds are invested for conquering cancer, current therapeutics against the cancer are still based on the radiation, chemical reagents and surgical removal of tumors. However, for the last decades, application of nanotechnology into cancer immunotherapy is significantly developed and lots of clinical trials such as magnetic resonance imaging (MRI), photodynamic therapy and drug delivery. Particularly, inorganic nanoparticles have advantages in synthesis, formation, modification by chemical conjugation chemistry.³⁷

There is a lot of other inorganic nanoparticles including poly(lactic-co-glycolic acid) (PLGA), PEG, quantum dot (QD), etc. Gold nanoparticles have been utilized as foreign drug carrier, which have exceptional affinity to thiol and amine residues for easy modification of therapeutics or biomolecules for biocompatibility (Figure 1.10). Also, their unique photodynamic ability allows site directed drug release and photothermal therapy of solid tumors, and another well-organized biocompatible nanoparticle is composed of iron oxide. These common nanoparticles have inexpensive, low-toxic and magnetized function for bio-application and diagnosis like a MRI. Magnetite(Fe_3O_4) is well-characterized source of iron oxide nanoparticle formation(IONP)³⁷⁻³⁹

1.2.4 Iron oxide nanoparticles

Iron oxides are very common source of iron in nature, with magnetite (Fe_3O_4), maghemite ($\gamma\text{-Fe}_2\text{O}_3$), and hematite ($\alpha\text{-Fe}_2\text{O}_3$) which are all unique characteristics of each iron oxides for industrial and medical application. Especially, the applications of IONP are focused as MRI contrast agents and drug vehicles for cancer therapeutics in the last decades. Also, IONP composed of magnetite and maghemite shows low toxicity *in vivo* application for biomedical applications because of their biocompatibility. Establish of stable IONP in physiological condition accelerate the application of biological and medical treatment. SPIONs, magnetized IONP with an external magnetic field utilized in local trafficking of certain drugs to the target organs or cells. This approach minimizes the side effects of drugs and local resident times for prolonging the drug efficiency. Furthermore, the surfaces of nanoparticles are capable to functionalize the additional modification with therapeutics (Figure1.11).³⁸⁻⁴³

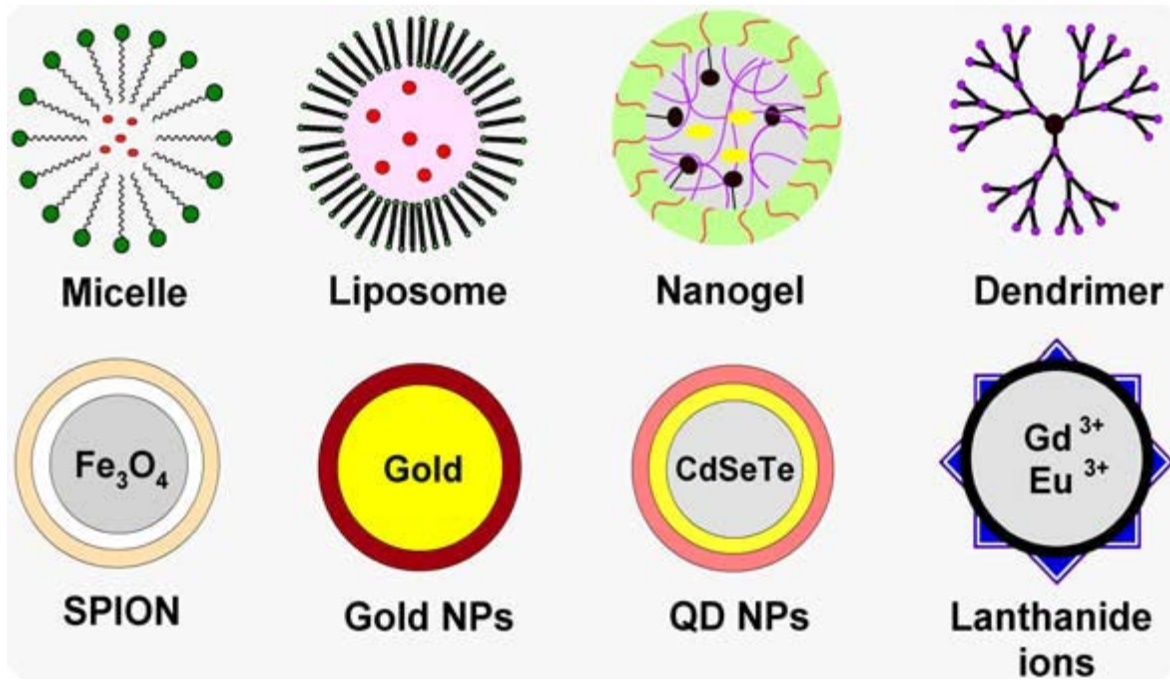


Figure 1.10 Schematic illustration of inorganic nanoparticles.

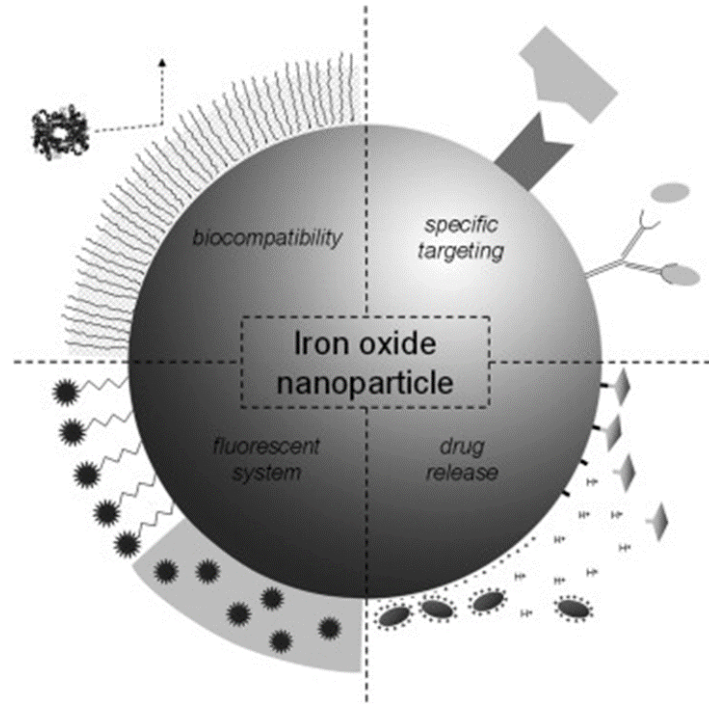


Figure 1.11 Representative illustration of application of IONP. IONP are biofunctionalized with oleic acid and water-soluble ligands are exchanged with oleic acid in water solution.

1.3 Nanoparticle-based cancer immunotherapy

For the development of vaccination history, traditional vaccines including live attenuated or killed microbes were the universal vaccine type to vaccinate infectious disease. Even though attenuated vaccines show powerful vaccination, some types of vaccines against diseases do not induce enough immune responses. Also, live attenuated vaccines still have a chance to infect patient according to the host immune condition. Subunit vaccines isolated antigenic proteins, polysaccharides or DNA from the part of attenuated or inactivated vaccines have benefits from improved safety dramatically as alternative. Although they have lots of advantages, subunit vaccines applied with alum-based adjuvant to overcome their limited vaccine capability, immunogenicity and longevity. On the other hand, these methods sometimes induce local reactions and may fail to generate adaptive immune responses. Therefore, there is a great need to develop novel adjuvants and delivery systems for the next generation of vaccines.^{10, 44}

Vaccine loading to protein cages VLPs originated from viral capsids are primary approaches to deliver the antigenic subunit vaccine to host the immune system. Self-assembling rod-shaped particles composed from protein capsid extracted from the tobacco mosaic virus, which did not contain genetic material, is first introduced in 1950s. A few decades later, Hepatitis B virus (HBV) surface antigen (HBsAg) was purified from infected human serum and discovered their spherical structure of protein nanoparticles without nucleic acid. VLPs effectively crosslink innate and adaptive immunity with intrinsic immunological characteristics by their self-adjuvating properties. However, VLPs originated from viral capsid have chances for recognition of antigenic epitopes and induce an immune response resulting that neutralization by antibodies. Even though VLPs are still promising in many fields, these approaches are not suitable for non-pathogen-derived diseases, such as cancers, rheumatis arthritis and Alzheimer disease. Therefore, non-VLP-originated protein cage nanoparticles may have alternatives and breakthroughs.⁴⁵

Well established drug carrier, ferritin, encapsulin protein cage nanoparticle demonstrated that antigenic peptides could be displayed internal or exterior cavity and efficiently delivered to DCs, leading to efficient activation of antigen specific immune responses against self-originated diseases. Genetically introducing model antigenic peptides, OT-1 (SIINFEKL), into the interior cavity or onto the exterior surface OT-1 (SIINFEKL) into the interior cavity or onto the exterior surface of FPCN-(OTs-FPCN). The high stability of peptide loaded FPCN offers the possibility as carrier of several types of antigenic peptides or small protein

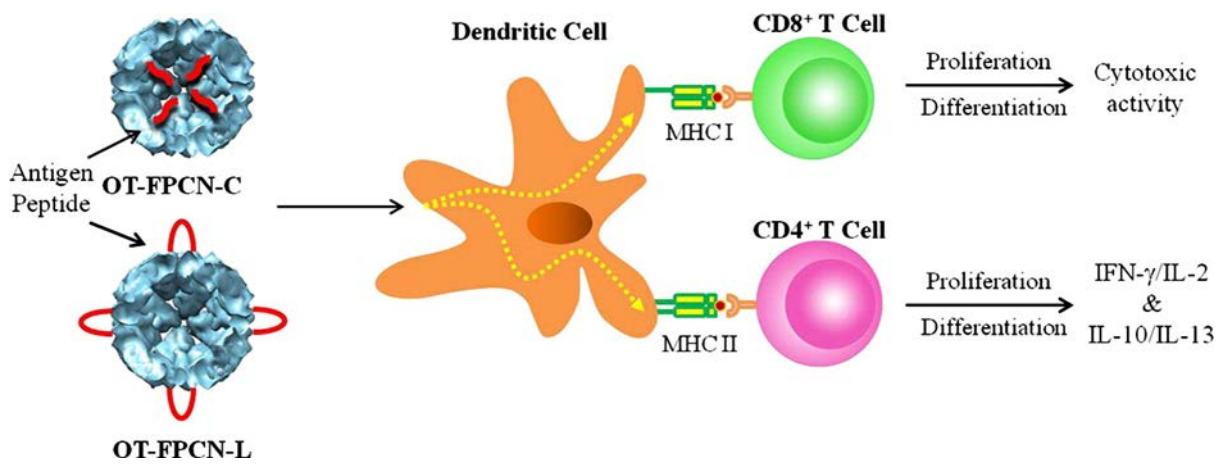


Figure 1.12 Antigen-specific T cell proliferations and subsequent immune responses induced by ferritin protein cage nanoparticles (FPCNs) carrying OT peptides.

antigens. All kinds of introduced FPCN derivatives carrying antigenic peptides of ovalbumin were efficiently phagocytosed and processed by specialized antigen presenting cells, DCs. Processed OT-1 and OT-2 peptides within endosomes were successfully presented on the surface of DCs and induced proper adaptive immune responses at low dosages of OTs-FPCNs except OT-FPCN-L *in vitro* and *in vivo* setting. The positions and configurations of antigenic peptides or proteins should be taken care of prior to the insertion for *in vivo* application (Figure 1.12.).^{25-26, 46}

Recently, the application of the adjuvants on the nanoparticles have been studied for enhancing the adjuvant effect by multivalence and affinity to APCs.⁴⁷ Primary adjuvant-protein cage nanoparticles are established by VLPs due to their origin, which basically have high immunogenicity and many accessible PAMPs as adjuvants. However, adjuvants of VLPs, originated from nucleic acids, can accidentally occur unwanted diseases. So, controlled and safe protein cage nanoparticles was developed independently from VLPs. Due to the nanoparticles' multivalence and polyvalence, one nanoparticle can carrying one or more functional moieties at once. Moreover, well-organized nanoparticles can be genetically or chemically modified with subunit vaccine and adjuvant like CpG. Multivalent decoration could promote immunogenicity of vaccines for adaptive immune responses against the target antigens with antigen cross-presentation (Figure1.13).⁴⁷⁻⁴⁸

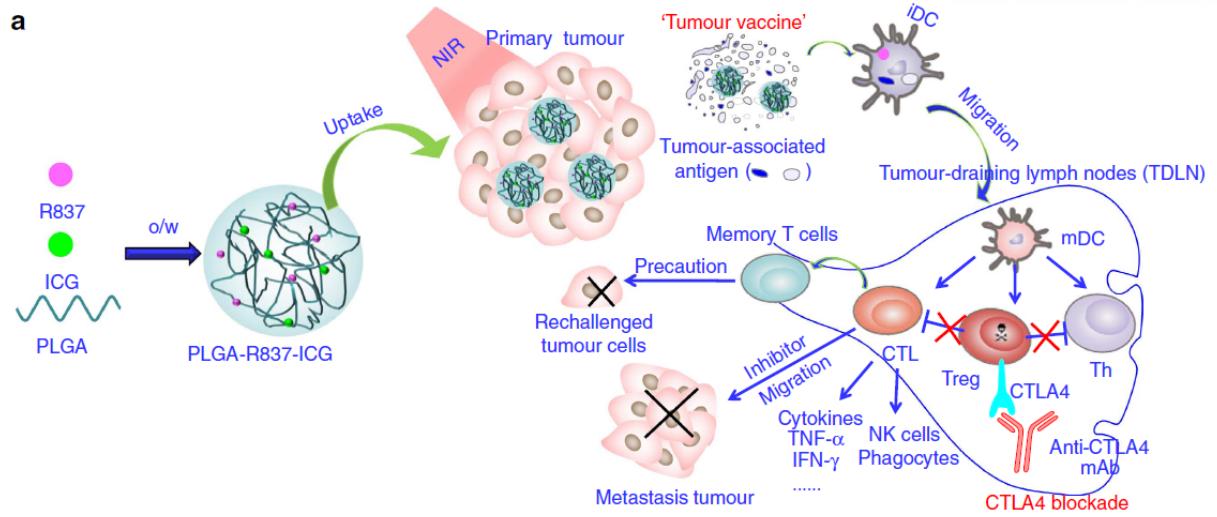


Figure 1.13 Representative study of cancer immunotherapy in combination with photothermal immune boosting of inorganic nanoparticles with immune checkpoint blockade.

1.4 References

1. Palucka, K.; Banchereau, J., Cancer immunotherapy via dendritic cells. *Nat Rev Cancer* 2012, 12 (4), 265-77.
2. Chen, D. S.; Mellman, I., Oncology meets immunology: the cancer-immunity cycle. *Immunity* 2013, 39 (1), 1-10.
3. Wang, M.; Zhao, J.; Zhang, L.; Wei, F.; Lian, Y.; Wu, Y.; Gong, Z.; Zhang, S.; Zhou, J.; Cao, K.; Li, X.; Xiong, W.; Li, G.; Zeng, Z.; Guo, C., Role of tumor microenvironment in tumorigenesis. *J Cancer* 2017, 8 (5), 761-773.
4. Vesely, M. D.; Kershaw, M. H.; Schreiber, R. D.; Smyth, M. J., Natural innate and adaptive immunity to cancer. *Annu Rev Immunol* 2011, 29, 235-71.
5. Dranoff, G., Cytokines in cancer pathogenesis and cancer therapy. *Nat Rev Cancer* 2004, 4 (1), 11-22.
6. Franciszkiwicz, K.; Boissonnas, A.; Boutet, M.; Combadiere, C.; Mami-Chouaib, F., Role of chemokines and chemokine receptors in shaping the effector phase of the antitumor immune response. *Cancer Res* 2012, 72 (24), 6325-32.
7. Ilyinskii, P. O.; Roy, C. J.; O'Neil, C. P.; Browning, E. A.; Pittet, L. A.; Altreuter, D. H.; Alexis, F.; Tonti, E.; Shi, J.; Basto, P. A.; Iannaccone, M.; Radovic-Moreno, A. F.; Langer, R. S.; Farokhzad, O. C.; von Andrian, U. H.; Johnston, L. P. M.; Kishimoto, T. K., Adjuvant-carrying synthetic vaccine particles augment the immune response to encapsulated antigen and exhibit strong local immune activation without inducing systemic cytokine release. *Vaccine* 2014, 32 (24), 2882-2895.
8. Medzhitov, R., Toll-like receptors and innate immunity. *Nat Rev Immunol* 2001, 1 (2), 135-45.
9. Palm, N. W.; Medzhitov, R., Pattern recognition receptors and control of adaptive immunity. *Immunological Reviews* 2009, 227, 221-233.
10. Rosenberg, S. A.; Yang, J. C.; Restifo, N. P., Cancer immunotherapy: moving beyond current vaccines. *Nat Med* 2004, 10 (9), 909-15.
11. Bobisse, S.; Genolet, R.; Roberti, A.; Tanyi, J. L.; Racle, J.; Stevenson, B. J.; Iseli, C.; Michel, A.; Le Bitoux, M. A.; Guillaume, P.; Schmidt, J.; Bianchi, V.; Dangaj, D.; Fenwick, C.; Derre, L.; Xenarios, I.; Michielin, O.; Romero, P.; Monos, D. S.; Zoete, V.; Gfeller, D.; Kandalaft, L. E.; Coukos, G.; Harari, A., Sensitive and frequent identification of high avidity neo-epitope specific CD8 (+) T cells in immunotherapy-naïve ovarian cancer. *Nat Commun* 2018, 9 (1), 1092.
12. Fesnak, A. D.; June, C. H.; Levine, B. L., Engineered T cells: the promise and challenges of cancer immunotherapy. *Nat Rev Cancer* 2016, 16 (9), 566-81.
13. Crossland, D. L.; Denning, W. L.; Ang, S.; Olivares, S.; Mi, T.; Switzer, K.; Singh, H.; Huls, H.; Gold, K. S.; Glisson, B. S.; Cooper, L. J.; Heymach, J. V., Antitumor activity of CD56-chimeric antigen receptor T cells in neuroblastoma and SCLC models. *Oncogene* 2018.
14. Drake, C. G.; Lipson, E. J.; Brahmer, J. R., Breathing new life into immunotherapy: review of melanoma, lung and kidney cancer. *Nat Rev Clin Oncol* 2014, 11 (1), 24-37.

15. Pardoll, D. M., The blockade of immune checkpoints in cancer immunotherapy. *Nat Rev Cancer* 2012, 12 (4), 252-64.
16. Buchbinder, E. I.; Desai, A., CTLA-4 and PD-1 Pathways: Similarities, Differences, and Implications of Their Inhibition. *Am J Clin Oncol* 2016, 39 (1), 98-106.
17. Baumeister, S. H.; Freeman, G. J.; Dranoff, G.; Sharpe, A. H., Coinhibitory Pathways in Immunotherapy for Cancer. *Annu Rev Immunol* 2016, 34, 539-73.
18. Ott, P. A., Immunotherapy: Immune-modified response criteria - an iterative learning process? *Nat Rev Clin Oncol* 2018, 15 (5), 267-268.
19. Sharpe, A. H., Introduction to checkpoint inhibitors and cancer immunotherapy. *Immunol Rev* 2017, 276 (1), 5-8.
20. Farkona, S.; Diamandis, E. P.; Blasutig, I. M., Cancer immunotherapy: the beginning of the end of cancer? *BMC Med* 2016, 14, 73.
21. Aumiller, W. M.; Uchida, M.; Douglas, T., Protein cage assembly across multiple length scales. *Chem Soc Rev* 2018.
22. Rother, M.; Nussbaumer, M. G.; Renggli, K.; Bruns, N., Protein cages and synthetic polymers: a fruitful symbiosis for drug delivery applications, bionanotechnology and materials science. *Chem Soc Rev* 2016, 45 (22), 6213-6249.
23. Uchida, M.; Kang, S.; Reichhardt, C.; Harlen, K.; Douglas, T., The ferritin superfamily: Supramolecular templates for materials synthesis. *Biochim Biophys Acta* 2010, 1800 (8), 834-45.
24. Theil, E. C.; Behera, R. K.; Tosha, T., Ferritins for Chemistry and for Life. *Coordination chemistry reviews* 2013, 257 (2), 579-586.
25. Han, J. A.; Kang, Y. J.; Shin, C.; Ra, J. S.; Shin, H. H.; Hong, S. Y.; Do, Y.; Kang, S., Ferritin protein cage nanoparticles as versatile antigen delivery nanoplatfoms for dendritic cell (DC)-based vaccine development. *Nanomed-Nanotechnol* 2014, 10 (3), 561-569.
26. Molino, N. M.; Wang, S. W., Caged protein nanoparticles for drug delivery. *Curr Opin Biotechnol* 2014, 28, 75-82.
27. Kang, Y. J.; Park, D. C.; Shin, H. H.; Park, J.; Kang, S., Incorporation of Thrombin Cleavage Peptide into a Protein Cage for Constructing a Protease-Responsive Multifunctional Delivery Nanoplatform. *Biomacromolecules* 2012, 13 (12), 4057-4064.
28. Zhen, Z.; Tang, W.; Chen, H.; Lin, X.; Todd, T.; Wang, G.; Cowger, T.; Chen, X.; Xie, J., RGD-Modified Apoferritin Nanoparticles for Efficient Drug Delivery to Tumors. *ACS Nano* 2013, 7 (6), 4830-4837.
29. Kang, Y. J.; Yang, H. J.; Jeon, S.; Kang, Y.-S.; Do, Y.; Hong, S. Y.; Kang, S., Polyvalent Display of Monosaccharides on Ferritin Protein Cage Nanoparticles for the Recognition and Binding of Cell-Surface Lectins. *Macromolecular Bioscience* 2014, 14 (5), 619-625.
30. Kang, H. J.; Kang, Y. J.; Lee, Y.-M.; Shin, H.-H.; Chung, S. J.; Kang, S., Developing an antibody-binding protein cage as a molecular recognition drug modular nanoplatfom. *Biomaterials* 2012, 33, 5423-5430.
31. Sutter, M.; Boehringer, D.; Gutmann, S.; Gunther, S.; Prangishvili, D.; Loessner, M. J.; Stetter,

- K. O.; Weber-Ban, E.; Ban, N., Structural basis of enzyme encapsulation into a bacterial nanocompartment. *Nat Struct Mol Biol* 2008, 15 (9), 939-47.
32. Moon, H.; Lee, J.; Min, J.; Kang, S., Developing Genetically Engineered Encapsulin Protein Cage Nanoparticles as a Targeted Delivery Nanoplatform. *Biomacromolecules* 2014, 15 (10), 3794-3801.
33. Giessen, T. W., Encapsulins: microbial nanocompartments with applications in biomedicine, nanobiotechnology and materials science. *Curr Opin Chem Biol* 2016, 34, 1-10.
34. Tamura, A.; Fukutani, Y.; Takami, T.; Fujii, M.; Nakaguchi, Y.; Murakami, Y.; Noguchi, K.; Yohda, M.; Odaka, M., Packaging Guest Proteins into the Encapsulin Nanocompartment from *Rhodococcus erythropolis* N771. *Biotechnol Bioeng* 2015, 112 (1), 13-20.
35. Moon, H.; Lee, J.; Min, J.; Kang, S., Developing Genetically Engineered Encapsulin Protein Cage Nanoparticles as a Targeted Delivery Nanoplatform. *Biomacromolecules* 2014, 15, 3794-3801.
36. Moon, H.; Lee, J.; Kim, H.; Heo, S.; Min, J.; Kang, S., Genetically Engineering Encapsulin Protein Cage Nanoparticle as a SCC-7 Cell Targeting Optical Nanoprobe. *Biomaterials research* 2014, 18, 21.
37. Rajabi, M.; Mousa, S. A., Lipid Nanoparticles and their Application in Nanomedicine. *Curr Pharm Biotechno* 2016, 17 (8), 662-672.
38. Gupta, A. K.; Gupta, M., Synthesis and surface engineering of iron oxide nanoparticles for biomedical applications. *Biomaterials* 2005, 26 (18), 3995-4021.
39. Teja, A. S.; Koh, P. Y., Synthesis, properties, and applications of magnetic iron oxide nanoparticles. *Prog Cryst Growth Ch* 2009, 55 (1-2), 22-45.
40. Wei, H.; Bruns, O. T.; Kaul, M. G.; Hansen, E. C.; Barch, M.; Wisniowska, A.; Chen, O.; Chen, Y.; Li, N.; Okada, S.; Cordero, J. M.; Heine, M.; Farrar, C. T.; Montana, D. M.; Adam, G.; Ittrich, H.; Jasanoff, A.; Nielsen, P.; Bawendi, M. G., Exceedingly small iron oxide nanoparticles as positive MRI contrast agents. *P Natl Acad Sci USA* 2017, 114 (9), 2325-2330.
41. Huber, D. L., Synthesis, properties, and applications of iron nanoparticles. *Small* 2005, 1 (5), 482-501.
42. Mahmoudi, M.; Sant, S.; Wang, B.; Laurent, S.; Sen, T., Superparamagnetic iron oxide nanoparticles (SPIONs): Development, surface modification and applications in chemotherapy. *Adv Drug Deliver Rev* 2011, 63 (1-2), 24-46.
43. Figuerola, A.; Di Corato, R.; Manna, L.; Pellegrino, T., From iron oxide nanoparticles towards advanced iron-based inorganic materials designed for biomedical applications. *Pharmacol Res* 2010, 62 (2), 126-43.
44. Gregory, A. E.; Titball, R.; Williamson, D., Vaccine delivery using nanoparticles. *Front Cell Infect Mi* 2013, 3.
45. Lopez-Sagasetta, J.; Malito, E.; Rappuoli, R.; Bottomley, M. J., Self-assembling protein nanoparticles in the design of vaccines. *Comput Struct Biotec* 2016, 14, 58-68.
46. Choi, B.; Moon, H.; Hong, S. J.; Shin, C.; Do, Y.; Ryu, S.; Kang, S., Effective Delivery of Antigen-Encapsulin Nanoparticle Fusions to Dendritic Cells Leads to Antigen-Specific Cytotoxic T

Cell Activation and Tumor Rejection. *Acs Nano* 2016, 10 (8), 7339-7350.

47. Chen, Q.; Xu, L. G.; Liang, C.; Wang, C.; Peng, R.; Liu, Z., Photothermal therapy with immune-adjuvant nanoparticles together with checkpoint blockade for effective cancer immunotherapy. *Nat. Comm.* 2016, 7.

48. Wilson, J. T.; Keller, S.; Manganiello, M. J.; Cheng, C.; Lee, C. C.; Opara, C.; Convertine, A.; Stayton, P. S., pH-Responsive Nanoparticle Vaccines for Dual-Delivery of Antigens and Immunostimulatory Oligonucleotides. *Acs Nano* 2013, 7 (5), 3912-3925.

2. Effective Delivery of Antigen-Encapsulin Nanoparticle Fusions to Dendritic Cells Leads to Antigen-Specific Cytotoxic T Cell Activation and Tumor Rejection

2.1 Abstract

In cancer immunotherapy, robust and efficient activation of cytotoxic CD8⁺ T cell immune responses is a promising, but challenging task. Dendritic cells (DCs) are well-known professional antigen presenting cells (APCs) that initiate and regulate antigen-specific cytotoxic CD8⁺ T cells that kill their target cells directly as well as secrete IFN- γ , a cytokine critical in tumor rejection. Here, we employed recently established protein cage nanoparticles, encapsulin (Encap), as antigenic peptide nanocarriers by genetically incorporating the OT-1 peptide (SIINFEKL) of ovalbumin (OVA) protein to the three different positions of Encap subunit. With them, we evaluated their efficacy in activating DC-mediated antigen-specific T cell cytotoxicity and consequent melanoma tumor rejection *in vivo*. DCs efficiently engulfed Encap and its variants (OT-1-Encaps), which carry antigenic peptides at different positions, and properly processed them within phagosomes. Delivered OT-1 peptides were effectively presented by DCs to naïve CD8⁺ T cells successfully resulting in the proliferation of antigen-specific cytotoxic CD8⁺ T cells. OT-1-Encap-vaccinations in B16-OVA melanoma tumor bearing mice effectively activated OT-1 peptide specific cytotoxic CD8⁺ T cells before or even after tumor generation resulting in significant suppression of tumor growth in prophylactic as well as therapeutic treatments. A large number of cytotoxic CD8⁺ T cells that actively produce both intracellular and secretory IFN- γ were observed in tumor infiltrating lymphocytes (TILs) collected from B16-OVA tumor masses originally vaccinated with OT-1-Encap-C upon the tumor challenges. The approaches we describe herein may provide opportunities to develop epitope-dependent vaccination systems that stimulate and/or modulate efficient and epitope-specific cytotoxic T cell immune responses in non-pathogenic diseases.

The effective generation of robust cytotoxic CD8⁺ T cell immune responses is considered a primary goal in cancer immunotherapy.¹ Functional cytotoxic CD8⁺ T cells not only kill their target cells directly but also secrete the cytokine IFN- γ , playing a critical role in tumor rejection by inhibiting tumor survival and angiogenesis and by recruiting innate and adaptive immune responses.² Dendritic cells (DCs) are known to be one of most powerful antigen presenting cells (APCs) and play a critical role in inducing adaptive immune responses by

educating antigen specific naïve T cells. DCs engulf tumor antigens, present them in the form of MHC/peptide complex on their surface, and consequently migrate to the secondary lymphoid sites where antigen-specific T cells are being educated,³ suggesting the importance of developing DC-mediated vaccines to activate antigen-specific cytotoxic CD8⁺ T cells. Since most tumors usually evade host immune systems by expressing low levels of antigenic epitopes, MHC, and costimulatory molecules which are poorly immunogenic to DCs⁴ it is essential in cancer immunotherapy to efficiently deliver tumor specific antigens to DCs, which strongly stimulate the maturation of DCs for the subsequent activation of antigen-specific cytotoxic CD8⁺ T cells.⁵⁻⁷

2.2 Introduction

Many of the approaches for vaccination have focused on utilizing inactivated or live attenuated disease-causing pathogens. However, there are limitations for developing vaccines for non-pathogen derived diseases, such as cancers and neurodegenerative disease, in these approaches. Therefore, it is necessary to develop simple and controllable antigen delivery systems which can carry a variety of protein antigens or antigenic peptides.

A variety of protein cage nanoparticles including virus-like particles (VLPs),⁸⁻²¹ ferritins²²⁻³⁰, lumazine synthase,³¹⁻³³ and encapsulin³⁴⁻³⁵ have been extensively studied as nano-scaled vehicles for delivering various types of diagnostics and/or therapeutics owing to their well-defined architecture and high biocompatibility.³⁶⁻³⁷ Protein cage nanoparticles are composed of multiple copies of one or two types of subunits to form well-defined spherical architecture and they are biochemically and genetically well-characterized. Therefore, any desired functions can be precisely incorporated through genetic and chemical modifications based on atomic resolution crystal structures.

For the development of vaccine platforms, VLPs, among many other protein cage nanoparticles, have been most popularly used in the genome-free and/or attenuated forms.^{14, 38-43} Many VLP-based vaccines have been used in clinics, and have significantly contributed to preventing numerous diseases caused by viruses, such as the Hepatitis B and human papilloma viruses.^{10, 44} However, these vaccines mainly utilize genuine coat proteins of VLPs as antigenic epitopes and generally induce an immune response that generates neutralizing antibodies specific for coat proteins of VLPs preventing subsequent infection of original pathogenic viruses. Therefore, these approaches are not suitable for non-pathogen derived diseases, such as cancers. Furthermore, many VLP-based vaccines occasionally exhibit unexpected self-adjuvanting effect that may cause undesired immunotherapeutic outcomes.⁴⁵⁻⁴⁷ As an alternative of VLPs, we previously employed ferritin protein cage nanoparticle as an antigen carriers and successfully demonstrated that antigenic peptides can be genetically introduced to protein cage nanoparticles and efficiently delivered to DCs leading to efficient activation of OT-1 peptide specific cytotoxic CD8⁺ T cells.⁴⁸ However, further investigation is essential to validate the efficacy of prophylactic and therapeutic vaccination driven by antigen-bearing protein cage nanoparticles and the possibility to use various types of protein cage nanoparticles as antigen nanocarriers.

We previously developed encapsulins (Encaps) as effective nanocarriers of therapeutic and diagnostic reagents using protein engineering.³⁴ Encapsulin is originally isolated from thermophile, *Thermotoga maritima*. It has 20 nm inner and 24 nm outer diameters and

icosahedral $T = 1$ symmetric spherical architecture which is self-assembled from 60 copies of identical 31-kDa subunits.⁴⁹ The genetic variants of Encap that we constructed were highly thermostable, maintaining their architecture.³⁴ Although Encap architecture is very similar to that of small icosahedral viruses, it does not contain any genomic DNA or RNA in its interior cavity, and its biological function in *T. maritima* has not been clearly understood yet. However, its crystal structure has been solved and its function was postulated to encapsulate functional proteins involved in oxidative stress responses.⁴⁹⁻⁵⁰

Ovalbumin (OVA) protein and the OT-1 transgenic mice are a widely used model system to study antigen-specific immune responses.⁵¹ The OT-1 peptide (SIINFEKL) corresponds to residues 257-264 of OVA protein, and its presentation by DCs to T cells induces proliferation and differentiation of OT-1-specific cytotoxic CD8⁺ T cells.⁵¹⁻⁵² B16 melanoma is a widely used tumor model to develop immunotherapeutic strategies with potential clinical applications based on its similarity to tumors found in patients.⁵³ B16-OVA cell line is a clone derived from the B16F10 melanoma cell line particularly transfected with OVA, suitable for studying OT-1 peptide-specific CD8⁺ T cell cytotoxicity and tumor rejection.⁵³⁻

54

In this study, we genetically introduced a model antigenic OT-1 peptide to Encap at various positions and evaluated their efficacies to induce DC-mediated antigen-specific T cell cytotoxicity and followed by B16-OVA tumor rejection (Figure 2.1).^{38,41,34,55}

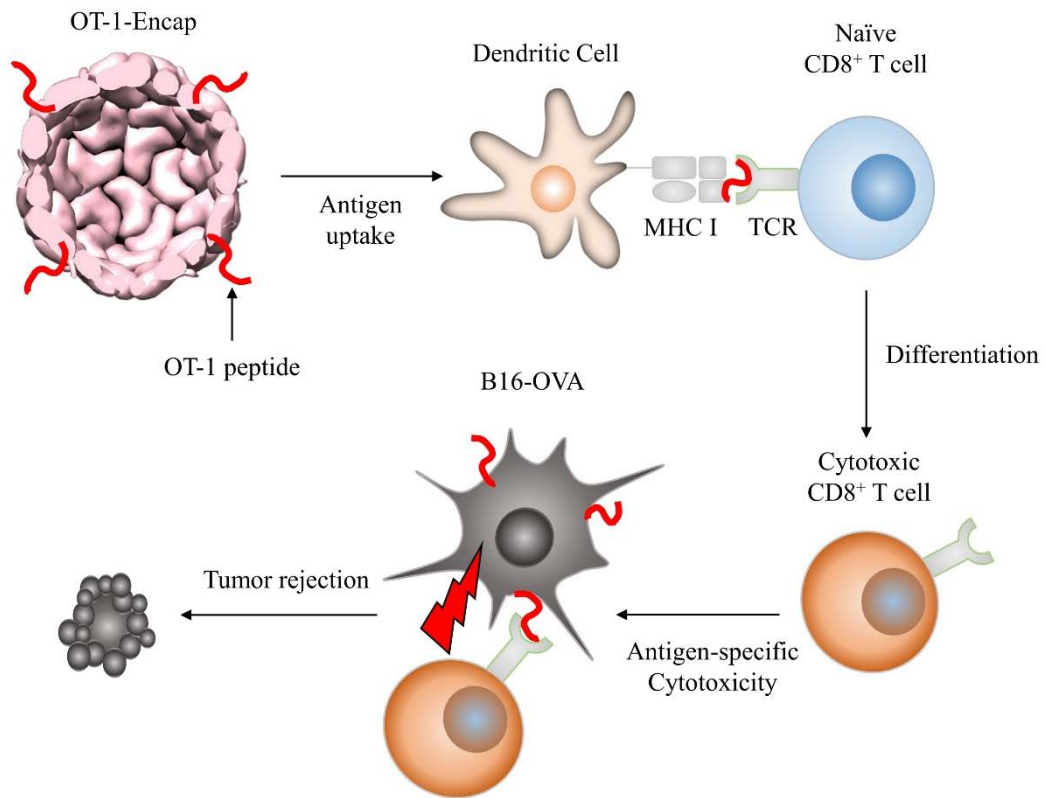


Figure 2.1 Schematic representation of OT-1-specific cytotoxic T cell differentiation and tumor rejection induced by OT-1-Encap-mediated prophylactic vaccinations

2.3 Materials and Methods

Construction and purification of encapsulins carrying the antigenic peptide OT-1

OT-1 peptides (SIINFEKL) were inserted into the loop region between residues 42 and 43 (loop42) or added to the N- or C-terminal ends of encapsulin (Encap) construct as described previously.³⁴ Encap and OT-1 Encaps were over-expressed and purified as described previously.³⁴ The endotoxin was taken away by using Triton X-114 (Sigma) and its levels of the resulting samples were quantified by using a Limulus Amoebocytes Lysate assay (Genescript). The resulting levels were all less than 0.15 EU/ml.

Protein concentrations used in this study were determined to ensure that the number of OT-1 peptides introduced to Encap is similar to the number of OT-1 peptides contained in soluble OVA protein. We calculated that 75 µg of OT-1-Encap contains approximately similar amounts of OT-1 peptides as that of 100 µg of soluble OVA protein, since each protein subunit has one OT-1 peptide and the molecular weight of OT-1-Encap subunit (33 kDa) is approximately 75 % of that of OVA protein (45 kDa).^{48,56} For the *in vitro* and *in vivo* assays, 1-5 mg/ml of OVA and 50-500 µg of OVA per mouse were used, respectively, which are the concentrations of model antigen OVA generally used in previous studies.⁴⁸

Mice and cell line

C57BL/6 and OT-1 transgenic mice were bought from Taconic and the Jackson Laboratory, respectively. OT-1 TCR expressed on CD8⁺ T cells is specific for the peptide OVA257–264 (SIINFEKL), bound to the class I MHC molecule H2-Kb.⁵² 64-65 All mice were utilized at 6-8 weeks and kept under the conditions of specific pathogen-free (SPF) following Ulsan National Institute of Science and Technology Institutional Animal Care and Use Committees (UNISTIACUC).

B16-F10 melanoma cell line and B16-OVA melanoma cell line, B16-F10 melanoma cells transfected with OVA gene, were generously provided by Dr. Byungsuk Kwon, Ulsan University, Korea. Tumor cells were grown and maintained in DMEM containing 5 % FBS (Hyclone) and antibiotics (Gibco). G418 was used as a selective marker (Calbiochem).

Isolation and analysis of primary cells

Spleens were ballooned and torn into small pieces. Subsequently, they were chopped and treated with 400 ManDI U/ml collagenase D (Roche) in 5 ml of Hank's balanced salt solution (HBSS, Thermofisher) by 25 G needle for 30 minutes. After treatment of 100 µl of 0.5M EDTA for additional 5 minutes, CD11c⁺ DCs were positively sorted by magnetic

activated cell sorting (MACS, Miltenyl Biotech) from single cell suspensions of splenocyte. Antigen-specific CD8⁺ T cells were prepared from the primed and boosted mice by indicated antigens (OT-1-Encap-C, OT-1-Encap-L, OT-1-Encap-N, or OVA protein). Briefly, single cell suspensions were obtained from spleens or lymph nodes and CD8⁺ T cells were selectively sorted (MACS, Miltenyl Biotech). Purity of sorted CD8⁺ T cells was higher than 98%. BD FACS Fortessa and FlowJo software (TreeStar) were used for collecting and analyzing all flow cytometry data, respectively.

Protein phagocytosis

Phagocytosis of Encap variants and OVA protein by DCs was determined by pHrodo dye (pHrodo succinimidyl ester, Invitrogen). Briefly, each one of the Encap variants and the OVA protein were labeled with 1 mg/ml of pH-sensitive lysine reactive pHrodo dyes, dialyzed overnight to remove unbound pHrodo dyes, and incubated with DCs at either 4 °C or 37 °C for 2 hours. pHrodo dye is an indicator of phagocytosis as it greatly increases in fluorescence at low pH.⁶⁵ The DCs were washed thoroughly and the fluorescent intensities of pHrodo were determined by flow cytometry.⁴⁸

Detection of antigen specific T cell proliferation using Carboxyfluorescein Diacetate Succinimidyl Ester (CFSE) dilution assay

For *in vitro* assay, 1×10^7 cells/ml of OT-1 specific T cells were labeled with 1 μ M of CFSE (Invitrogen) at 37 °C for 7 min. DCs were pulsed with indicated proteins (OT-1-Encap-C, OT-1-Encap-L, OT-1-Encap-N, or OVA protein) for 3 hours and co-cultured with OT-1 specific T cells labeled with CFSE (1:3 ratio) with poly (I:C) (InvivoGen) at 37 °C. 3 days later, cultured cells were collected and treated with fluorescent dye-conjugated V α 2, V β 5 and CD8 antibodies (all from BD Biosciences).

For *in vivo* assay, 5 μ M CFSE-labeled OT-1 T cells were intravenously introduced into naïve C57BL/6 mice. Mice were immunized with OVA proteins, Encap and OT-1 Encaps in the footpads subcutaneously with 50 μ g of poly (I:C) one day later. At day 4, single cell suspensions were obtained from lymph nodes and treated with fluorescent dye-conjugated V α 2, V β 5 and CD8 antibodies (all from BD Biosciences).

V β 5.1/5.2⁺V α 2⁺CD8⁺-based OT-1 specific T cells were gated and a diluted series of CFSE fluorescence per cells were analyzed. Proliferation index of each groups (bottom panels) was analyzed by Modfit LT software.⁶⁶

Cytotoxic T lymphocyte (CTL) assay

For *in vivo* CTL assay, mice were injected intraperitoneally with PBS or the indicated proteins (OT-1-Encap-C, OT-1-Encap-L, OT-1-Encap-N, or OVA protein) with 50 µg of poly (I:C) as an adjuvant. Mice were intravenously injected with 1:1 mixtures, 7×10^6 of each, of OT-1 peptide-pulsed (5 µM CFSE-labeled, CFSE^{hi}) and unpulsed (0.5 µM CFSE-labeled, CFSE^{low}) syngeneic splenocytes at day seven. Fourteen to sixteen hours later, single cell suspensions were collected from lymph nodes and the OT-1 specific CTL activity was evaluated by flow cytometry.

Measurement of total IFN-γ productions of functional CD8⁺ cytotoxic T cells

Single cells were collected from spleens and lymph nodes of each one of the CTL experimental groups as described above stimulated again with 1 µM of OT-1 peptides in a 96-well plate at 37 °C for 48 hours. Cultured supernatants were harvested and the amounts of produced IFN-γ were determined by cytometric beads assay (CBA) flex sets (BD Biosciences) and flow cytometry. All collected data were analyzed with FCAP Array software.

Tetramer assay of OT-1 peptide specific TCR

Single cells were isolated from spleens of the *in vivo* CTL experimental groups as described above and stimulated again with 1 µM of OT-1 peptides in a 96-well plate at 37 °C for 2 hours. The population of antigen-specific TCR expressing CD8⁺ T cells from re-stimulated splenocytes was analyzed by staining with PE conjugated MHC I tetramer (glycotope) and flow cytometry.⁵⁷ All collected data were analyzed with FlowJo software (TreeStar).

Prophylactic vaccination against B16-OVA or B16-F10 tumor challenges

Mice were primed with PBS, OVA proteins, Encap, or OT-1-Encap-C with 50 µg of poly (I:C) as an adjuvant, were and boosted with the same antigens 14 days later. At day 21, the vaccinated mice were subcutaneously challenged with 0.5×10^6 cells of B16-OVA melanoma cells or B16-F10 cells on the right flank. Every two or three days for 26 days, tumor sizes were measured with a caliper. PBS-immunized mice were used as a positive control. Mice were sacrificed at 26 days post tumor challenges, and tumor masses were subsequently collected. Tumor volume was calculated according to $V = \text{Width} \times \text{Height}^2$.

Therapeutic vaccination against B16-OVA or B16-F10 tumor challenges

Mice were subcutaneously challenged with 0.5×10^6 cells of B16-OVA or B16-F10

melanoma cells on the right flank. At day 10, tumor bearing mice were therapeutically vaccinated with PBS, OVA proteins, Encap, or OT-1-Encap-C with 50 µg of poly (I:C) as an adjuvant. Tumor sizes were measured and calculated as mentioned in prophylactic vaccination methods.

Isolation of tumor infiltrating lymphocytes

Tumor infiltrating lymphocytes (TILs) were isolated from tumor masses using centrifugation with discontinuous Ficoll gradient. Tumor masses were collected from mice, cut into small pieces, and incubated with collagenase D/DNase I mixture at 37 °C for 30 min with gentle shaking. A mixture was prepared with 1670 ManDI U/ml of collagenase D, 0.2 mg/ml DNase in HBSS buffer. Subsequently, incubating solutions were pipetted up and down multiple times to disaggregate tumor cells and filtered with a 70 µm strainer. Single cells were suspended with 4 ml of 75 % Ficoll (GE healthcare), laid on 4 ml of 100 % Ficoll, and centrifuged gently at 280 g for 30 min. TILs were collected from the interphase and washed with a solution of 1 mM PBS/EDTA mixture. Cells were stained with CD3⁺CD45.2⁺CD44⁺CD4⁺CD8⁺ antibodies (BD Biosciences) and ratio of CD4⁺ and CD8⁺ was analyzed by flow cytometry.

Measurement of intracellular IFN-γ production of functional CD8⁺ cytotoxic T cells

TILs were obtained as described above. Isolated cells were stimulated again with 2 µM of OT-1 peptide or 1 µg/ml of αCD3 and 2 µg/ml of αCD28 mAbs (Biolegend) for 2 hours followed by the addition of 10 µg/ml of BFA (Biolegend) for additional 4 hours. Fcγ receptors were blocked with anti-CD16/CD32 antibodies, and extracellular markers were stained with anti-CD3 and CD8 at 4 °C for 30 minutes. Cells were fixed and permeabilized with Cytotfix/Cytoperm kit (BD Biosciences) and intracellular IFN-γ was stained along with their isotypes (Biolegend) at 4 °C for 25 minutes. Data were analyzed by flow cytometry.

2.4 Results

Encapsulin protein cage nanoparticles (Encaps) were used here as antigen nanocarriers to directly activate the antigen-specific CD8⁺ T cell cytotoxicity mediated by DCs and evaluate their efficacy of tumor rejection (Figure 2.1). OT-1 peptides were genetically introduced to three different positions of Encap subunit, the N- and C-terminal ends and the loop region between residues 42 and 43 (loop42) (Figure 2.2A and Figure S1A and S2A). Crystal structure of Encap indicated that the N-terminal end and the loop42 are positioned in the inner cavity, and the C-terminal end is slightly exposed to the exterior surface.⁴⁹ OT-1 peptide insertions into each position were validated by molecular mass measurements of dissociated subunits (Figure 2.2B and Figure S1B and S2B). The molecular mass of the OT-1 peptide-inserted dissociated subunits of encapsulin at the C-terminal end (OT-1-Encap-C) was observed to be 33073.0 Da that is agreed well with the theoretical value (33071.4 Da) (Figure 2.2B). OT-1 peptide-inserted encapsulins (OT-1-Encaps) were eluted at the same position on the size exclusion chromatography as wild-type Encap (WT Encap) (Figure 2.2C and Figure S1C and S2C). The transmission electron microscopic (TEM) analyses of negatively stained OT-1-Encaps also confirmed their spherical morphology having 24 nm in outer diameter (Figure 2.2D and Figure S1D and S2D). These results reveal that the OT-1 peptide insertions into three different positions do not significantly alter their cage architecture and stoichiometry and provide a rationale for incorporation of other antigenic peptides.

We have previously demonstrated that ferritin protein cage nanoparticles carrying antigenic peptides are efficiently phagocytosed by DCs and processed in phagosomes.⁴⁸ Here, we also showed that pHrodo-labeled Encap and OT-1-Encaps are successfully taken up by DCs as the control soluble OVA protein (Figure S3A) and fluorescein-labeled OT-1-Encap-C are processed in phagosomes (Figure S3B) by flow cytometry analysis and visualizing their intracellular localization with a confocal microscope, respectively. To determine whether OT-1-Encap-C induces proper maturation of immature DCs, we co-incubated immature DCs with OT-1-Encap-C, OVA protein, or OT-1 peptides with poly (I:C) for 18 hours, the maturation markers (CD80, CD86, and MHC II) were detected with PE conjugated antibodies, and subsequently evaluated the degree of DC maturation with flow cytometry. All the DC maturation markers were successfully observed in OT-1-Encap-C treated DCs similar to those of OVA protein or OT-1 peptide treated DCs suggesting that OT-1-Encap-C successfully induced proper maturation of immature DCs (Figure S4). Therefore, we hypothesized that efficient processing of the phagocytosed OT-1-Encaps and the properly

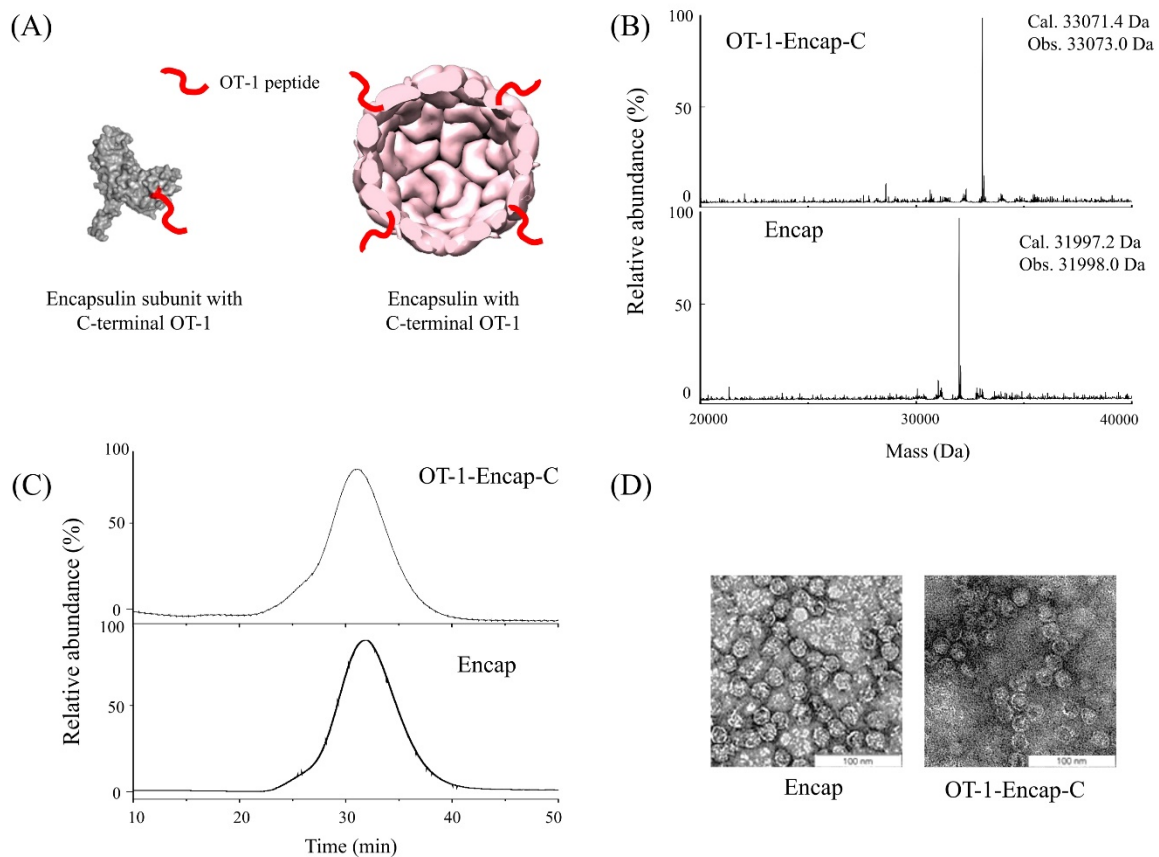


Figure 2.2 Characterization of Encap containing OT-1 peptides at the C-termini (OT-1-Encap-C).

(A) Schematic representation of OT-1 peptide addition to the C-termini of Encap. (B) Molecular mass measurements of the dissociated subunits of Encap (bottom) and OT-1-Encap-C (top). Calculated and observed molecular masses were indicated. (C) Size exclusion elution profiles (280 nm) of Encap (bottom) and OT-1-Encap-C (top). (D) Transmission electron micrographic (TEM) image of 2% uranyl acetate stained Encap (left) and OT-1-Encap-C (right). Scale bars (100 nm) were indicated.

presenting processed OT-1 peptides to CD8⁺ T cells would lead to successful proliferation and differentiation of antigen-specific CD8⁺ T cells. To examine this hypothesis, we initially attached the lysine-reactive fluorescent dye carboxyfluorescein succinyl ester (CFSE) to the surface of naïve CD8⁺ T cells and carried out a CFSE dilution assay *in vitro* and *in vivo*. Clonal expansions of CFSE-labeled naïve CD8⁺ T cells driven by antigen-specific stimulations would result in serial dilutions of CFSE.⁵⁶ We first pulsed DCs with OT-1-Encap variants (OT-1-Encap-C, OT-1-Encap-L or OT-1-Encap-N) for three hours *in vitro*, followed by extensive washing to ensure the presentation of only processed antigenic peptides, and incubated them with CFSE-labeled OT-1 transgenic CD8⁺ T cells. The degree of CD8⁺ T cell proliferation was evaluated with flow cytometry three days later.⁵⁶ All OT-1-Encap variants exhibited finger-like peaks with lower CFSE signals similar to that of the positive control, OVA protein, whereas untreated and Encap treated showed no changes (Figure 2.3A). These results indicate that all OT-1-Encap variants up-taken by DCs were efficiently processed within DC phagosomes and the processed OT-1 peptides were successfully presented to naïve CD8⁺ T cells, leading to effective OT-1 peptide-specific CD8⁺ T cell proliferation. At lower dosages of OT-1-Encap variants, we observed configuration-dependent proliferative responses (Figure S5). OT-1-Encap-C showed almost identical proliferative responses to those of OVA protein even at very low concentrations, whereas OT-1-Encap-N and OT-1-Encap-L induced proliferative responses only at high and moderate concentrations (Figure S5). This difference could be attributed to less effective processing of OT-1 peptides inserted in loop region and at the N-terminal, compared to those inserted at the C-terminal of end, consistent with our previous study.⁴⁸

Next, the antigen-specific proliferation of CD8⁺ T cells was investigated *in vivo*. Naïve mice received CFSE-labeled OT-1 CD8⁺ T cells intravenously and were challenged the next day with OT-1-Encap variants (OT-1-Encap-C, OT-1-Encap-L or OT-1-Encap-N). Splenocytes were collected from the mice three days later, and the CFSE signals were measured with flow cytometry to determine the degree of antigen-specific proliferation of CD8⁺ T cells. Similar to *in vitro* studies, all OT-1-Encap variant treated groups exhibited serially decreased signal intensities as that of OVA protein treated group did (Figure 2.3B). We also directly observed stable cognate interactions between OT-1-Encap-C treated mature DCs and CD8⁺ T cells⁵⁷ (Figure S6) confirming that the mature DCs properly processed OT-1 peptides and presented them directly to CD8⁺ T cells inducing proliferation and differentiation of antigen-specific CD8⁺ T cells.

In conclusion, *in vitro* and *in vivo* CFSE dilution assay data clearly indicated that genetically inserted OT-1 peptides were successfully delivered to DCs by Encap, processed

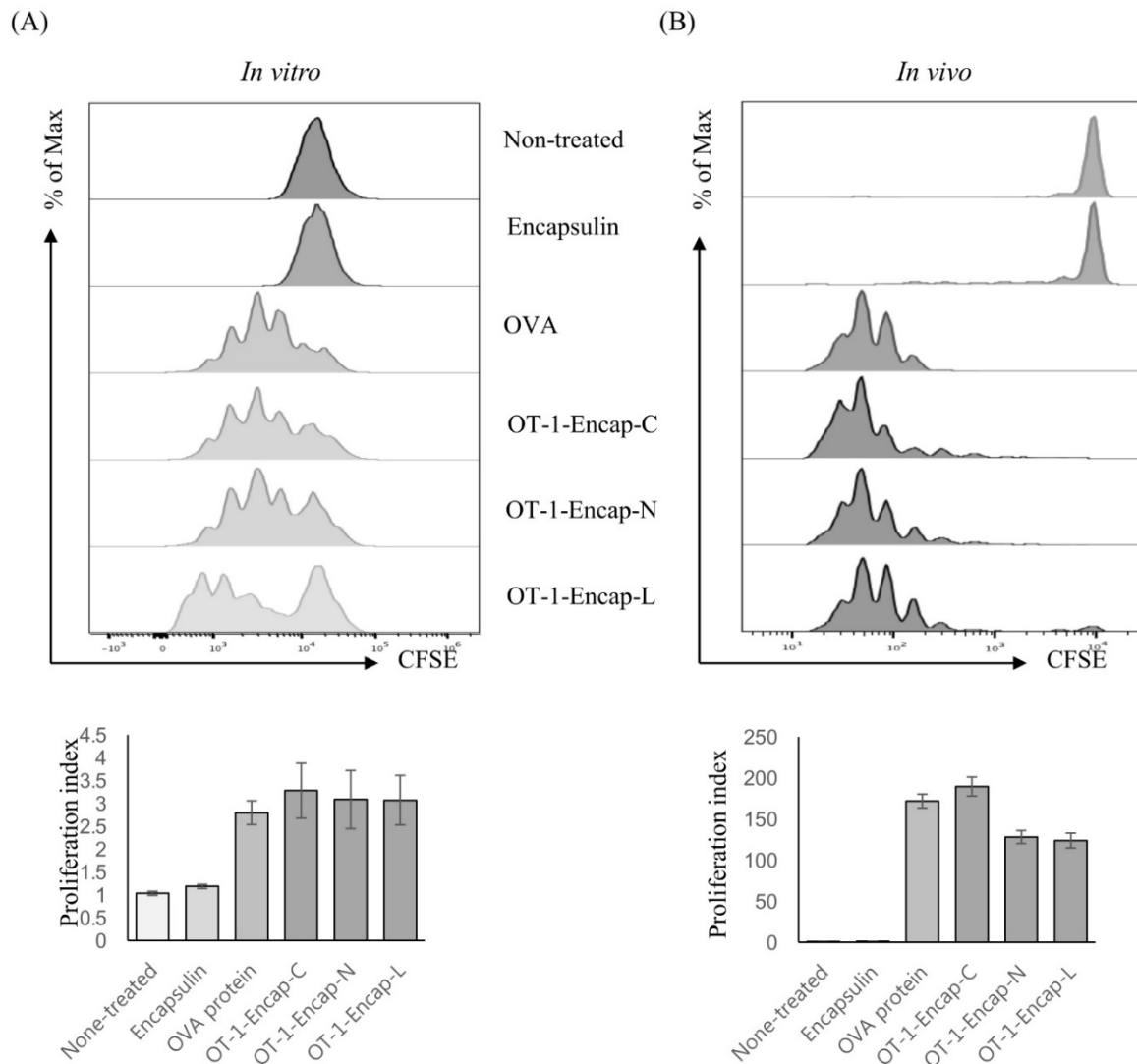


Figure 2.3 OT-1 peptides delivered to DCs by OT-1-Encap variants induce OT-1 specific CD8⁺ T cell proliferation *in vivo* and *in vitro*. (A) DCs harvested from naïve C57BL/6 mice were pulsed either with media, Encap, OVA protein, OT-1-Encap-C, OT-1-Encap-N or OT-1-Encap-L (from top to bottom) for 3 hours and co-cultured with CFSE-labeled OT-1 T cells at a ratio of 1:3. Four days later, the proliferation of OT-1 specific CD8⁺ T cells was measured by flow cytometry. (B) Naïve C57BL/6 mice were adoptively transferred with CFSE-labeled OT-1 T cells and on the next day, they were immunized subcutaneously either with PBS, OVA protein, Encap, OT-1-Encap-C, OT-1-Encap-N or OT-1-Encap-L (from top to bottom) in the presence of poly (I:C) as an adjuvant. Three days later, the proliferation of OT-1 specific CD8⁺ T cells was measured by flow cytometry. Proliferation index of each groups (bottom panels) was analyzed by Modfit LT software.

efficiently, and presented properly to naïve CD8⁺ T cells to effectively induce their proliferation as antigen-specific CD8⁺ T cells.

Successful vaccination should effectively generate functional cytotoxic CD8⁺ T cells that recognize target cells and kill them in an antigen-specific manner. To explore whether the CD8⁺ T cells that were induced to proliferate by OT-1-Encap-C immunization acquired cytotoxic functions, we performed a cytotoxic T lymphocyte (CTL) assay *in vivo*. If the proliferated CD8⁺ T cells are effectively differentiated as OT-1 specific cytotoxic T cells by delivered OT-1 peptides, they would selectively kill OT-1 peptide-pulsed target cells, leaving irrelevant splenocytes intact.⁵⁸ Naïve mice were immunized with PBS, OVA protein, Encap or OT-1-Encap-C subcutaneously with poly (I:C). Seven days after immunization, they were intravenously challenged with 1.4×10^7 of CFSE-labeled syngeneic splenocytes; 1:1 mixtures of splenocytes previously pulsed with 1 μM of OT-1 peptide for 1 hour (7×10^6 of 5 μM CFSE-labeled, CFSE^{hi}) and unpulsed (7×10^6 of 0.5 μM CFSE-labeled, CFSE^{low}). One day later, single cells were harvested from spleens and lymph nodes of each group and CFSE fluorescence intensities were measured by flow cytometry. Once OT-1 peptide specific CD8⁺ cytotoxic T cells are generated, they would kill OT-1 peptide pulsed target cells (CFSE^{hi}), resulting in reduced CFSE fluorescence intensities. Significant population reductions of CFSE^{hi} syngeneic splenocytes isolated from spleens (Figure 2.4A) or lymph nodes (Figure S7A) were observed in the OVA protein or OT-1-Encap-C immunized groups, whereas there was no meaningful signal change in the negative control groups (PBS or Encap, Figure 2.4A and S7A). Interestingly, the OT-1-Encap-C immunized group showed most significant reduction of CFSE^{hi} populations, even more than that of the OVA protein immunized group (Figure 2.4A and S7A), suggesting that OT-1 peptides delivered by OT-1-Encap-C generate more efficient CD8⁺ cytotoxic T cells. Since the IFN- γ production level of CD8⁺ T cells generally reflects the cytotoxicity of CD8⁺ T cells,⁵⁹ we measured the IFN- γ productions of functional CD8⁺ cytotoxic T cells. Naïve mice were also immunized with simple pulsing of OT-1 peptides onto Encap. It has been known that small antigenic peptides do not effectively generate antigen-specific functional CD8⁺ cytotoxic T cells *in vivo* because of low antigenicity of small size of peptides.⁶⁰⁻⁶¹ Simple pulsing of OT-1 peptides onto Encap did not generate noticeable antigen-specific cytotoxicity (Figure S8). OT-1 peptides covalently attached to large-sized Encap may allow generating more efficient CD8⁺ cytotoxic T cells (Figure 2.4).

Single cells were harvested from spleens and lymph nodes of each one of the CTL experimental groups and stimulated again with 1 μM of OT-1 peptides for 48 hours. Subsequently, cultured supernatants were harvested and the amounts of produced IFN- γ

were analyzed with the cytometric beads assay (CBA). Isolated single cells from OT-1-Encap-C immunized groups produced the largest amounts of IFN- γ (Figure 2.4B and S7B). To directly detect the response of antigen-specific CD8⁺ T cells further, mice were immunized with PBS, OVA protein, Encap, OT-1-Encap-C or OT-1 peptides along with poly (I:C) and CD8⁺ T cells were separated from whole splenocytes. OT-1 peptide-specific CD8⁺ T cells was detected with PE conjugated SIINFEKL-MHC I tetramers and their populations were subsequently analyzed by flow cytometry. OVA protein or OT-1-Encap-C immunized mice exhibited increased populations of antigen-specific CD8⁺ T cells compared to those of PBS, Encap, or OT-1 peptide immunized mice (Figure S9). These data imply that OT-1 peptides delivered by OT-1-Encap-C efficiently generate high-quality functional OT-1 specific CD8⁺ cytotoxic T cells leading to effective target cell killing observed in the CTL assay (Figure 2.4A and S7A).⁵⁹

To further investigate the OT-1-Encap-C mediated adaptive immune responses in prophylactic vaccination, we utilized the B16-OVA tumor challenge model and examined whether the activated CD8⁺ cytotoxic T cells could selectively reject the generation of OT-1 peptide expressing tumors. If OT-1-Encap-C successfully activates OT-1 specific cytotoxic CD8⁺ T cells through DCs, they would infiltrate the tumor sites and kill B16-OVA melanoma cells selectively. We challenged mice with B16-F10 which does not express OT-1 peptide as a negative control to confirm antigenic peptide-specific vaccination.^{4,53}

For prophylactic vaccination, mice were first primed with PBS, OVA proteins, Encap or OT-1-Encap-C with 50 μ g of poly (I:C), and boosted with the same antigens 14 days later. At day 21, vaccinated mice subcutaneously received 0.5×10^6 cells of B16-OVA or B16-F10 on the right flank, and afterwards tumor sizes were recorded every two or three days (Figure 2.5A and S10). Twenty six days after tumor challenges, mice were sacrificed and tumor masses were collected (Figure 2.5B and S10). While large-sized B16-OVA tumor masses were generated in PBS- or Encap-immunized mice, tumor generation in OT-1-Encap-C or OVA protein immunized mice were significantly suppressed (Figure 2.5A and 2.5B). The OVA protein or OT-1-Encap-C immunized groups in B16-F10 tumor challenges successfully generated efficient OT-1 specific CD8⁺ T cells which kill OT-1 peptide-pulsed target cells (CFSE^{hi}) (Figure S10A). However, their cytotoxicity was OT-1 specific and they, therefore, did not kill B16-F10 cells or suppress tumor growth (Figure S10B and S10C). These results suggest that OT-1-Encap-C or OVA protein vaccinations resulted in the effective activation of antigenic peptide specific cytotoxic CD8⁺ T cells prior to tumor generation, allowing subsequent infiltration of OT-1 specific cytotoxic CD8⁺ T cells into the tumor sites to suppress tumor growth upon the tumor challenges.

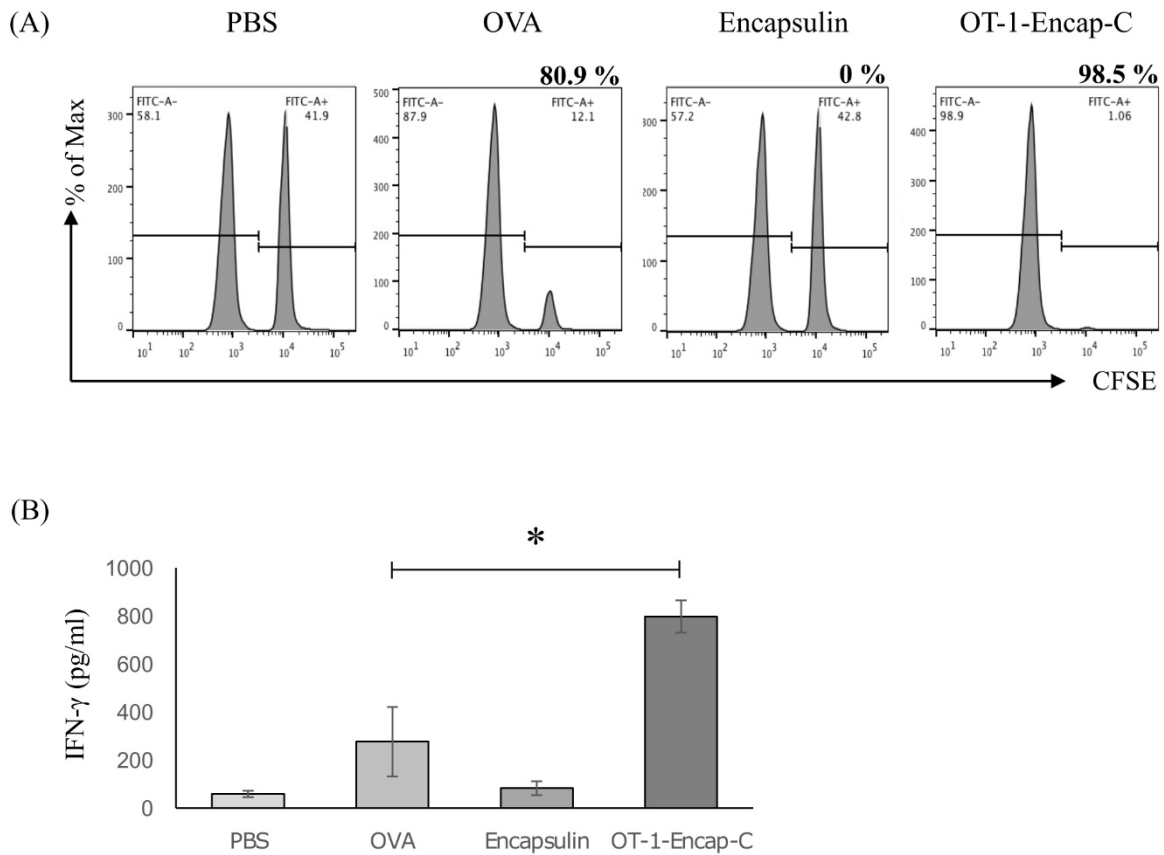
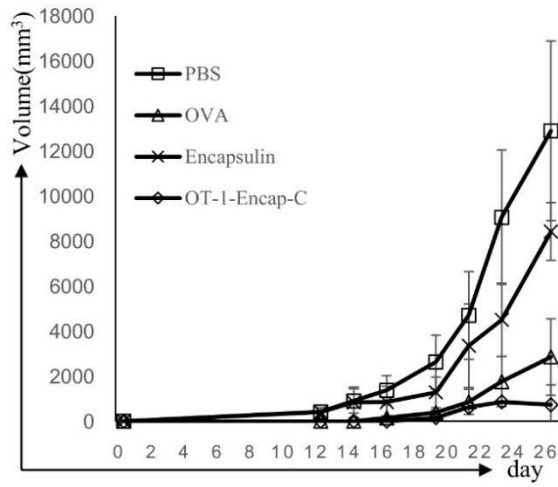


Figure 2.4 OT-1 peptides delivered to DCs by OT-1-Encap-C induce the differentiation of functional effector CD8⁺ T cells in spleens. (A) Naïve C57BL/6 mice were immunized subcutaneously either with PBS, OVA protein, Encap, or OT-1-Encap-C in the presence of poly (I:C) as an adjuvant. Mice were intravenously injected with CFSE-labeled syngeneic splenocytes pulsed with (CFSE^{hi}) or without (CFSE^{low}) OT-1 peptide seven days later. Next day, cytotoxicity of OT-1 specific CD8⁺ T cell was measured by flow cytometry. (B) Single cells were isolated from spleens and stimulated again with OT-1 peptides for 2 days. The amounts of IFN- γ produced were measured with CBA from cultured supernatants. The P values < 0.05 were considered significant (*).

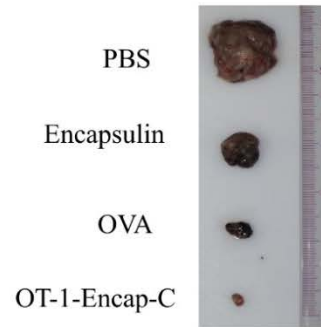
To test this hypothesis, we isolated tumor-infiltrating lymphocytes (TILs) and analyzed the contents of CD8⁺ T cells and their IFN- γ productions. At 21 days after tumor challenges, tumor masses were isolated from each group (Figure S11A) and cut into small pieces. They were incubated with collagenase D/DNase I mixture at 37 °C for 30 min and cells were subsequently disaggregated and filtered for single cell preparation. Single cells were suspended in 75% Ficoll, laid on 100% Ficoll, and centrifuged gently. TILs were collected from interphase within Ficoll and the populations of CD4⁺ and CD8⁺ T cells in TILs were evaluated with flow cytometry (Figure 2.5C). TILs collected from OT-1-Encap-C vaccinated B16-OVA tumors contained larger CD8⁺ T cell populations than PBS, Encap or even OVA protein vaccinated groups (Figure 2.5C, bottom right) suggesting that activated cytotoxic T cells are effectively infiltrated to the tumor sites. While CD4⁺ and CD8⁺ T cells were similarly populated in TILs collected from OVA protein vaccinated B16-OVA tumors, CD8⁺ T cells were much more populated than CD4⁺ T cells in TILs collected from OT-1-Encap-C vaccinated ones (Figure 2.5C and S11B), indicating the selective activation of cytotoxic CD8⁺ T cells by OT-1 peptides delivered by OT-1-Encap-C and their effective infiltration into the tumor sites. Slightly better tumor suppression observed in B16-OVA tumors vaccinated with OT-1-Encap-C might have resulted from more activated cytotoxic CD8⁺ T cell populations in tumor sites. Functional properties of infiltrated cytotoxic CD8⁺ T cells, like their intracellular and total IFN- γ production, were further investigated with intracellular cytokine staining (ICS) assay and CBA, respectively. Isolated TILs were stimulated again with 1 μ M of OT-1 peptides for 2 hours followed by the addition of 10 μ g/ml of BFA for 4 hours. Fc γ receptors were blocked and extracellular markers were subsequently detected with antibodies to CD3 and CD8. The populations of IFN- γ producing cells were evaluated with flow cytometry (Figure 2.5D). Cytotoxic CD8⁺ T cells obtained from TILs of OT-1-Encap-C or OVA-vaccinated B16-OVA tumors produced and accumulated IFN- γ intracellularly at equivalent levels, whereas those of PBS or Encap vaccinated ones did not (Figure 2.5D). CBA results also confirmed IFN- γ production of TILs of OT-1-Encap-C- or OVA-vaccinated B16-OVA tumors (Figure S11C). Taken together, these data strongly support our hypothesis that OT-1-Encap-C selectively activates cytotoxic CD8⁺ T cells, allowing efficient infiltration of them to the tumor sites and subsequent suppression of tumor growth upon the tumor challenges.

Most tumor cells generally have evasion systems that produce inhibitory signals to escape from their host immune systems. Thus, we investigated whether OT-1-Encap-C vaccination can effectively kill the target cells at the early tumor challenging conditions. Ten days after tumor challenges in prophylactic vaccination, the mice were intravenously injected with a

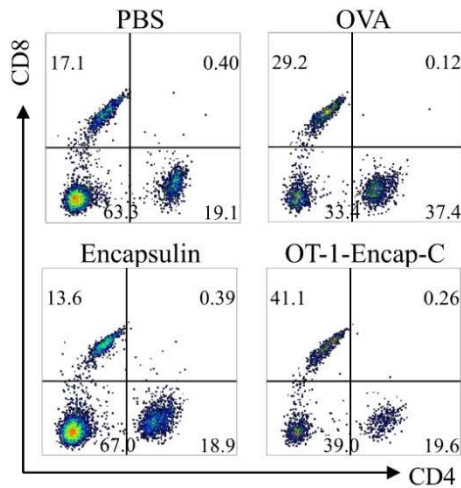
(A)



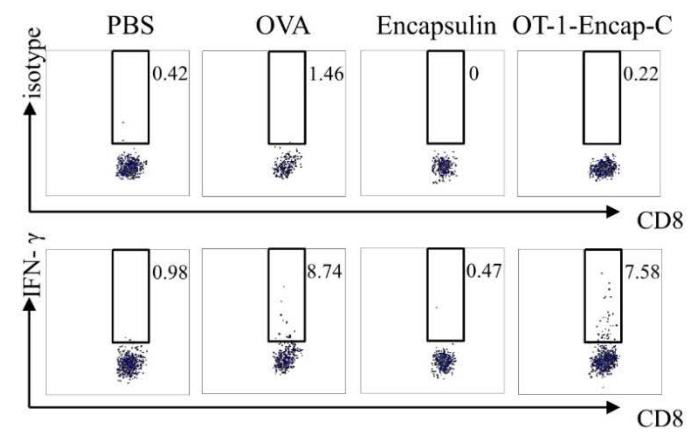
(B)



(C)



(D)



(E)

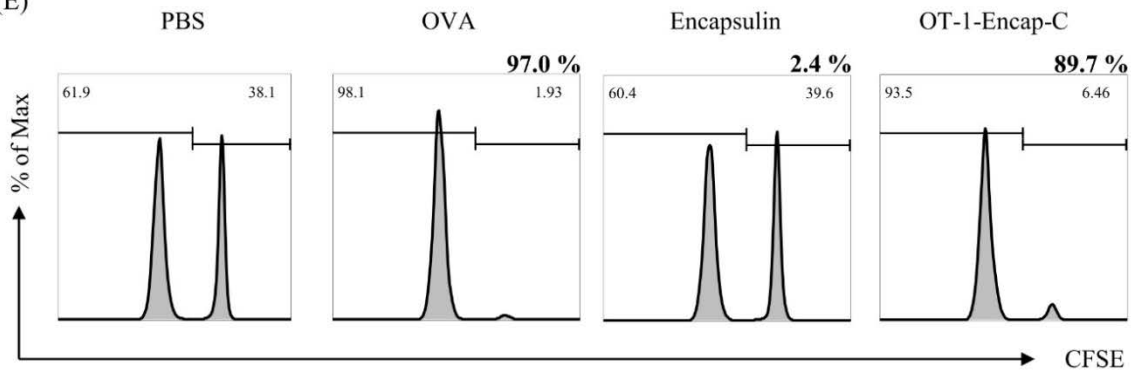


Figure 2.5 Prophylactic vaccination with OT-1-Encap-C suppressed B16-OVA tumor growth.

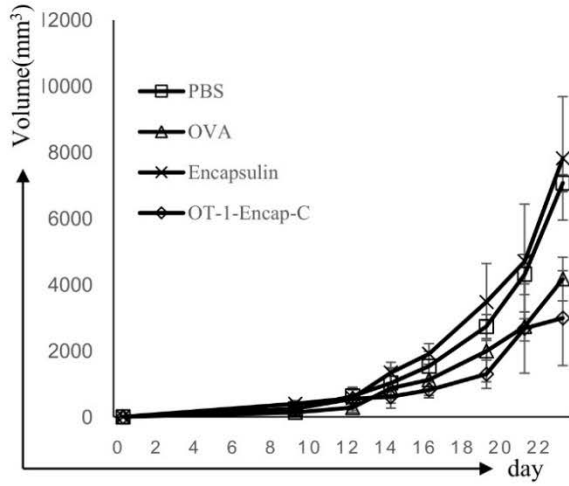
(A) Mice were primed intraperitoneally either with PBS, OVA protein, Encap or OT-1-Encap-C in the presence of poly (I:C) as an adjuvant and boosted with the same antigens 14 days later. At day 21, 0.5×10^6 of B16-OVA melanoma cells were subcutaneously injected onto the right flank. Tumor sizes were measured afterwards with a caliper every two or three days (n=5). (B) Mice were sacrificed at day 26 after tumor challenges and tumor masses were isolated presented. (C) TILs were isolated from tumor masses (Figure S11A) of the mice 21 days after the tumor challenges and the percentages of CD4⁺ T cells and CD8⁺ T cells were measured by flow cytometry. (D) Isolated TILs were stimulated again with 1 μ M of OT-1 peptides, accumulated intracellular IFN- γ was stained along with their isotypes, and the IFN- γ secreting CD8⁺ T cells were measured by flow cytometry. (E) After 10 days of tumor challenges, tumor bearing mice were intravenously injected with CFSE-labeled syngeneic splenocytes pulsed with (CFSE^{hi}) or without (CFSE^{low}) OT-1 peptide. OT-1 specific CD8⁺ T cell cytotoxicity was measured by flow cytometry.

mixed splenocytes which have OT-1 peptide-pulsed CFSE^{hi} or unpulsed CFSE^{low}, as we described in the *in vivo* CTL assays. Single cells were harvested from spleen the next day and CFSE signals were analyzed by flow cytometry (Figure 2.5E). Similarly to CTL assays performed without tumor challenges, populations of CFSE^{hi}-labeled OT-1 peptide-pulsed syngeneic splenocytes isolated from spleens were significantly reduced in groups immunized with OVA protein or OT-1-Encap-C, whereas they remained unchanged in the control groups (PBS or Encap) (Figure 2.5E). These data indicate that OT-1 peptides delivered by OT-1-Encap-C effectively induced OT-1 specific cytotoxic CD8⁺ T cells even under early tumor challenged conditions and killed OT-1 specific target cells.

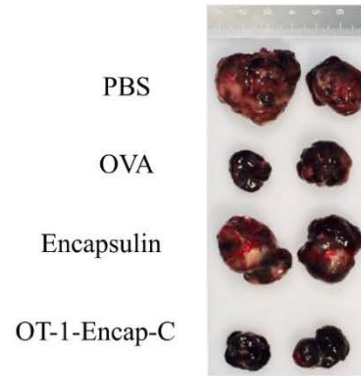
Most of tumors occur spontaneously in various conditions and the majority of patients recognize its occurrence only after tumor has already progressed. Therefore, the effective therapeutic vaccination against progressed tumors is very important and essential in cancer treatment. Since OT-1-Encap-C vaccination effectively killed the target cells shortly after prophylactic vaccination (Figure 2.5E), we anticipated that OT-1-Encap-C may effectively activate OT-1 specific cytotoxic CD8⁺ T cells even under the presence of OT-1 bearing tumor and may suppress tumor progression. To answer this question, we carried out therapeutic vaccination experiments. Ten days after B16-OVA or B16-F10 tumor challenges, mice were therapeutically vaccinated with PBS, OVA proteins, Encap or OT-1-Encap-C with 50 μg of poly (I:C) as an adjuvant and their tumor sizes were measured for 23 days (Figure 2.6). B16-OVA tumor generations in OT-1-Encap-C or OVA protein immunized mice were greatly suppressed compared to those of PBS or Encap immunized groups (Figure 2.6A and 6B), whereas B16-F10 tumors were almost equally generated in all groups (Figure S12A and S12B). However, their tumor-suppression efficiencies were not as effective as above prophylactic vaccination, probably due to the lack of a boosting injection. The population of CD8⁺ T cells and the IFN-γ secretion of those cells were dramatically increased in isolated TILs as in prophylactic vaccination suggesting that tumor infiltrated CD8⁺ T cells were functionally activated (Figure 2.6C and 2.6D). Ten days after therapeutic vaccination, mice were intravenously injected with a mixed splenocytes which have OT-1 peptide-pulsed CFSE^{hi} and unpulsed CFSE^{low}. On the next day, single cells were isolated from spleen the next day and the CFSE signals were analyzed by flow cytometry to evaluate how much OT-1 specific cytotoxicity is generated (Figure 2.6E and S12C). Similarly to CTL assays performed with prophylactic vaccination, populations of CFSE^{hi}-labeled OT-1 peptide-pulsed syngeneic splenocytes were reduced in groups immunized with OVA protein or OT-1-Encap-C (Figure 2.6E). However, their cytotoxic activities were not as strong as those of prophylactic treatments consistent with their tumor suppression capability (Figure 2.6A and

2.6B). These data suggest that OT-1-Encap-C also efficiently deliver OT-1 peptide to DCs to educate cytotoxic CD8⁺ T cells as tumor antigen-specific killers in early stages of tumor generation and provide opportunity to be utilized as tumor therapeutic vaccines.

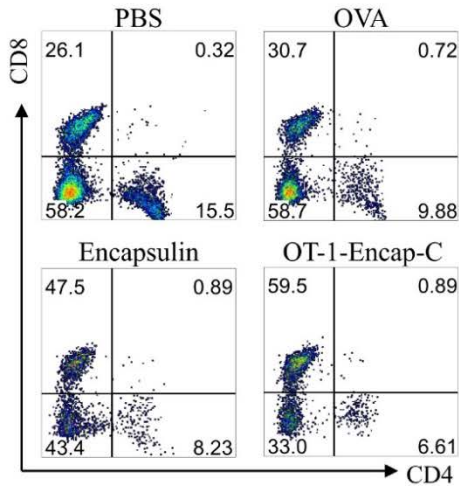
(A)



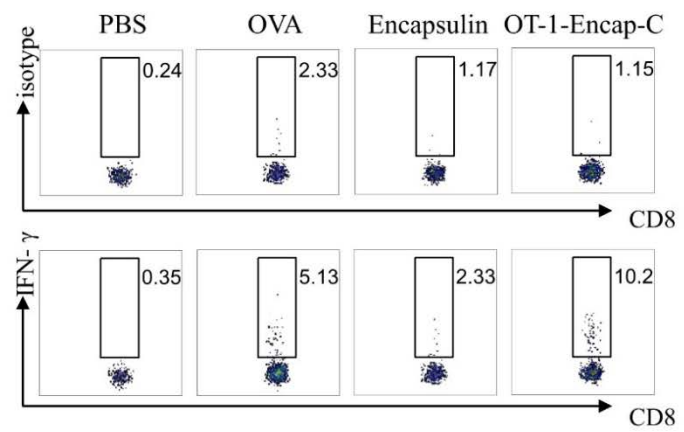
(B)



(C)



(D)



(E)

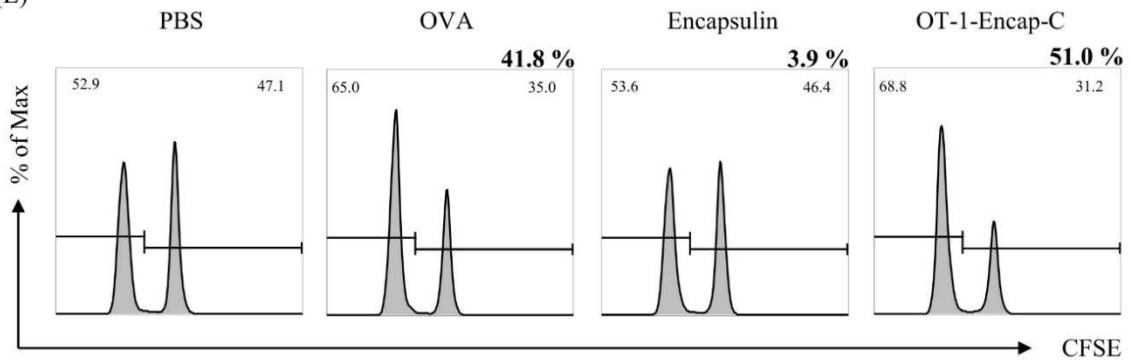


Figure 2.6 Therapeutic vaccination with OT-1-Encap-C suppressed B16-OVA tumor growth. (A) Mice were subcutaneously injected with 0.5×10^6 of B16-OVA melanoma onto the right flank. 10 days later, the mice were introduced either with PBS, OVA protein, Encap or OT-1-Encap-C in the presence of poly (I:C) as an adjuvant intraperitoneally. Tumor sizes were measured afterwards with a caliper every two or three days for 23 days (n=7). (B) Mice were sacrificed at day 23 after tumor challenges and tumor masses were isolated presented. (C) TILs were isolated from tumor masses of the mice 21 days after the tumor challenges and the percentages of CD4⁺ T cells and CD8⁺ T cells were measured by flow cytometry. (D) Isolated TILs were stimulated again with 1 μ M of OT-1 peptides, accumulated intracellular IFN- γ was stained along with their isotypes, and the IFN- γ secreting CD8⁺ T cells were measured by flow cytometry. (E) After 10 days of therapeutic vaccination, tumor bearing mice were intravenously injected with CFSE-labeled syngeneic splenocytes pulsed with (CFSE^{hi}) or without (CFSE^{low}) OT-1 peptide. OVA-specific CD8⁺ T cell cytotoxicity was measured by flow cytometry.

2.5 Discussion

In this study, we genetically introduced OT-1 peptides (SIINFEKL) to three various positions of the Encap subunit, the N- and C-terminal ends and the loop region between residues 42 and 43 (loop42) and confirmed that these three regions are tolerant of the peptide insertion. Encap and OT-1-Encaps were effectively phagocytosed by DCs and processed within phagosomes. The processed OT-1 peptides were effectively presented by DCs to naïve CD8⁺ T cells leading to the efficient proliferation of antigen-specific CD8⁺ T cells *in vivo* as well as *in vitro*. OT-1-Encap-C exhibited almost identical proliferative responses to those of OVA protein even at very low concentrations, whereas OT-1-Encap-N and OT-1-Encap-L exhibited proliferative responses only at high and moderate concentrations. Our data suggest that OT-1 peptides in the loop region and at the N-terminal end are not processed as efficiently as those at the C-terminal end. Therefore, the position of antigenic epitopes should be carefully considered for *in vivo* application.

OT-1-Encap-C-immunized naïve mice efficiently induced the OT-1 peptide specific cytotoxic T cells leading to selective killing of externally inserted OT-1 peptide-bearing target cells. Isolated single cells from OT-1-Encap-C-immunized mice secreted large amounts of IFN- γ and such high-quality functional OT-1 specific CD8⁺ cytotoxic T cells generated by OT-1-Encap-C resulted in most effective target cell killing in CTL assays. In a B16-OVA melanoma challenge experiment, considerable tumor growth suppressions we observed with the OT-1-Encap-C vaccination in both prophylactic and therapeutic treatments. TILs obtained from the OT-1-Encap-C-vaccinated B16-OVA tumor group included many cytotoxic CD8⁺ T cells which produce a large quantity of both intracellular and secretory IFN- γ cytokines. Although CD8⁺ T cells infiltrate into tumor generation sites, Tregs accumulated by tumor microenvironment generally do not allow naïve CD8⁺ T cells to differentiate into functional cytotoxic T cells.⁶²⁻⁶³ OT-1-Encap-C vaccination effectively generated OT-1 specific cytotoxic CD8⁺ T cells before and, furthermore, even after tumor generation and led to subsequent infiltration of OT-1 specific cytotoxic CD8⁺ T cells into the tumor sites upon the tumor challenges, providing tumor suppression.

Encapsulin has multiple addressable sites for introducing additional activities and cargo molecules in both interior cavity and exterior surface. Various type of antigenic epitopes, adjuvant molecules, and DC targeting ligands can be incorporated genetically and/or chemically. The approach and Encap variants we described here may provide opportunities to develop epitope-dependent vaccination systems that stimulate and/or modulate efficient and peptide-specific cytotoxic T cell immune responses in non-pathogen originated diseases, for example, cancers and neurodegenerative diseases.

2.6 References

1. Uto, T.; Wang, X.; Sato, K.; Haraguchi, M.; Akagi, T.; Akashi, M.; Baba, M., Targeting of Antigen to Dendritic Cells with Poly (γ -glutamic acid) Nanoparticles Induces Antigen-Specific Humoral and Cellular Immunity. *J. Immunol.* 2007, 178, 2979-2986.
2. Ikeda, H.; Old, L. J.; Schreiber, R. D., The Roles of IFN- γ in Protection Against Tumor Development and Cancer Immunoediting. *Cytokine Growth Factor Rev.* 2002, 13, 95-109.
3. Steinman, R. M., Lasker Basic Medical Research Award. Dendritic Cells: Versatile Controllers of the Immune System. *Nat. Med.* 2007, 13, 1155-1159.
4. Aranda, F.; Llopiz, D.; Diaz-Valdes, N.; Riezu-Boj, J. I.; Bezunartea, J.; Ruiz, M.; Martinez, M.; Durantez, M.; Mansilla, C.; Prieto, J.; Lasarte, J. J.; Borrás-Cuesta, F.; Sarobe, P., Adjuvant Combination and Antigen Targeting as a Strategy to Induce Polyfunctional and High-Avidity T-cell Responses Against Poorly Immunogenic Tumors. *Cancer Res.* 2011, 71, 3214-3224.
5. Steinman, R. M.; Banchereau, J., Taking Dendritic Cells into Medicine. *Nature* 2007, 449, 419-426.
6. Steinman, R. M.; Pope, M., Exploiting Dendritic Cells to Improve Vaccine Efficacy. *J. Clin. Invest.* 2002, 109, 1519-1526.
7. Tacke, P. J.; de Vries, I. J.; Torensma, R.; Figdor, C. G., Dendritic-Cell Immunotherapy: from *ex vivo* Loading to *in vivo* Targeting. *Nat. Rev. Immunol.* 2007, 7, 790-802.
8. Banerjee, D.; Liu, A. P.; Voss, N. R.; Schmid, S. L.; Finn, M. G., Multivalent Display and Receptor-Mediated Endocytosis of Transferrin on Virus-Like Particles. *ChemBioChem* 2010, 11, 1273-1279.
9. Destito, G.; Yeh, R.; Rae, C. S.; Finn, M. G.; Manchester, M., Folic Acid-Mediated Targeting of Cowpea Mosaic Virus Particles to Tumor Cells. *Chem. Biol.* 2007, 14, 1152-1162.
10. Kushnir, N.; Streatfield, S. J.; Yusibov, V., Virus-Like Particles as a Highly Efficient Vaccine Platform: Diversity of Targets and Production Systems and Advances in Clinical Development. *Vaccine* 2012, 31, 58-83.
11. Lucon, J.; Qazi, S.; Uchida, M.; Bedwell, G. J.; LaFrance, B.; Prevelige, P. E.; Douglas, T., Use of the Interior Cavity of the P22 Capsid for Site-Specific Initiation of Atom-Transfer Radical Polymerization with High-Density Cargo Loading. *Nat. Chem.* 2012, 4, 781-788.

12. Min, J.; Jung, H.; Shin, H.-H.; Cho, G.; Cho, H.; Kang, S., Implementation of P22 Viral Capsids as Intravascular Magnetic Resonance T1 Contrast Conjugates via Site-Selective Attachment of Gd(III)-Chelating Agents. *Biomacromolecules* 2013, 14, 2332-2339.
13. Min, J.; Moon, H.; Yang, H. J.; Shin, H.-H.; Hong, S. Y.; Kang, S., Development of P22 Viral Capsid Nanocomposites as Anti-Cancer Drug, Bortezomib (BTZ), Delivery Nanoplatfroms. *Macromol. Biosci.* 2014, 14, 557-564.
14. Patterson, D. P.; Rynda-Apple, A.; Harmsen, A. L.; Harmsen, A. G.; Douglas, T., Biomimetic Antigenic Nanoparticles Elicit Controlled Protective Immune Response to Influenza. *ACS Nano* 2013, 7, 3036-3044.
15. Stephanopoulos, N.; Tong, G. J.; Hsiao, S. C.; Francis, M. B., Dual-Surface Modified Virus Capsids for Targeted Delivery of Photodynamic Agents to Cancer Cells. *ACS Nano* 2010, 4, 6014-6020.
16. Zeng, Q.; Wen, H.; Wen, Q.; Chen, X.; Wang, Y.; Xuan, W.; Liang, J.; Wan, S., Cucumber Mosaic Virus as Drug Delivery Vehicle for Doxorubicin. *Biomaterials* 2013, 34, 4632-4642.
17. Farkas, M. E.; Aanei, I. L.; Behrens, C. R.; Tong, G. J.; Murphy, S. T.; O'Neil, J. P.; Francis, M. B., PET Imaging and Biodistribution of Chemically Modified Bacteriophage MS2. *Mol. Pharm.* 2013, 10, 69-76.
18. Pokorski, J. K.; Hovlid, M. L.; Finn, M. G., Cell Targeting with Hybrid Q β Virus-Like Particles Displaying Epidermal Growth Factor. *ChemBioChem* 2011, 12, 2441-2447.
19. Bruckman, M. A.; Jiang, K.; Simpson, E. J.; Randolph, L. N.; Luyt, L. G.; Yu, X.; Steinmetz, N. F., Dual-Modal Magnetic Resonance and Fluorescence Imaging of Atherosclerotic Plaques *in vivo* Using VCAM-1 Targeted Tobacco Mosaic Virus. *Nano Lett.* 2014, 14, 1551-1558.
20. Li, K.; Chen, Y.; Li, S.; Nguyen, H. G.; Niu, Z.; You, S.; Mello, C. M.; Lu, X.; Wang, Q., Chemical Modification of M13 Bacteriophage and Its Application in Cancer Cell Imaging. *Bioconjug. Chem.* 2010, 21, 1369-1377.
21. Yildiz, I.; Shukla, S.; Steinmetz, N. F., Applications of Viral Nanoparticles in Medicine. *Curr. Opin. Biotechnol.* 2011, 22, 901-908.
22. Aime, S.; Frullano, L.; Geninatti Crich, S., Compartmentalization of a Gadolinium Complex in the Apoferritin Cavity: A Route to Obtain High Relaxivity Contrast Agents for Magnetic Resonance Imaging. *Angew. Chem. Int. Ed. Engl.* 2002, 41, 1017-1019.
23. Kang, Y. J.; Park, D. C.; Shin, H.-H.; Park, J.; Kang, S., Incorporation of Thrombin Cleavage Peptide into a Protein Cage for Constructing a Protease-Responsive

- Multifunctional Delivery Nanoplatform. *Biomacromolecules* 2012, 13, 4057-4064
24. Kang, Y. J.; Yang, H. J.; Jeon, S.; Kang, Y.-S.; Do, Y.; Hong, S. Y.; Kang, S., Polyvalent Display of Monosaccharides on Ferritin Protein Cage Nanoparticles for the Recognition and Binding of Cell-Surface Lectins. *Macromol. Biosci.* 2014, 14, 619-625.
 25. Kwon, C.; Kang, Y. J.; Jeon, S.; Jung, S.; Hong, S. Y.; Kang, S., Development of Protein-Cage-Based Delivery Nanoplatforms by Polyvalently Displaying β -Cyclodextrins on the Surface of Ferritins Through Copper(I)-Catalyzed Azide/Alkyne Cycloaddition. *Macromol. Biosci.* 2012, 12, 1452-1458.
 26. Uchida, M.; Flenniken, M. L.; Allen, M.; Willits, D. A.; Crowley, B. E.; Brumfield, S.; Willis, A. F.; Jackiw, L.; Jutila, M.; Young, M. J.; Douglas, T., Targeting of Cancer Cells with Ferrimagnetic Ferritin Cage Nanoparticles. *J. Am. Chem. Soc.* 2006, 128, 16626-16633.
 27. Uchida, M.; Kosuge, H.; Terashima, M.; Willits, D. A.; Liepold, L. O.; Young, M. J.; McConnell, M. V.; Douglas, T., Protein Cage Nanoparticles Bearing the LyP-1 Peptide for Enhanced Imaging of Macrophage-Rich Vascular Lesions. *ACS Nano* 2011, 5, 2493-2502.
 28. Terashima, M.; Uchida, M.; Kosuge, H.; Tsao, P. S.; Young, M. J.; Conolly, S. M.; Douglas, T.; McConnell, M. V., Human Ferritin Cages for Imaging Vascular Macrophages. *Biomaterials* 2011, 32, 1430-1437.
 29. Zhen, Z.; Tang, W.; Chen, H.; Lin, X.; Todd, T.; Wang, G.; Cowger, T.; Chen, X.; Xie, J., RGD-Modified Apoferritin Nanoparticles for Efficient Drug Delivery to Tumors. *ACS Nano* 2013, 7, 4830-4837.
 30. Kang, H. J.; Kang, Y. J.; Lee, Y.-M.; Shin, H.-H.; Chung, S. J.; Kang, S., Developing an Antibody-Binding Protein Cage as a Molecular Recognition Drug Modular Nanoplatform. *Biomaterials* 2012, 33, 5423-5430.
 31. Min, J.; Kim, S.; Lee, J.; Kang, S., Lumazine Synthase Protein Cage Nanoparticles as Modular Delivery Platforms for Targeted Drug Delivery. *RSC Adv.* 2014, 4, 48596-48600.
 32. Ra, J.-S.; Shin, H.-H.; Kang, S.; Do, Y., Lumazine Synthase Protein Cage Nanoparticles as Antigen Delivery Nanoplatforms for Dendritic Cell-Based Vaccine Development. *Clin. Exp. Vaccine. Res.* 2014, 3, 227-234.
 33. Kim, H.; Kang, Y. J.; Min, J.; Choi, H.; Kang, S., Development of an Antibody-Binding Modular Nanoplatform for Antibody-Guided Targeted Cell Imaging and Delivery. *RSC Adv.* 2016, 6, 19208-19213.
 34. Moon, H.; Lee, J.; Min, J.; Kang, S., Developing Genetically Engineered Encapsulin Protein Cage Nanoparticles as a Targeted Delivery Nanoplatform. *Biomacromolecules* 2014, 15, 3794-3801.
 35. Moon, H.; Lee, J.; Kim, H.; Heo, S.; Min, J.; Kang, S., Genetically Engineering

Encapsulin Protein Cage Nanoparticle as a SCC-7 Cell Targeting Optical Nanoprobe. *Biomater. Res.* 2014, 18, 21.

36. MaHam, A.; Tang, Z.; Wu, H.; Wang, J.; Lin, Y., Protein-Based Nanomedicine Platforms for Drug Delivery. *Small* 2009, 5, 1706-1721.

37. Zufferey, F.; Sherr, E. H.; Beckmann, N. D.; Hanson, E.; Maillard, A. M.; Hippolyte, L.; Mace, A.; Ferrari, C.; Kutalik, Z.; Andrieux, J.; Aylward, E.; Barker, M.; Bernier, R.; Bouquillon, S.; Conus, P.; Delobel, B.; Faucett, W. A.; Goin-Kochel, R. P.; Grant, E.; Harewood, L.; et al., A 600 kb Deletion Syndrome at 16p11.2 Leads to Energy Imbalance and Neuropsychiatric Disorders. *J. Med.Genet.* 2012, 49, 660-668.

38. Elamanchili, P.; Lutsiak, C. M. E.; Hamdy, S.; Diwan, M.; Samuel, J., "Pathogen-Mimicking" Nanoparticles for Vaccine Delivery to Dendritic Cells. *J. Immunother.* 2007, 30, 378-395.

39. Manayani, D. J.; Thomas, D.; Dryden, K. A.; Reddy, V.; Siladi, M. E.; Marlett, J. M.; Rainey, G. J. A.; Pique, M. E.; Scobie, H. M.; Yeager, M.; Young, J. A. T.; Manchester, M.; Schneemann, A., A Viral Nanoparticle with Dual Function as an Anthrax Antitoxin and Vaccine. *PLoS Pathog.* 2007, 3, 1422-1431

40. Peacey, M.; Wilson, S.; Baird, M. A.; Ward, V. K., Versatile RHDV Virus-Like Particles: Incorporation of Antigens by Genetic Modification and Chemical Conjugation. *Biotechnol. Bioeng.* 2007, 98, 968-977.

41. Richert, L. E.; Servid, A. E.; Harmsen, A. L.; Rynda-Apple, A.; Han, S.; Wiley, J. A.; Douglas, T.; Harmsen, A. G., A Virus-Like Particle Vaccine Platform Elicits Heightened and Hastened Local Lung Mucosal Antibody Production after a Single Dose. *Vaccine* 2012, 30, 3653-3665.

42. Savard, C.; Guerin, A.; Drouin, K.; Bolduc, M.; Laliberte-Gagne, M. E.; Dumas, M. C.; Majeau, N.; Leclerc, D., Improvement of the Trivalent Inactivated Flu Vaccine Using PapMV Nanoparticles. *PLoS One* 2011, 6, e21522.

43. Tacke, P. J.; Zeelenberg, I. S.; Cruz, L. J.; van Hout-Kuijter, M. A.; van de Glind, G.; Fokkink, R. G.; Lambeck, A. J. A.; Figdor, C. G., Targeted Delivery of TLR Ligands to Human and Mouse Dendritic Cells Strongly Enhances Adjuvanticity. *Blood* 2011, 118, 6836-6844.

44. Roldao, A.; Mellado, M. C. M.; Castilho, L. R.; Carrondo, M. J. T.; Alves, P. M., Virus-Like Particles in Vaccine Development. *Expert Rev. Vaccines* 2010, 9, 1149-1176.

45. Grgacic, E. V. L.; Anderson, D. A., Virus-Like Particles: Passport to Immune Recognition. *Methods* 2006, 40, 60-65.

46. Molino, N. M.; Anderson, A. K. L.; Nelson, E. L.; Wang, S.-W., Biomimetic Protein

Nanoparticles Facilitate Enhanced Dendritic Cell Activation and Cross-Presentation. *ACS Nano* 2013, 7, 9743-9752.

47. Plummer, E. M.; Manchester, M., *Viral Nanoparticles and Virus-Like Particles: Platforms for Contemporary Vaccine Design*. Wiley Interdiscip. Rev. Nanomed. Nanobiotechnol. 2011, 3, 174-196.

48. Han, J.-A.; Kang, Y. J.; Shin, C.; Ra, J.-S.; Shin, H.-H.; Hong, S. Y.; Do, Y.; Kang, S., *Ferritin Protein Cage Nanoparticles as Versatile Antigen Delivery Nanoplatforams for Dendritic Cell (DC)-Based Vaccine Development*. *Nanomedicine* 2014, 10, 561-569.

49. Sutter, M.; Boehringer, D.; Gutmann, S.; Gunther, S.; Prangishvili, D.; Loessner, M. J.; Stetter, K. O.; Weber-Ban, E.; Ban, N. *Structural Basis of Enzyme Encapsulation into a Bacterial Nanocompartment*. *Nat. Struct. Mol. Biol.* 2008, 15, 939-947.

50. Rahmanpour, R.; Bugg, T. D. H., *Assembly *in vitro* of Rhodococcus Jostii RHA1 Encapsulin and Peroxidase DypB to Form a Nanocompartment*. *FEBS J.* 2013, 280, 2097-2104.

51. Shimonkevitz, R.; Colon, S.; Kappler, J. W.; Marrack, P.; Grey, H. M., *Antigen Recognition by H-2-Restricted T-Cells. 2. A Tryptic Ovalbumin Peptide that Substitutes for Processed Antigen*. *J. Immunol.* 1984, 133, 2067-2074.

52. Clarke, S. R.; Barnden, M.; Kurts, C.; Carbone, F. R.; Miller, J. F.; Heath, W. R., *Characterization of the Ovalbumin-Specific TCR Transgenic Line OT-I: MHC Elements for Positive and Negative Selection*. *Immunol. Cell Biol.* 2000, 78, 110-117.

53. Fidler, I. J., *Biological Behavior of Malignant Melanoma Cells Correlated to Their Survival *in vivo**. *Cancer Res.* 1975, 35, 218-224.

54. Mayordomo, J. I.; Zorina, T.; Storkus, W. J.; Zitvogel, L.; Celluzzi, C.; Falo, L. D.; Melief, C. J.; Ildstad, S. T.; Kast, W. M.; Deleo, A. B.; Lotze, M. T., *Bone Marrow-Derived Dendritic Cells Pulsed with Synthetic Tumour Peptides Elicit Protective and Therapeutic Antitumour Immunity*. *Nat. Med.* 1995, 1, 1297-1302.

55. Berzofsky, J. A.; Ahlers, J. D.; Belyakov, I. M., *Strategies for Designing and Optimizing New Generation Vaccines*. *Nat. Rev. Immunol.* 2001, 1, 209-219.

56. Lyons, A. B., *Analysing Cell Division *in vivo* and *in vitro* Using Flow Cytometric Measurement of CFSE Dye Dilution*. *J. Immunol. Methods* 2000, 243, 147-154.

57. Mittelbrunn, M.; Martinez del Hoyo, G.; Lopez-Bravo, M.; Martin-Cofreces, N. B.; Scholer, A.; Hugues, S.; Fetler, L.; Amigorena, S.; Ardavin, C.; Sanchez-Madrid, F., *Imaging of Plasmacytoid Dendritic Cell Interactions with T cells*. *Blood* 2009, 113, 75-84.

58. Oehen, S.; Brduscha-Riem, K., *Differentiation of Naive CTL to Effector and Memory CTL: Correlation of Effector Function with Phenotype and Cell Division*. *J. Immunol.* 1998,

161, 5338-5346.

59. Sad, S.; Marcotte, R.; Mosmann, T. R., Cytokine-Induced Differentiation of Precursor Mouse CD8⁺ T cells into Cytotoxic CD8⁺ T cells Secreting Th1 or Th2 Cytokines. *Immunity* 1995, 2, 271-279.
60. Kast, W. M.; Brandt, R. M.; Melief, C. J., Strict Peptide Length is not Required for the Induction of Cytotoxic T Lymphocyte-Mediated Antiviral Protection by Peptide Vaccination. *Eur. J. Immunol.* 1993, 23, 1189-1192.
61. Toes, R. E.; Blom, R. J.; Offringa, R.; Kast, W. M.; Melief, C. J., Enhanced Tumor Outgrowth after Peptide Vaccination. Functional Deletion of Tumor-Specific CTL Induced by Peptide Vaccination Can Lead to the Inability to Reject Tumors. *J. Immunol.* 1996, 156, 3911-3918.
62. Gajewski, T. F.; Schreiber, H.; Fu, Y. X., Innate and Adaptive Immune Cells in the Tumor Microenvironment. *Nat. Immunol.* 2013, 14, 1014-1022.
63. Spranger, S.; Spaapen, R. M.; Zha, Y.; Williams, J.; Meng, Y.; Ha, T. T.; Gajewski, T. F., Up-Regulation of PD-L1, IDO, and T(regs) in the Melanoma Tumor Microenvironment is Driven by CD8(+) T cells. *Sci. Transl. Med.* 2013, 5, 200ra116.
64. Hogquist, K. A.; Jameson, S. C.; Heath, W. R.; Howard, J. L.; Bevan, M. J.; Carbone, F. R., T cell Receptor Antagonist Peptides Induce Positive Selection. *Cell* 1994, 76, 17-27.
65. Miksa, M.; Komura, H.; Wu, R.; Shah, K. G.; Wang, P., A Novel Method to Determine the Engulfment of Apoptotic Cells by Macrophages Using pHrodo Succinimidyl Ester. *J. Immunol. Methods* 2009, 342, 71-77
66. Yuan, Y.; Shen, H.; Franklin, D. S.; Scadden, D. T.; Cheng, T., *In vivo* Self-Renewing Divisions of Haematopoietic Stem Cells are Increased in the Absence of the Early G1-Phase Inhibitor, p18INK4C. *Nat. Cell Biol.* 2004, 6, 436-442.

3. Covalent Conjugation of Small-Molecule Adjuvants to Nanoparticles Induces Robust Cytotoxic T Cell Responses via DC Activation

3.1 Abstract

Specific recognitions of pathogen associated molecular patterns by Toll-like receptors (TLRs) initiate dendritic cell (DC) activation, which are critical for coordinating innate and adaptive immune responses. Imidazoquinolines as small-molecule TLR7 agonists often suffer from their prompt dissemination and short half-life in the bloodstream, preventing their localization to the corresponding receptors and effective DC activation. We postulated that covalent incorporation of imidazoquinoline moieties onto the surface of biocompatible nanoparticles (~30 nm size) would enhance their chemical stability, cellular uptake efficiency, and adjuvanticity. The fully synthetic adjuvant-nanocomplexes led to successful DC activation at lower nanomolar doses compared with free small-molecule agonists. Once a model antigen such as ovalbumin was used for immunization, we found that the nanocomplexes promoted an unusually strong cytotoxic T lymphocyte response, revealing their unique immunostimulatory capacity benefiting from multivalency and efficient transport to endosomal TLR7.

3.2 Introduction

DCs are the most potent APCs, which coordinate between the innate and adaptive immune systems.¹ They are specialized to engulf and process antigens and subsequently present epitopes to elicit robust immune responses.²⁻⁴ APCs express various types of pattern recognition receptors including lectins or TLRs to distinguish between self- and non-self-structures. Recognition of PAMPs by TLRs generally induces DC activation.^{5,6,7} Activated DCs present foreign epitopes of antigens onto MHCs and increase the expression of co-stimulatory molecules (CD80, CD86) to help cognate interaction with TCR. The expression of chemokine receptor CCR7 leads DCs to migrate into lymph nodes, where naïve T cells are transformed into functional T lymphocytes including CTLs.^{8,9}

TLR7, located within endosomal compartment, is a promising adjuvant target-site for DC-mediated immunization. It recognizes nucleotide-derived compounds, including single-stranded RNA or low-molecular-weight imidazoquinoline derivatives, such as R837 (imiquimod) and R848 (resiquimod).^{5,8,10} Yet, promotion of robust CTL responses by small-molecule adjuvants is highly challenging due to their prompt dissemination through diffusion.^{8,11-13} To overcome these hurdles, polymeric or inorganic nanoparticles (NPs) encapsulating imidazoquinolines have been introduced to enhance stability and biodistribution of TLR7 agonists, consequently improving DC activation efficiency.¹⁴⁻¹⁷ Here, we describe the first synthetic approach for preparing covalently linked imidazoquinoline-nanoconjugates for inducing robust CTL responses (Figure 3.1). Our design can entirely avoid the potential time-based release of small-molecule agonists from the non-covalently functionalized nanocarriers through the interactions between cell membranes and engineered NPs. However, the challenges associated with our approach are two-fold. First, the design of nanocomplexes requires multi-step reactions to achieve a molecularly well-defined structure. Second, the synthetic nanocomplexes should effectively initiate TLR-mediated DC activation and subsequently induce T cell immunity. To validate our working hypothesis, we designed alkyne-functionalized imidazoquinoline derivatives and covalently conjugated them with biocompatible NPs to examine their role in DC maturation and generation of CTL response.

3.3 Materials and Methods

Reagents

N,N,N',N'-Tetramethyl-*O*-(1*H*-benzotriazol-1-yl)uronium hexafluorophosphate (HBTU, 98%), 4-pentynoic acid (95%), copper(II) sulfate pentahydrate (98%), (+)-sodium L-ascorbate (98%), and *N*-hydroxysuccinimide (NHS, 98%) were purchased from Sigma-Aldrich. Amine-functionalized iron oxide (Fe₃O₄) magnetic nanoparticles (aqueous solution, 5 mg Fe/mL) were supplied by Ocean nanotech. Triethylamine (TEA, 99%) was obtained from Alfa Aesar. NHS-fluorescein (5/6-carboxyfluorescein succinimidyl ester) was purchased from Thermo Scientific.

Synthesis of Adjuvant 1

Adjuvant **2**²¹ (400 mg, 1.11 mmol) and TEA (547 μ L, 3.89 mmol, 3.5 equiv) were dissolved in DCM (80 mL). 4-pentynoic acid (142 mg, 1.45 mmol, 1.3 equiv) and HBTU (549 mg, 1.45 mmol, 1.3 equiv) were added at 0 °C, and the solution left to stir overnight at room temperature. The reaction mixture was concentrated *in vacuo* and the residue was purified by flash column chromatography (DCM:MeOH:NH₄OH = 9.5:0.5:0.1) to yield the title compound as a clear oil (261 mg, 53%). ¹H NMR (400 MHz, MeOD) δ_{H} 0.92 (t, *J* 7.4 Hz, 3H), 1.42 (dt, *J* 14.7, 7.4 Hz, 2H), 1.77 (dt, *J* 15.4, 7.6 Hz, 2H), 2.20 (t, *J* 2.6 Hz, 1H), 2.34-2.49 (m, 4H), 4.33 (s, 2H), 5.82 (s, 2H), 7.00 (d, *J* 8.1 Hz, 2H), 7.09 (m, 1H), 7.27 (d, *J* 8.1 Hz, 2H), 7.41 (m, 1H), 7.65 (dd, *J* 8.3, 0.4 Hz, 1H), 7.78 (d, *J* 7.8 Hz, 1H); ¹³C NMR (150 MHz, MeOD) δ_{C} 14.1, 15.7, 23.4, 27.8, 30.7, 35.9, 43.6, 49.5, 70.3, 83.5, 115.7, 121.5, 123.4, 126.2, 126.7, 126.9, 128.5, 129.4, 135.4, 136.0, 139.8, 144.8, 152.5, 156.0, 173.8.; HRMS (ESI): Calcd for C₂₇H₃₀N₅O⁺ [M+H]⁺: 440.2445, found 440.2445.

Synthesis of Azido-NPs

Spacer **3**³⁷ (30 mg, 116 μ mol) dissolved in DMF was added to the Amine-NPs (1.5 mg Fe). Mixture was stirred at room temperature for a day, then dialyzed in DI water was conducted for 3 times to remove non-conjugated molecules in excess.

Synthesis of Adjuvant-NPs: Adjuvant **1** (2.55 mg, 5.80 μ mol, 15 equiv) dissolved in DMF, CuSO₄·6H₂O (1.45 mg, 5.80 μ mol, 15 equiv) and (+)-sodium L-ascorbate (1.15 mg, 5.80

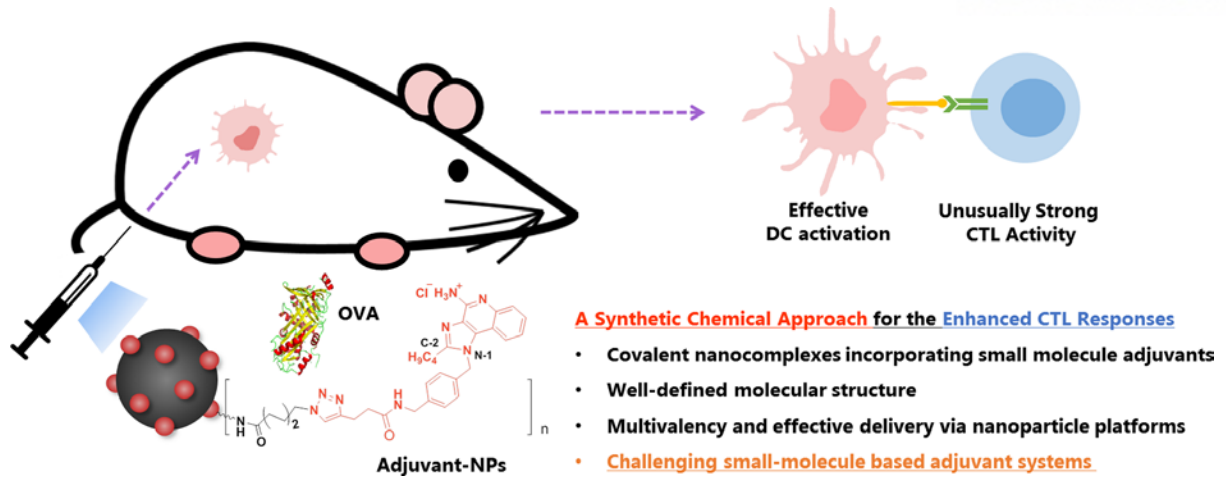


Figure 3.1 General attributes of Adjuvant-NPs in inducing DC activation and a robust CTL response.

μmol , 15 equiv) was added to Azide-NPs and stirred at room temperature for a day. The reaction mixture was dialyzed in DI water for two times then, treated with 0.1 M Tris buffer (pH 6) for 2 times to form ammonium salt of imidazoquinoline moiety. Solution was filtered through 0.2 μm pore size filter and concentrated to 3 mg/mL Fe dissolved in autoclaved PBS buffer by using centrifugal filter (3000 rpm, 12 min).

Synthesis of Fluorescein-Adjuvant-NPs

For the fluorescence analysis and confocal analysis of DC uptake with nanoparticle, NHS-fluorescein was utilized to append fluorescein to Adjuvant-NPs (Figure 3.S1). To a solution of Adjuvant-NPs in PBS buffer was added NHS-fluorescein (0.92 mg, 1.94 μmol , 5 equiv to Amine-NPs (1.5 mg Fe)) and stirred for 1 day at room temperature. NHS-fluorescein in excess was removed by DI water dialysis (for 3 times) and the solution was centrifuged (3000 rpm, 12 min, for 3 times). Then Fluorescein-Adjuvant-NPs were concentrated to 3 mg Fe/mL in autoclaved PBS buffer.

Instruments

Proton nuclear magnetic resonance and carbon nuclear magnetic resonance spectra were recorded by an Agilent 400-MR DD2 and an Agilent VNMRS 600. Low resolution mass spectra were measured by a Bruker HCT Basic System with electrospray ionization (ESI) source. High resolution mass spectra were measured by an ABI API-3000 ESI mass spectrometer. Fluorescence spectra were measured by using an Agilent Cary Eclipse fluorescence spectrophotometer. UV-Vis spectra were recorded by a Jasco V-670 spectrometer. Dynamic light scattering (DLS) measurements were performed by a Brookhaven Instrument Corporation's NanoDLS. Transmission electron microscopy (TEM) images were taken by a JEOL JEM-1400.

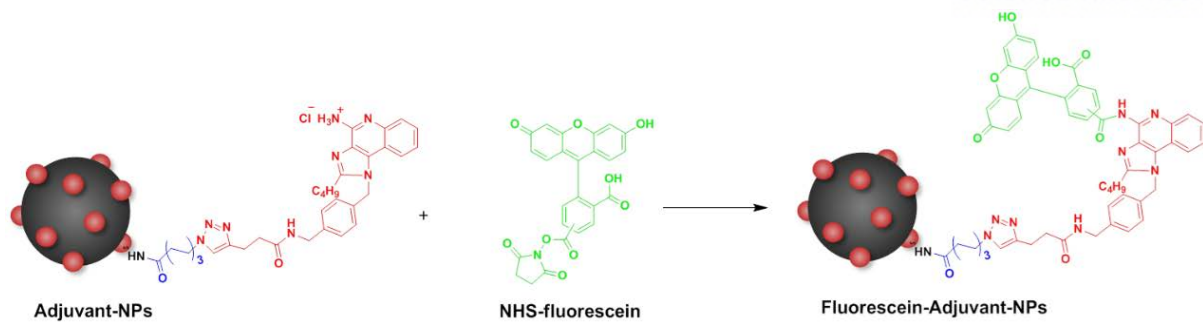


Figure 3.S1 Synthesis of Fluorescein-Adjuvant-NPs.

Mice

Female C57BL/6 mice were purchased from Taconic. All mice were maintained under specific pathogen-free (SPF) conditions and used at 6-8 weeks with Institutional Animal Care and Use guidelines. The Institutional Animal Care and Use Committee of the Ulsan National Institute of Science and Technology (UNISTIACUC) approved the *in vivo* animal experiments conducted in this study

DC Maturation

Mice were injected intraperitoneally (I.P.) with R848 (InvivoGen, San Diego, CA), adjuvant 1', amine-NPs, adjuvant-NPs, or PBS for *in vivo* DC maturation. Mice were sacrificed after 18 hours of injection. Whole splenocytes were harvested and stained with CD11c FITC. Cells were subsequently stained with CD80 PE, CD86 PE, MHC II PE, CCR7 PE and isotypes control (supplied by BioLegend®). Maturation of CD11c⁺ DC were measured by BD FACS Fortessa and analyzed by FlowJo software (TreeStar).

DC Isolation

Spleens were harvested from mice to HBSS buffer (GIBCO), then, ballooning with 400 Mandl U/ml collagenase D (Roche) and tear them into small pieces by 25G needle and 3 ml syringe. CD11c⁺ cells were positively enriched with magnetic activated cell sorting (MACS, Miltenyi Biotech). Sorted T cells showed >98 % purity, as detected by flow cytometry. All flow cytometry data were acquired by BD FACS Fortessa and analyzed by FlowJo software (TreeStar).

Confocal Microscopic Imaging of DCs

1×10^6 Cells/ml of immature DCs were isolated and incubated on coverslip in 24 wells plate with indicated PBS or NP 7 with 5 μ g of OVA protein as model antigens onto cover slip for 18 hours at 37 °C. Matured DCs were treated with 50 nM of lysotracker (Thermo-Fisher scientific) to stain the lysosome with red fluorescence for last 2 hours. Nucleus was stained with DAPI and images of green fluorescence of NP and red fluorescence of lysosome were obtained by FV1000 confocal microscopy (Olympus).

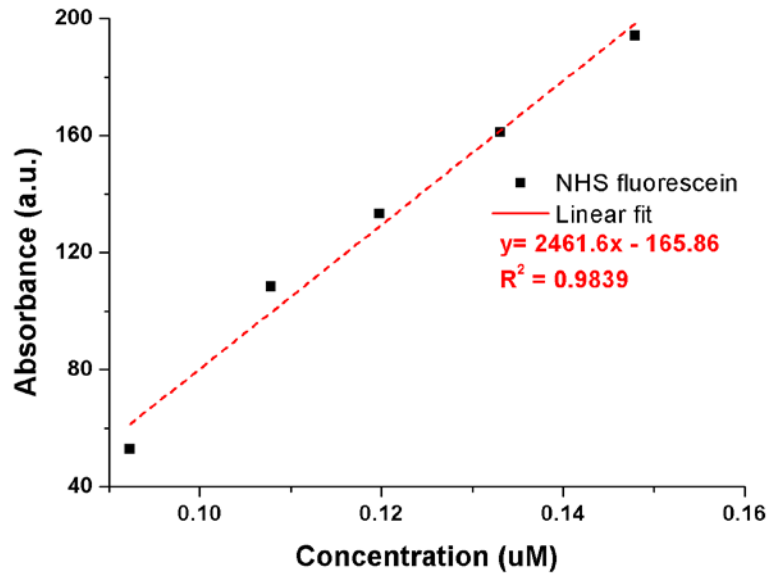


Figure 3.S2. A calibration curve of NHS fluorescein.

***In vivo* CTL Assay**

For *in vivo* CTL assay, mice were immunized with 50 µg of OVA protein with indicated adjuvant intraperitoneally; list indicated adjuvants. After 7 days, mice were re-immunized to boost immune responses. Then, mice were intravenously injected with 1:1 mixtures of OT-I peptide-pulsed (5 µM CFSE-labeled, CFSE^{hi}) and unpulsed (0.5 µM CFSE-labeled, CFSE^{low}) syngeneic splenocytes (7×10^6 of each). 18 Hours later, single cells were harvested from lymph nodes and spleens from each mouse. OT-I specific CTL activity was evaluated by flow cytometry. We repeated *in vivo* CTL assay three times and three mice were used in each group (total 9 mice/experimental set).

Tetramer assay

To investigate OVA epitope (OT-I peptide) specificity induced by adjuvant-NPs vaccination, immunized mice as CTL experiment were sacrificed and single homogenized splenocytes were harvested. Cells were meshed with 70 µm pore strainer, then, re-stimulated with OT-I peptide (1 µM) in 96 well plate (5×10^5 cells/ 200 µl) at humidified incubator for 4 days. OT-I peptide specific T cell receptor expressing T cells were stained with PE-conjugated MHC I tetramer (glycotope), then, analyzed by flow cytometry.

3.4 Results

Although live-attenuated vaccines can elicit long-term immunity, they have a potential risk of infection, and practically not suitable to vaccine against pathogens such as influenza, HIV, or Ebola virus.¹⁸ In contrast, subunit vaccines provide superior safety profiles and allow tunable design at the molecular-level to elicit predictable immune responses. However, they are short-lived and poorly immunogenic. Thus, immunostimulatory adjuvants are required to generate potent T cell immunity.^{8,18} The advent of engineered nanocomplexes loaded with imidazoquinoline analogues opens up new opportunities to effectively target TLR7, yet investigations have been established on the basis of non-covalent encapsulation chemistry. Although CpG oligodeoxynucleotide-NP complexes have been previously demonstrated,^{19,20} NPs covalently incorporating the small-molecule cognate ligands without repeating monomer units have not been reported so far.

To synthesize well-defined molecular adjuvant-nanocomplexes, we designed and prepared an imidazoquinoline analogue (adjuvant **1**) with a terminal alkyne moiety to couple with azide coated iron oxide NPs (see Figure 3.2a). Adjuvant **2** was synthesized from 2,4-quinolinediol as previously described by the David group.²¹⁻²⁴ Based on the previous structure-activity relationship studies,^{21,25-28} *n*-butyl group was introduced at C-2 position to increase TLR7 agonistic potency. Further, an alkyne functionality as a versatile anchor was placed at N-1 position for next-stage chemical reactions, since the site modification does not significantly compromise agonistic potency. Molecular structure of TLR7 agonist, Adjuvant **1**, was confirmed by ¹H and ¹³C NMR spectra (Figures 3.2b and 3.2c). For the conjugation platform displaying multivalency, water-soluble and surface-engineered iron oxide NPs were selected because of their biocompatibility and monodisperse size.^{29,30} Biocompatible NPs with monodisperse size ranges of ~30 nm can be used as nanocarriers *in vivo*, which are optimal for internalization by immature DCs by facilitating endolysosomal pathway, and can be trafficked into the draining lymph nodes, thereby enhancing their adjuvanticity.^{11,20,31-34} Amine-surface-modified iron oxide NPs (Amine-NPs) were then reacted with Spacer **3** with an activated ester moiety, to afford Azide-NPs, since azido functionality can be readily installed and is highly orthogonal and versatile for further transformations. Finally, Adjuvant **1** was conjugated by Cu^I-catalyzed Huisgen 1,3-dipolar cycloaddition reaction and treated with 0.1 M Tris buffer (pH 6) to form Adjuvant-NPs (for the details, see the Experimental Section and the Supporting Information).

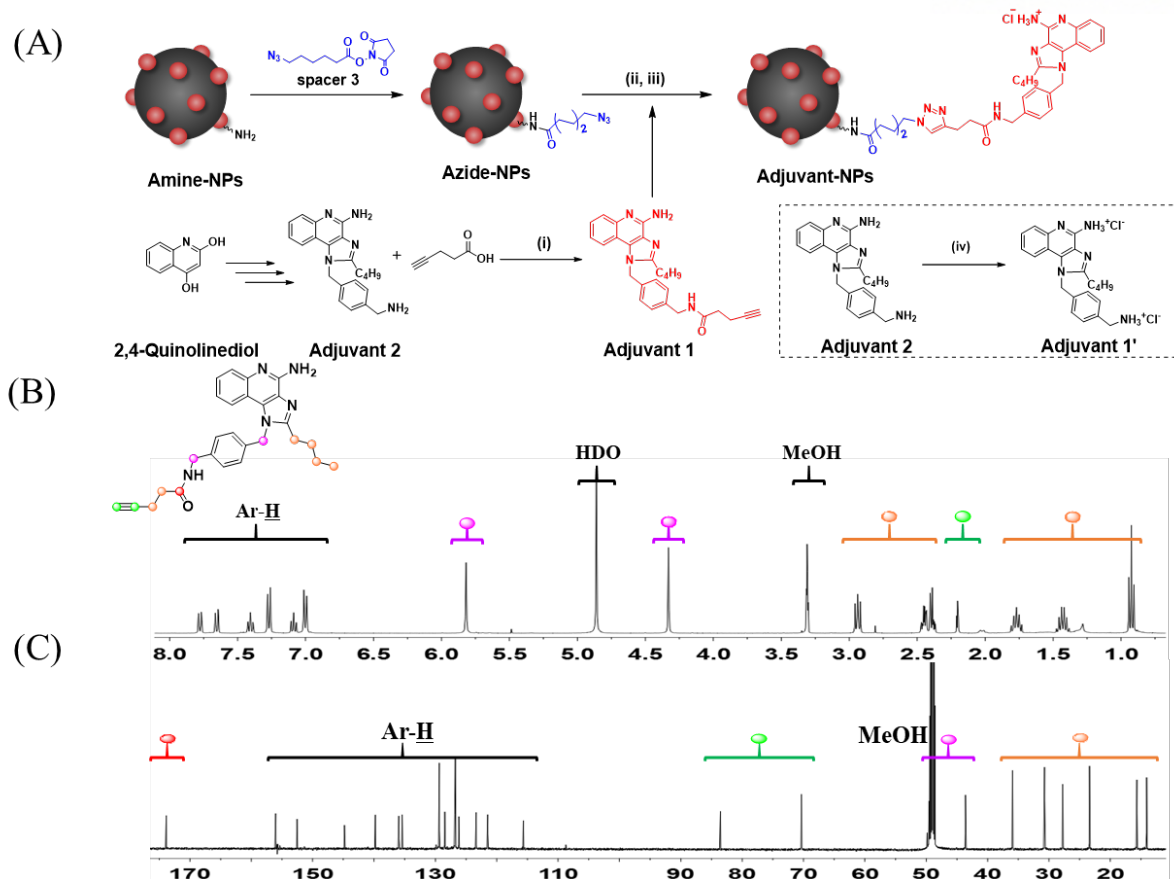


Figure 3.2 (A) Synthetic scheme of Adjuvant-NPs (i) HBTU, TEA, DCM, (ii) $\text{CuSO}_4 \cdot 5\text{H}_2\text{O}$, sodium ascorbate, DMF, (iii) 0.1 M Tris buffer (pH 6), and (iv) diluted hydrogen chloride solution. (B, C) ^1H and ^{13}C NMR spectra (MeOD) of Adjuvant 1.

Core- and hydrodynamic sizes of the synthetic nanocomplexes were determined by transmission electron microscopy (TEM) and dynamic light scattering (DLS) analyses, respectively (Figures 3.3a and 3.3b). TEM image revealed spherical and monodisperse particles with ~11 nm core diameters of Adjuvant-NPs without any signs of particle aggregation, even after multi-step chemical modifications. DLS data analysis showed an effective diameter of 31.6 nm and a narrow size distribution with polydispersity index (PDI) = 0.258. Previously NPs having ~30 nm size have been demonstrated to be efficiently uptaken by DCs.^{19,20} Moreover, we carried out spectroscopic studies to examine the effectiveness of imidazoquinoline conjugation. UV-Vis spectrum of Adjuvant-NPs showed distinct imidazoquinoline peaks at about 225, 246, and 321 nm with slight peak shifts (Figure 3.3c). To quantify the loading level, a fluorescence assay was conducted (Figure 2.3d), since iron oxide NPs are weakly fluorescent. NHS-fluorescein is an amine reactive fluorescent probe bearing an activated ester moiety, thus fluorophore can be appended to Adjuvant-NPs to generate Fluorescein-Adjuvant-NPs. Based on the standard curve of NHS-fluorescein and iron concentration of NPs, the loading amount of imidazoquinolines in Adjuvant-NPs was estimated to be 0.139 $\mu\text{mol}/[\text{mg Fe}]$ (see Supporting Information, Figures S1 and S2).

Further, we evaluated DC activation efficacies by using synthetic TLR7 agonists. Adjuvant-NPs or free Adjuvant **1'** were intraperitoneally injected into mice, and their DCs were harvested 18 hours later. DC activation markers including CD80, CD86, MHC I, and CCR7 were stained with phycoerythrin (PE)-conjugated antibodies and analyzed by flow cytometry. R848,¹⁰ Adjuvant-NPs, or Adjuvant **1'** effectively increased the expression levels of the activation markers (Figure 3.4 and Figures S3-S5). Highly water-soluble Adjuvant **1'** acted as an effective stimulant of DC activation at 115.6 nmol or even at a concentration as low as 69.4 nmol (Figure S3). Amine-NPs showed weak self-adjutant effect (Figure S5). Remarkably, 13.9 nmol of Adjuvant-NPs (concentration in loading levels of cognate ligands) and 115.6 nmol of free Adjuvant **1'** induced comparable immunostimulatory activities. This is attributed to the enhanced avidity as well as effective internalization of the nanocomplexes to the endosomal TLR7 of DCs.

Since TLR7 is expressed inside endosomal compartments of DCs, effective delivery of antigens and adjuvants into DCs is indispensable for their proper activation and subsequent immune response. However, free small molecules hardly localize to TLRs; thus, they require effective delivery vehicles. To examine cellular internalization of the nanocomplexes and their appropriate localization in DCs, we prepared Fluorescein-Adjuvant-NPs as probes (see Supporting Information) and studied their uptake using

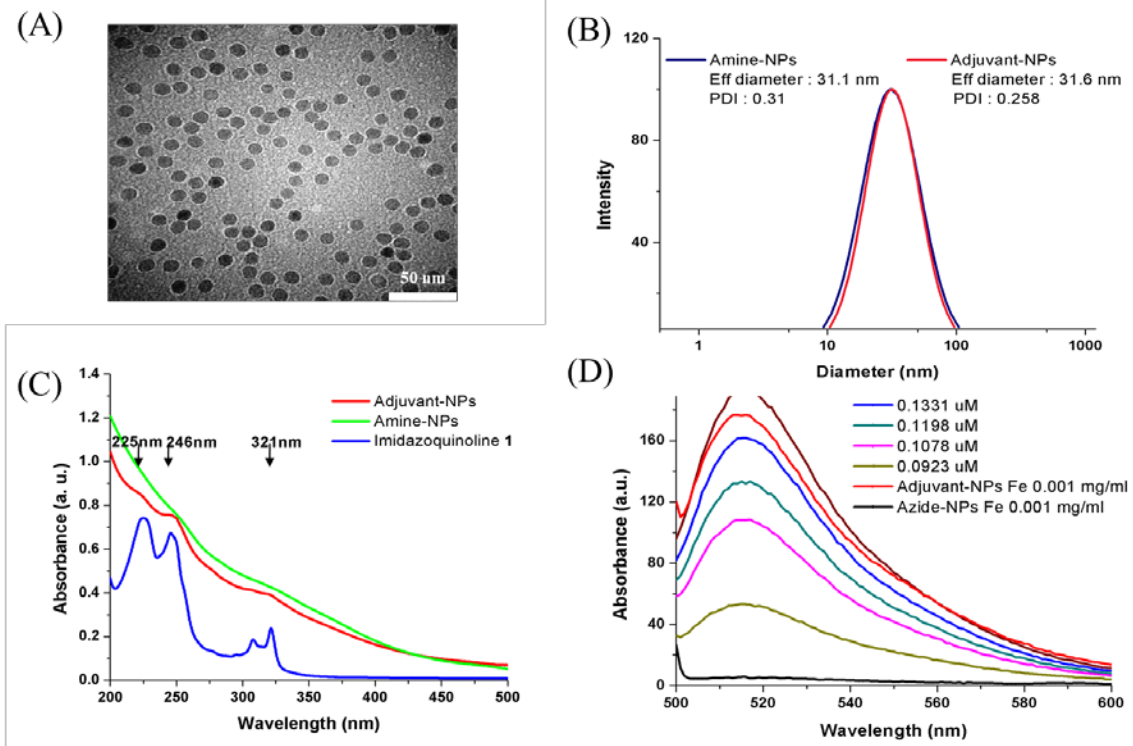


Figure 3.3. Characterization of Adjuvant-NPs. (A) TEM image of Adjuvant-NPs, (B) DLS analysis, (C) UV-vis spectra, and (D) fluorescence spectra.

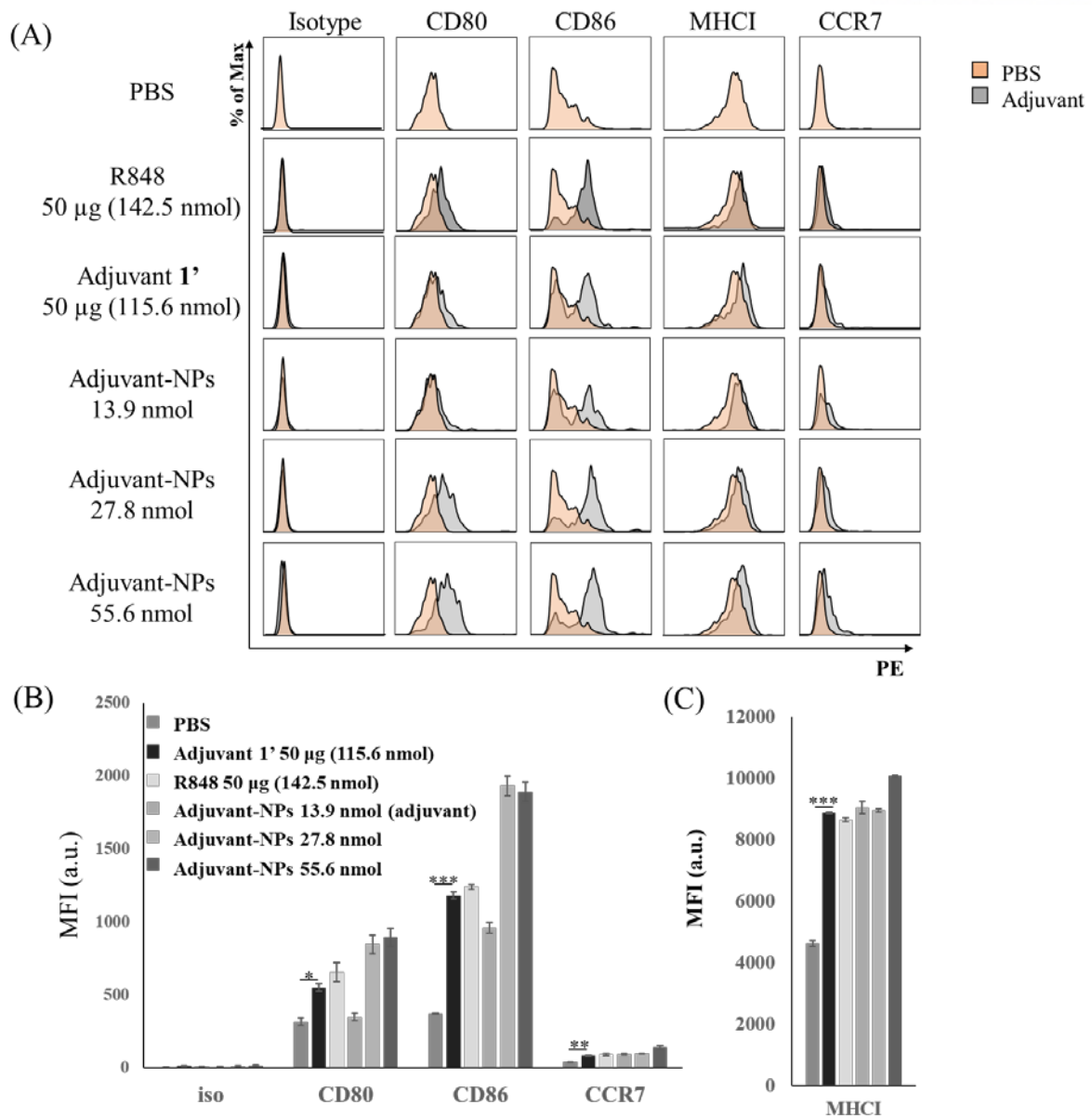


Figure 3.4 Adjuvant effects on *in vivo* DC activation: (A) flow cytometry analyses, and (B, C) the mean fluorescence intensity (MFI) levels of DC activation markers (CD80, CD86, CCR7, and MHC I). The P values of <0.05 (*), <0.01 (**), and <0.001 (***) were considered significant.

confocal fluorescence microscopy (Figure 3.5a). The complexes were cultured with immature DCs *in vitro* in the presence of OVA as a model antigen. After 18 hours, the cells were fixed, and the nuclei and low pH endosomes were stained with DAPI and LysoTracker, respectively. Fluorescein-Adjuvant-NPs were localized within endosomes thanks to their suitable particle size (~30 nm) (Figure 3.5b).^{19,20} Also, properly activated DCs secrete high quantity of pro-inflammatory cytokines to activate further immune responses. (Koch, F. et al. The Journal of experimental medicine 1996, 184, 741-6.) ELISA assay to detect IL-12p40 from DC supernatant cultured with adjuvant NPs and OVA suggest almost equal secretion of IL-12p40 compared with adjuvant 1 (Figure 3.5c), which can assist imidazoquinoline cognate agonists effectively interact with TLR7 within DC endosomes.

The efficient DC activation and nanocomplex internalization prompted us to test whether these mature DCs can elicit sufficient cytotoxic CD8⁺ T cell responses. We performed an *in vivo* CTL assay based on the CFSE assay to monitor OVA-specific T cell proliferation.^{35,36} Mice were intraperitoneally immunized with 25 µg of OVA protein as an antigen in the presence of PBS, R848, Amine-NPs, or Adjuvant-NPs as TLR7 agonists. Groups of mice were primarily immunized for 2 weeks, and additionally boosted for 1 week. After immunization, mice were intravenously injected with 1:1 mixtures of OT-1 peptide-pulsed (CFSE^{hi}) and unpulsed (CFSE^{low}) syngeneic splenocytes to evaluate OVA-specific CTL activity. The population of OT-1 peptide pulsed target cells was analyzed by flow cytometry. It is speculated that if OT-1 specific T cells are effectively stimulated by mature DCs with OVA protein and adjuvants, the OT-1 peptide-pulsed (CFSE^{hi}) syngeneic splenocytes would be lysed and their population decreased. Remarkably, injection of Adjuvant-NPs with 27.8 nmol of adjuvant together with OVA protein caused 84% target cell lysis (Figure 3.6). In contrast, small-molecule R848 (28.5 or 142.5 nmol) or Amine-NPs showed negligible to poor (0-25%) cytotoxic responses. It is speculated that superior CD8⁺ T cell efficacy of Adjuvant-NPs at low doses of imidazoquinoline moiety is associated with the enhanced avidity of fully synthesized multivalent adjuvant-NPs and effective DC internalization.

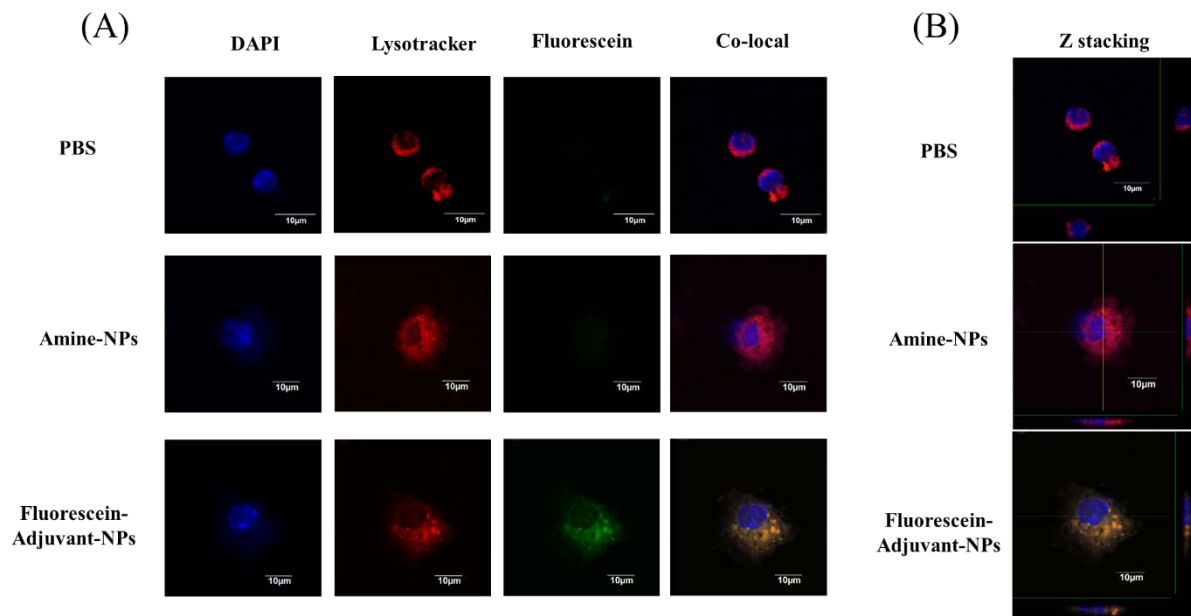


Figure 3.5 Fluorescence imaging studies to examine the internalization of Fluorescein-Adjuvant-NPs in DCs. (A, B) Samples were characterized by confocal fluorescent microscopy.

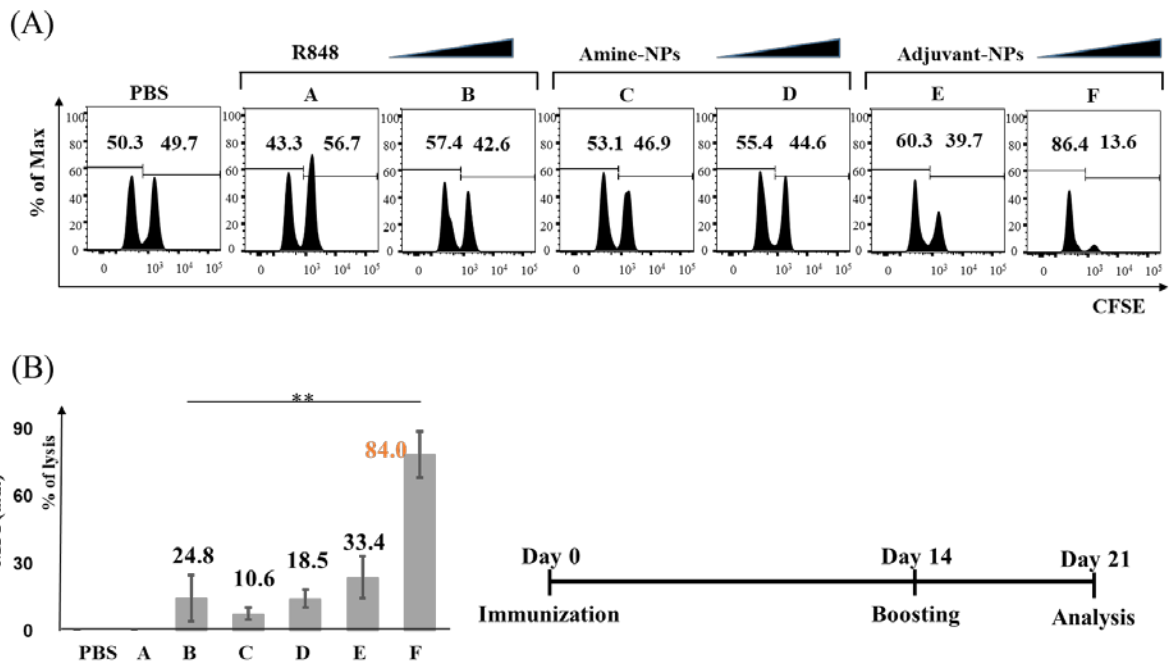


Figure 3.6 *In vivo* CTL assay on splenocytes. (A) Percentages of OT-1 peptide unpulsed CFSE^{low} (left) and that of pulsed CFSE^{high} (right) were analyzed by flow cytometry. Each group was stimulated with indicated adjuvants: Sample A: R848 10 μ g, 28.5 nmol; sample B: R 848 50 μ g, 142.5 nmol; sample C: amine-NPs 100 μ g Fe; sample D: amine NPs 200 μ g Fe; sample E: Adjuvant-NPs (100 μ g Fe, 13.9 nmol of imidazoquinoline); sample F: Adjuvant-NPs (200 μ g Fe, 27.8 nmol of imidazoquinoline) along with OVA protein. (B) Conversion of the percentages of CFSE^{high} based on the negative control of PBS treated group. The P values of <0.01(**) were considered significant.

3.5 Discussion

We chemically synthesized structurally well-defined molecular adjuvant-nanoparticle conjugates through multi-step reactions and investigated their potency of their immunostimulatory activity. The nanocomplexes displaying multiple low-molecular-weight ligands were efficiently internalized by immature DCs, and they subsequently enhanced *in vivo* DC activation by facilitating multivalent interactions between imidazoquinoline moieties and endosomal TLR7. In addition, they induced increased expression levels of activation markers in the low nanomolar range. Their cellular localization was validated by fluorescent labeling of the nanocomplexes. Co-administration of the synthetic adjuvant-nanocomplexes and OVA protein elicited unusually robust antigen-specific cytotoxic T cell responses. Considering the significant challenges generating cell-mediated immunity via small-molecule based adjuvant systems, we believe that our synthetic approach can provide a versatile platform for the rational designing of next-generation vaccines.

3.6 References

1. Tacke, P. J., de Vries, I. J. M., Torensma, R., and Figdor, C. G. (2007) Dendritic-cell immunotherapy: from ex vivo loading to *in vivo* targeting. *Nat. Rev. Immunol.* 7, 790–802.
2. Palucka, K., and Banchereau, J. (2012) Cancer immunotherapy via dendritic cells. *Nat. Rev. Cancer* 12, 265–277.
3. Mandal, S., Hammink, R., Tel, J., Eksteen-Akeroyd, Z. H., Rowan, A. E., Blank, K., and Figdor, C. G. (2015) Polymer-based synthetic dendritic cells for tailoring robust and multifunctional T cell responses. *ACS Chem. Biol.* 10, 485–492.
4. Mandal, S., Eksteen-Akeroyd, Z. H., Jacobs, M. J., Hammink, R., Koepf, M., Lambeck, A. J. A., van Hest, J. C. M., Wilson, C. J., Blank, K., Figdor, C. G., et al. (2013) Therapeutic nanoworms: towards novel synthetic dendritic cells for immunotherapy. *Chem. Sci.* 4, 4168–4174.
5. O’Neill, L. A. J., Golenbock, D., and Bowie, A. G. (2013) The history of Toll-like receptors-redefining innate immunity. *Nat. Rev. Immunol.* 13, 453–460.
6. Iwasaki, A., and Medzhitov, R. (2010) Regulation of adaptive immunity by the innate immune system. *Science* 327, 291–295.
7. Tom, J. K., Dotsey, E. Y., Wong, H. Y., Stutts, L., Moore, T., Davies, D. H., Felgner, P. L., and Esser-Kahn, A. P. (2015) Modulation of innate immune responses via covalently linked TLR agonists. *ACS Cent. Sci.* 1, 439–448.
8. Moyle, P. M., and Toth, I. (2013) Modern subunit vaccines: development, components, and research opportunities. *ChemMed-Chem* 8, 360–376.
9. Palucka, K., Banchereau, J., and Mellman, I. (2010) Designing vaccines based on biology of human dendritic cell subsets. *Immunity* 33, 464–478.
10. Hemmi, H., Kaisho, T., Takeuchi, O., Sato, S., Sanjo, H., Hoshino, K., Horiuchi, T., Tomizawa, H., Takeda, K., and Akira, S. (2002) Small anti-viral compounds activate immune cells via the TLR7/MyD88-dependent signaling pathway. *Nat. Immunol.* 3, 196–200.
11. Moon, J. J., Huang, B., and Irvine, D. J. (2012) Engineering nano- and microparticles to tune immunity. *Adv. Mater.* 24, 3724–3746.
12. Rajagopal, D., Paturel, C., Morel, Y., Uematsu, S., Akira, S., and Diebold, S. S. (2010) Plasmacytoid dendritic cell-derived type I interferon is crucial for the adjuvant activity of Toll-like receptor 7 agonists. *Blood* 115, 1949–1957.
13. Warshakoon, H. J., Hood, J. D., Kimbrell, M. R., Malladi, S., Wu, W. Y., Shukla, N. M., Agnihotri, G., Sil, D., and David, S. A. (2009) Potential adjuvant properties of innate immune stimuli. *Hum. Vaccines* 5, 381–394.

14. Kasturi, S. P., Skountzou, I., Albrecht, R. A., Koutsonanos, D., Hua, T., Nakaya, H. I., Ravindran, R., Stewart, S., Alam, M., Kwissa, M., et al. (2011) Programming the magnitude and persistence of antibody responses with innate immunity. *Nature* 470, 543–550.
15. Heo, M. B., and Lim, Y. T. (2014) Programmed nanoparticles for combined immunomodulation, antigen presentation and tracking of immunotherapeutic cells. *Biomaterials* 35, 590–600.
16. Ilyinskii, P. O., Roy, C. J., O’Neil, C. P., Browning, E. A., Pittet, L. A., Altreuter, D. H., Alexis, F., Tonti, E., Shi, J., Basto, P. A., et al. (2014) Adjuvant-carrying synthetic vaccine particles augment the immune response to encapsulated antigen and exhibit strong local immune activation without inducing systemic cytokine release. *Vaccine* 32, 2882–2895.
17. Tacke, P. J., Zeelenberg, I. S., Cruz, L. J., van Hout-Kuijper, M. A., van de Glind, G., Fokink, R. G., Lambeck, A. J. A., and Figdor, C. G. (2011) Targeted delivery of TLR ligands to human and mouse dendritic cells strongly enhances adjuvanticity. *Blood* 118, 6836–6844.
18. Coffman, R. L., Sher, A., and Seder, R. A. (2010) Vaccine adjuvants: putting innate immunity to work. *Immunity* 33, 492–503.
19. de Titta, A., Ballester, M., Julier, Z., Nembrini, C., Jeanbart, L., van der Vlies, A. J., Swartz, M. A., and Hubbell, J. A. (2013) Nanoparticle conjugation of CpG enhances adjuvancy for cellular immunity and memory recall at low dose. *Proc. Natl. Acad. Sci. U. S. A.* 110, 19902–19907.
20. Molino, N. M., Anderson, A. K. L., Nelson, E. L., and Wang, S.-W. (2013) Biomimetic protein nanoparticles facilitate enhanced dendritic cell activation and cross-presentation. *ACS Nano* 7, 9743–9752.
21. Shukla, N. M., Malladi, S. S., Mutz, C. A., Balakrishna, R., and David, S. A. (2010) Structure-activity relationships in human toll-like receptor 7-active imidazoquinoline analogues. *J. Med. Chem.* 53, 4450–4465.
22. Shukla, N. M., Mutz, C. A., Ukani, R., Warshakoon, H. J., Moore, D. S., and David, S. A. (2010) Syntheses of fluorescent imidazoquinoline conjugates as probes of Toll-like receptor 7. *Bioorg. Med. Chem. Lett.* 20, 6384–6386.
23. Shukla, N. M., Lewis, T. C., Day, T. P., Mutz, C. A., Ukani, R., Hamilton, C. D., Balakrishna, R., and David, S. A. (2011) Toward selfadjuvanting subunit vaccines: model peptide and protein antigens incorporating covalently bound toll-like receptor-7 agonistic imidazoquinolines. *Bioorg. Med. Chem. Lett.* 21, 3232–3236.
24. Shukla, N. M., Mutz, C. A., Malladi, S. S., Warshakoon, H. J., Balakrishna, R., and

- David, S. A. (2012) Toll-like receptor (TLR)-7 and -8 modulatory activities of dimeric imidazoquinolines. *J. Med. Chem.* 55, 1106–1116.
25. Schiaffo, C. E., Shi, C., Xiong, Z., Olin, M., Ohlfest, J. R., Aldrich, C. C., and Ferguson, D. M. (2014) Structure-activity relationship analysis of imidazoquinolines with Toll-like receptors 7 and 8 selectivity and enhanced cytokine induction. *J. Med. Chem.* 57, 339–347.
26. Shi, C., Xiong, Z., Chittepudi, P., Aldrich, C. C., Ohlfest, J. R., and Ferguson, D. M. (2012) Discovery of imidazoquinolines with Toll-like receptor 7/8 independent cytokine induction. *ACS Med. Chem. Lett.* 3, 501–504.
27. Ryu, K. A., Stutts, L., Tom, J. K., Mancini, R. J., and Esser-Kahn, A. P. J. (2014) Stimulation of innate immune cells by light-activated TLR7/8 agonists. *J. Am. Chem. Soc.* 136, 10823–10825.
28. Yoo, E., Salunke, D. B., Sil, D., Guo, X., Salyer, A. C. D., Hermanson, A. R., Kumar, M., Malladi, S. S., Balakrishna, R., Thompson, W. H., et al. (2014) Determinants of activity at human Toll-like receptors 7 and 8: quantitative structure-activity relationship (QSAR) of diverse heterocyclic scaffolds. *J. Med. Chem.* 57, 7955–7970.
29. Dobrovolskaia, M. A., and McNeil, S. E. (2007) Immunological properties of engineered nanomaterials. *Nat. Nanotechnol.* 2, 469–478.
30. Gupta, A. K., and Gupta, M. (2005) Synthesis and surface engineering of iron oxide nanoparticles for biomedical applications. *Biomaterials* 26, 3995–4021.
31. Na, H. B., Song, I. C., and Hyeon, T. (2009) Inorganic nanoparticles for MRI contrast agents. *Adv. Mater.* 21, 2133–2148.
32. de Vries, I. J. M., Lesterhuis, W. J., Barentsz, J. O., Verdijk, P., van Krieken, J. H., Boerman, O. C., Oyen, W. J., Bonenkamp, J. J., Boezeman, J. B., Adema, G. J., et al. (2005) Magnetic resonance tracking of dendritic cells in melanoma patients for monitoring of cellular therapy. *Nat. Biotechnol.* 23, 1407–1413.
33. Song, X., Gong, H., Yin, S., Cheng, L., Wang, C., Li, Z., Li, Y., Wang, X., Liu, G., and Liu, Z. (2014) Ultra-small iron oxide doped polypyrrole nanoparticles for *in vivo* multimodal imaging guided photothermal therapy. *Adv. Funct. Mater.* 24, 1194–1201.
34. Yang, K., Hu, L., Ma, X., Ye, S., Cheng, L., Shi, X., Li, C., Li, Y., and Liu, Z. (2012) Multimodal imaging guided photothermal therapy using functionalized graphene nanosheets anchored with magnetic nanoparticles. *Adv. Mater.* 24, 1868–1872.
35. Irvine, D. J., Hanson, M. C., Rakhra, K., and Tokatlian, T. (2015) Synthetic nanoparticles for vaccines and immunotherapy. *Chem. Rev.* 115, 11109–11146.
36. Leleux, J., and Roy, K. (2013) Micro and nanoparticle-based delivery systems for

vaccine immunotherapy: an immunological and materials perspective. *Adv. Healthcare Mater.* 2, 72–94.

37. Mintern, J. D., Percival, C., Kamphuis, M. M. J., Chin, W. J., Caruso, F., and Johnston, A. P. R. (2013) Targeting dendritic cells: the role of specific receptors in the internalization of polymer capsules. *Adv. Healthcare Mater.* 2, 940–944.

38. Smith, D. M., Simon, J. K., and Baker, J. R. (2013) Applications of nanotechnology for immunology. *Nat. Rev. Immunol.* 13, 592–605.

39. Koch, F., Stanzl, U., Jennewein, P., Janke, K., Heufler, C., Kampgen, E., Romani, N., and Schuler, G. (1996) High level IL-12 production by murine dendritic cells: upregulation via MHC class II and CD40 molecules and downregulation by IL-4 and IL-10. *J. Exp. Med.* 184, 741–746.

40. Han, J.-A., Kang, Y. J., Shin, C., Ra, J.-S., Shin, H.-H., Hong, S. Y., Do, Y., and Kang, S. (2014) Ferritin protein cage nanoparticles as versatile antigen delivery nanoplatfoms for dendritic cell (DC)-based vaccine development. *Nanomedicine* 10, 561–569.

41. Quah, B. J. C., Warren, H. S., and Parish, C. R. (2007) Monitoring lymphocyte proliferation *in vitro* and *in vivo* with the intracellular fluorescent dye carboxyfluorescein diacetate succinimidyl ester. *Nat. Protoc.* 2, 2049–2056.

42. Lampkins, A. J., O’Neil, E. J., and Smith, B. D. (2008) Bioorthogonal phosphatidylserine conjugates for delivery and imaging applications. *J. Org. Chem.* 73, 6053–6058.

4. Conclusion

In this dissertation, I studied about the novel methods and candidates for enhancing the cancer immunotherapy based on the nanotechnology. Unlike conventional and clinical treatment of radiation and chemotherapeutics, immunology-based cancer therapeutics are now on the clinical trials for clearing the various cancer development and metastasis. Also, these types of approaches have importance in prolonged or even permanent immune responses to residual or metastatic cancer cells.

Here, I proved that engineered nanoparticles could be utilized in DC based vaccination of cancer antigens for inducing antigen specific cytotoxic CD8⁺ T lymphocytes via multi-valently decoration of cancer antigens to encapsulin or imidazoquinoline adjuvant to biocompatible IONP, respectively.

Encapsulin, protein cage nanoparticles have lots of advantages for additional modification for interior or exterior with easy chemical or genetical access. *In vitro* and *in vivo* studies with nanoparticles provide the evidence of enhancement in adaptive immune responses which came from antigen multivalence.

Additionally, introducing the synthetic adjuvant to IONP by chemical methods could maximize the immune responses inducing the maturation and education of DCs with specific antigens. These approaches may induce proper and powerful immune response for the low immunogenic cancer immune therapy by generation of antigen specific immune responses via small-molecule based adjuvant systems.

The adaptive immune responses acquired from both approaches show considerable activation of antigen specific cytotoxic CD8⁺ T lymphocytes for the rejection of cancer cells or solid tumor itself. The studies described here may provide opportunities to develop the novel cancer immunotherapy that manipulate the DC activation with subsequent cancer antigen-specific cytotoxicity.

5. Acknowledgement

유니스트에서 7년 동안 대학원 생활을 하며 멀게만 느껴졌던 졸업을 눈 앞에 두고 있습니다. 아마, 여러분들의 도움이 없었다면 저 혼자서는 절대 여기까지 오지 못했을 것입니다. 마지막으로 감사 인사를 드리면서 제 마음을 전하고자 합니다.

우선, 3년이 조금 넘는 시간 동안 저를 지도해주신 지도 교수님, 강세병 교수님께 진심으로 감사드립니다. 고 도윤경 교수님의 제자였던 저를 구성원으로 받아들인다는 선택이 지금에 와서야 얼마나 심사숙고한 어려운 선택이었는지 와 닿습니다. 그 이후로 교수님의 제자로서 받았던 아낌없는 조언과 가르침은 제가 그 단시간에 실험을 배우고 적응을 할 수 있는 원동력이 되었습니다. 교수님께서 멘토로서 보여주신 열정과 지도를 가슴 깊이 새기도록 하겠습니다.

그리고 저의 부족함에도 끝까지 믿어 주시고 응원 해 주셨던 고 도윤경 교수님께 감사의 말을 드립니다. 제가 길을 찾지 못해 방황할 때에는 어김없이 저에게 과학자로서 가져야 될 사고와 제가 개선해야 할 점, 그리고 지금 당장 할 수 있는 일에 대해 조언해 주셨습니다. 언제나처럼 다시 돌아오실 것만 같았던 교수님을 더 이상 뵈 수 없지만, 교수님께서 우리에게 바라셨던 것처럼 자신의 자리에서 할 수 있는 일을 하겠습니다.

또한 제 박사 졸업까지 아낌없는 조언을 해 주신 저의 위원회 교수님들, 이창욱 교수님, 박찬영 교수님, 홍성유 교수님, 류성호 교수님께 진심으로 감사드립니다. 그리고 실험실을 옮겨온 저를 빠르게 적응할 수 있게 물심양면으로 도와 주신 문효진 누나에게도 감사드립니다. 또, 갑자기 들어온 선배 때문에 많이 당황하고 적응하느라 힘들었을 우리 후배들에게도 고맙다는 말을 전합니다. 매사 덩덤하게 그 자리에서 꾸준하게 해내는 김한솔 후배, 그리고 영특한 최혁준 후배, 실험실 굿은 일을 도맡아가며 성실한 배윤지 후배, 잘 해 나가고 있는 막내 박성국 후배, 앞으로의 긴 대학원생활도 충분히 잘 해낼 수 있을 거라 믿습니다.

갓 대학원생이 된 어리고 철없는 후배를 가족같이 대하며 아낌없는 지원을 해 주신 신창식 선배님께 진심으로 감사드립니다. 지금 하시는 고된 미국 생활도 잘 마무리되어 저와 재아, 형 모두 우스개처럼 이야기했던 높은 데서 다시 만날 수 있으면 좋겠습니다. 또 다른 제 직속

선배이신 영지누나, 실험에 철두철미한 전문적인 모습이 너무 존경스러웠습니다. 오래 함께하지 못했지만 많은 것을 배웠습니다. 감사합니다. 또, 저와 같이 다사다난한 대학원생활을 보낸 친구이자 또 다른 가족, 한재아 선배님께도 감사드립니다. 그의 날카로운 지적과 자유로운 언어능력은 언제나 저에게 새로운 자극을 주었고 새로운 시선으로 문제를 해결할 수 있음을 보여주었습니다. DISNI lab.의 연구원으로 오랜 시간 헌신해주신 라재선 선생님께도 이 기회를 빌어 감사의 말을 드립니다. 그리고 DISNI lab.에서 인연으로 맺어졌지만 지금은 흩어진 우리 인턴 학생들에게도 감사 인사 드립니다. 자신의 꿈을 향해 달려간 조용빈 후배, 말은 바 열심히 하는 정형민 후배, 소신있게 자신의 길을 택한 홍성준 후배, 한결 같은 밝음과 꾸준함이 장점인 류은진 후배 모두 응원해 주셔서 고맙고 다들 멋지게 삶을 헤쳐 나갈 것이라 믿습니다.

그리고 대학원 동기 송은경 누나, 누나의 밝음과 생기는 언제나 주변 사람들을 즐겁게 했습니다. 많이 의지하고 많은 도움을 받았습니다. 또, 제 선배이며 친구였던 조주형 선배, 형한테는 정말 많은 이야기를 했던 것 같습니다. 제가 살갑게 남을 챙기지 못 해 늘 죄송하지만 형이 있었기 때문에 더 즐겁게 대학원 생활을 했습니다. 또 오랫동안 제 고민을 함께 해준 임한솔 동생에게도 감사의 말을 전합니다. 박경수 선생님, 박수아 선생님 그리고 다른 동물실험실 식구들, 여러분께서 주신 많은 도움, 진심으로 감사드립니다.

끝으로 무심하고 부족한 아들을 전폭적으로 지지해주시고 믿어 주신 부모님, 멀리서 무심한 듯 응원하며 마음 써준 누나, 저를 믿어주고 의지해주는 사랑하는 동생, 여동생처럼 응원해준 처제, 부족한 사위에게 위로와 격려를 아끼지 않으신 장인어른, 장모님께 진심으로 감사드립니다. 그리고 10 여년의 시간동안 지금까지 곁을 지켜준 친구, 인생 선배이자 존경하는 제 반쪽 헤림이, 저를 지금까지 믿어주고 격려해 줘서 정말 고맙습니다. 앞으로 우리가 같이 할 많은 일들도 지금처럼 서로를 아끼며 의지하며 잘 헤쳐 나가길 바랍니다. 언제든 어디에 있던 항상 마음 한 켠에 있는 친구들 태훈이, 현아, 지환이, 필구, 정민이, 태욱이, 정환이, 창만이 너희 격려와 조언은 정말 큰 힘이 되었다. 고맙다.

여기에 다 언급하지 못 했지만 지난 7 년간 저와 인연을 같이 했던 모든 분들께 고마운 마음을 전합니다. 이 곳에서 배운 지식과 경험을 바탕으로 앞으로의 제가 가는 길에서 참된 과학자가 될 수 있도록 노력하겠습니다.